DETERMINATION OF EFFECTIVE POLARIZABILITIES AND RADIATIVE FORCING OF ATMOSPHERIC AEROSOLS:

IMPACTS ON VARIATIONS WITH WAVELENGTHS AND RELATIVE HUMIDITIES

BY

UBA, SHUAIBU

DEPARTMENT OF PHYSICS

FACULTY OF SCIENCE

AHMADU BELLO UNIVERSITY,

ZARIA – NIGERIA

AUGUST, 2016

DETERMINATION OF EFFECTIVE POLARIZABILITIES AND RADIATIVE FORCING OF ATMOSPHERIC AEROSOLS:

Impacts on Variations with Wavelengths and Relative Humidities

BY

UBA Shuaibu, B.Sc. Physics (B.U.K. 2002), M.Sc.

Theoretical Physics (B.U.K. 2008)

PH.D./SCIEN/03869/2008-2009

A THESIS SUBMITTED TO THE SCHOOL OF POSTGRADUATE SCHOOL, AHMADU BELLO UNIVERSITY, ZARIA, NIGERIA

IN PARTIAL FULFILLMENT OF THE REQUIREMENTS FOR THE AWARD OF DOCTOR OF PHILOSOPHY ATMOSPHERIC PHYSICS

DEPARTMENT OF PHYSICS

FACULTY OF SCIENCE

AHMADU BELLO UNIVERSITY,

ZARIA – NIGERIA

AUGUST, 2016

DECLARATION

I hereby declare that, this thesis titled **"Determination of Effective Polarizabilities and Radiative Forcing of Atmospheric Aerosols: *Impacts in variations with wavelengths and relative humidities"*** has been originally written by me in the department of Physics, Ahmadu Bello University, Zaria - Nigeria and it is account for my own research. No part of this thesis was previously presented for another Degree or Diploma at any University anywhere around the world. All references has been duly cited.

_____, _____,

UBA Shuaibu Date

CERTIFICATION

This thesis tittle **"Determination of Effective Polarizabilities and Radiative Forcing of Atmospheric Aerosols:** ***Impacts in variations with wavelengths and relative humidities"*** by Uba Shuaibu meets the regulations governing the award of the Doctor of Philosophy (Physics) of Ahmadu Bello University, Zaria and is approved for its contribution to knowledge and literary presentation.

Dr. B.I. Tijjani …… ……..……

(Chairman Supervisory Committee)

Professor. G. I. Balogun ……

(Member Supervisory Committee)

Professor Rabiu Nasiru …… ……..……

(Member Supervisory Committee)

Dr. Y. I. Zakari …… ……..……

Head of Physics Department

Professor Kabiru Bala …… ……..…… (Dean, School of Postgraduate Studies)

DEDICATION

This Thesis Is Dedicated to My Beloved Parents and members of my family.

ACKNOWLEDGMENT

I wish to express my profound gratitude to the Chairman Supervisory committee, Dr. B.I. Tijjani of the Department of Physics, Bayero University, Kano for his numerous contributions, encouragement, and assistance towards the successful compilation of the research. I am greatly indebted to the members of the supervisory committee; Professor G.I. Balogun, Center for Energy Research and Training (CERT) Ahmadu Bello University, Zaria and Professor Rabiu Nasiru of the Department of Physics, Ahmadu Bello University, Zaria for their desirable contributions, suggestions, advice and assistance for the successful compilation of this work. Equally my thanks go Dr. U. Sadiq, the Head of Department Physics, Dr. I.Y. Zakari and Dr. A.A. Abdelmalek to mention few, for their assistance, encouragement and suggestions from all angles. My appreciations goes to all staff of the Department of Physics, Ahmadu Bello University, Zaria whom in way or the other contributed toward the success of this work.

I sincerely acknowledge the support by the TETFUND 2011, friends, relatives and my beloved parents Mal. Uba Hussein and Mrs. Safiyya Uba Hussein for the supports and prayers. A special acknowledgement is also owed the members of my family, especially my beloved wife Murjanatu Shuaibu and all my children.

ABSTRACT

In this research, I reviewed and applied the Claussi Massoti together with Maxwell relations $\varepsilon = n^2$ and derived the Lorentz – Lorentz relation. We computed the effective Polarizabilities for each atmospheric aerosol components. Hence, the effective polarizabilities for six types of model extracted from OPAC. The six models are: Artic, Antarctic, Maritime Tropical, Urban, Desert/Saharan and Continental Clean aerosols. The respective effective Polarizabilities were computed numerically within 61 wavelengths spectral ranges and eight different types of relative Humidities (RH 00%, 50%, 70%, 80%, 90%, 95%, 98%, and 99%) respectively. The three wavelengths spectral range are: Part I (0.25 to 0.8 μm), Near UV region to visible range. Part II (0.8 to 6.0 μm), Near infrared to medium spectral range and Part III (6.0 to 40.0 μm), Far IR region. The results were analyzed graphically within the three different spectral regions. We have found that the range of effective polarizabilities for six models are as follows: continental clean aerosols 0.491 to 0.541Å^3, Urban aerosols 0.00667 to 0.0073 Å^3, for Antarctic aerosols, 0.0063 to 0.256 Å^3, Artic aerosols 0.000333 to 0.00311 Å^3, Maritime aerosols 0. 000144 to 0.000205 Å^3 finally, for Saharan aerosols is 0.000663 to 0.0000909 Å^3 respectively.

Similarly for the Radiative Forcings (RF) were computed numerically using the concept of Chylek and Wong. The vibrational frequency were determined for each spectral region of the model. With changes of relative humidity in the atmosphere, condensation or evaporation of water take place on the aerosols and this at the same time changes the aerosols optical parameters It is evident that, when the relative humidity increases, the size of an aerosol particle increases through the accretion of water. At RH above 95%. together with the growth in size, the complex refractive index of the aerosol also varies.

The research reveals that; the magnitude of Polarizabilities have shown clear decrease with increases in RH for all the aerosols models but have extraordinary values at different wavelength bands. The contributions mainly was due to the effect of the strongly or

loosely bound electrons that create the dipoles. The magnitude of the mean polarizabilities is minimum near IR region, moderate at Near UV to Visible and maximum at far IR spectral range.

Similarly, for the RF, the cooling effects occurred as RH and λ decrease. While the warming effect occurred for Saharan aerosols at all the wavelengths range and persisted as the wavelength increases. The results have clear shown that the vibrational polarizabilities increases with increase in RH.

The optical depth of the atmospheric aerosols were determined for each model and analyzed graphically, the results have shown the clear decreases in size with increase in wavelengths but increases with increase in RH. The statistical analysis using SPSS was used for further interpretations. The statistical regression analysis shows that, the aerosol optical depth decreases with increase in λ. As the RH increases, the aerosol increases in size and the dipole decreases hence the polarizabilities decreases with increase in RH. Finally, we observed that, Sahara aerosols model has the lowest polarizabilities resulted in highest warming effect and continental clean aerosols model has the highest value of effective polarizability and resulted the cooling effect.

TABLE OF CONTENTS

Contents

List of Table

Table Page

LIST OF FIGURES

Figure
Page

CHAPTER ONE

INTRODUCTION

1.1 Research Background

The charge redistributions that occur when a particle is exposed to an electric field is characterized by a set of constants called polarizabilities. Physically, the polarizability is the fundamental property that characterizes the particle-field interactions.

For every one cubic centimeter of atmospheric air contains approximately 2.5 x 10^{19} molecules. About 10^{3} of these may be charged (ions). The average distance between the molecules is about ten times molecular sizes. In addition, one cubic centimetercontains a substantial number of particles varying in size from a few Angstrom to several microns. These particles arise from a number of natural sources as well as from activities of the earth's inhabitants. The particles can have complex chemical composition and morphologies; the suspension of particles in gas is known as aerosols (Meszaros, 1981).

All matter is polarized in direct proportion to the strength of the external field, where the proportionality constant is called the polarizability. Optical properties of aerosols are also characterized by their polarizabilities (Yangang and Peter, 2008**).** Electric polarizability has long been the subject of investigations . As a natural phenomenon, electricity was known in ancient times,several attempts were made as early as ninetieth century to correlate the dielectric constants with the microscopic structure of matter (Yangang and Peter, 2008**).** In 1847, following Faraday in considering the dielectric to be composed of conducting spheres in a non-conducting medium, Mossotti succeeded

in deriving a relation between the dielectric constant and the volume fraction occupied by the conducting particles in the dielectric. However, this expression remained relatively unknown until it was again derived probably independently 1879 by Clausius(Doyle, 1978).

Electric polarizability is routinely associated with fundamental characteristics of atomic and molecular systems: hardness, softness and hyper softness, stiffness and compressibility. The basic theory of electric polarizability and its higher order (hyperpolarizability) is of central importance to the rational approach to the description and interpretation of a wide range of phenomena in aerosol scattering and phenomena induced by intermolecular and atmospheric interaction with radiations. It is also present as a key element in the rigorous analysis of spectroscopic observations. In recent years, the theoretical determination of electric polarizability and hyper polarizability is making decisive contributions to new fields with important potential for advanced technological applications. Such fields are the atmospheric and aerosol sciences, molecular simulation and modeling of fundamental processes and the search for new aerosol and optical materials.The increasing demand for accurate polarizability values has resulted in intense investigations on all computational aspects of its determination. At a relatively early stage, the agreement between theory and experiment for these quantities was a major issue. The careful analysis of the observed discrepancies has brought about an effective rapprochement between theory and experiment. The development of theoretical methods of high predictive capability and reliable computational strategies has transformed computational aerosol science into a true vehicle of progress for modern technological advancement.

Polarizability is the ability for a molecule or aerosol to be polarized. It is a property of matter. Polarizabilities determine the dynamical response of a bound system to external fields, and provide insight into a molecule's or aerosols internal structure. Electric polarizability is the relative tendency of a charge distribution, like the electron cloud of an atom or molecule and aerosols to be distorted from its normal shape by an external electric field, which may usually be caused by the presence of a nearby ion or dipole.

The electronic polarizability (α) is defined as the ratio of the induced dipole moment (**P**) of an atom to the electric field (**E**) that produces this dipole moment. Or

$$\vec{p} = \alpha \vec{E} \quad (1.1)$$

Polarizability has the SI units of $C \cdot m^2 \cdot V^{-1} = A^2 \cdot s^4 \cdot kg^{-1}$, while its cgs unit is cm^3. Usually it is expressed in cgs units as a so called polarizability volume, instead of cm^3 it is sometimes expressed in $Å^3 = 10^{-24}\ cm^3$.

The polarizability α as defined above is a scalar quantity. This implies that the applied electric fields can only produce polarization components parallel to the field. For instance, an electric field in the x- direction can only produce an x-component in **p**. However, it can happen that an electric field in the x-direction, produces a y or z component in the vector **p** . In this case α is described as a tensor of rank 2, which is represented with respect to a given system of axes by a 3 x 3 matrix. In thisresearch, we adopt the scalarformulation technique.

Generally, polarizability increases as volume occupied by electrons or aerosols increases. Likewise, larger molecules are generally more polarizable than smaller ones. It is important to note that ground state electron configuration models are often inadequate in studying the polarizability of bonds because dramatic changes in molecular structure occur in a reaction.

The earliest observation of an effect that could subsequently be directly related to a molecular polarizability was the first notice of anomalous dispersion by Fox Talbot 1840 (Sihvola et al, 2004; Ottcher, 1952).It was Stoke (Stoke, 1966) who first made the crucial proposal those molecules could be treated as having their own natural vibrational frequencies that result in observable effects when interacting with light at a different frequency. This proposition, made in 1852.(Ottcher, 1952).

The most important process responsible for energy transfer in the atmosphere is electromagnetic radiation. This radiation travels in wave form, and all electromagnetic waves travel at the same speed, the speed of light, that is $2.99793 \pm 1 \times 10^{8}$m sec^{-1} in a vacuum and very nearly the same speed in air. Visible light, gamma rays, x-rays, ultraviolet light, infrared radiation, microwaves, television signals, and radio waves constitute the electromagnetic spectrum (Liou, 2002).

The Atmospheric processes influence almost all aspects of the life of the humanity. The processes of transformations of radiation energy of the Sun in the atmosphere and on the surface, and the formation of different types of atmospheric radiations as components of the radiation balance of the planet (polarization and other characteristics of radiation fields).Optical properties of particulate atmospheric

constituents that is aerosol particles and clouds affect local radiative forcing, the radiation balance of the earth, and thus climate **(**Thomas'2006; Ulrich, 2012).

Moreover, these properties are essential for remote sensing, both of the constituents themselves and with respect to the masking effect against other quantities. The Polarizabilities effects of aerosol particles dominate in the solar spectral range are not negligible at other wavelengths.The optical propertiesof aerosol particles are highly variable, in both time and space. This is valid for the number density, that is, the amount of particles per volume, for the microphysical properties, like size distribution, refractive index and shape, and for the height distribution. Moreover, in most cases, the actual properties are not wellknown (Thomas, 2006).

For this reason,it is necessary to reduce the variability of naturally occurring aerosols to typical cases, but without neglecting possible fluctuations (Hess et al, 1998).

When aerosols interact with radiation, two different processes usually occurred, (Akhter, 1985; Igor, 2010).

First, the aerosol can reradiate the received energy without changing the wavelength (scattering).

Second, the received energy can be re-emitted at a different wavelengths or transformed into heat energy (absorption).

The sum of these two processes is called extinction. The direction of scattered light can be describe by the asymmetry factor **g**, which is the fraction of the incident light scattered in forward direction. If all light is scattered forward, the asymmetry factor is

1 and if it tends towards -1, more light is scattered backwards (reflected). The ratio between the fraction of light lost due to scattering (scattering coefficient) and to extinction (extinction coefficient) is called the single scatting albedo ω, where $0 \le \omega \le 1$(Akhter, 1985, Igor, 2010). The larger the single scattering albedo, the more light attenuation is caused by scattering. When integrating the extinction coefficient over a vertical column the optical thickness τ is obtained. The aerosol optical thickness describes the degree to which aerosols attenuate light on its way through the atmosphere.

1.2 Classification of Atmospheric Aerosols

The term "atmospheric aerosol" encompasses a wide range of particle types having different compositions, sizes, shapes, and optical properties. Aerosol loading, or amount in the atmosphere, is usually quantified by mass concentration or by an optical measure, aerosol optical depth (AOD). AOD is the vertical integral through the entire height of the atmosphere of the fraction of incident light either scattered or absorbed by airborne particles (Mian Chin, 2009).

Depending on its composition or sources, the atmospheric aerosol is subdivided into the following types (Deepak, 1982; Deirmendjian, 1969;Twomey, 1977).

1.2.1 The Aerosol of natural origin

The aerosols that have natural origin are:

i. Products of evaporation of sea splashes: salt particles.
ii. Mineral dust lifted into the atmosphere by the wind**.**

iii. Volcanic aerosol, both directly ejected into the atmosphere(ash) and formed as a result of gas phase reactions (sulphuric acid particles);

iv. particles of biogenous origin, both those directly ejected into the atmosphere and formed

as a result of condensation of volatile organic compounds and chemical reactions between these compounds;

v. Products of natural gas phase reactions. (for example, sulphates, formed as a result of oxidation of SO_2).

1.2.2Aerosol of the Antropogenous origin:

The aerosols that have antropogenous origin are:

i. Industrial emissions of particles(soot, smog, road dust, etc.);
ii. Products of agricultural activity **(**for example, dust formed during plowing);
iii. Products of gas phase reactions (formed in the same manner as natural products in reactions of antropogenous trace gases).

The atmospheric aerosol is also subdivided into tropospheric and stratospheric (on the basis of the features of location in the appropriate layer of the atmosphere) and also into primary aerosols falling into the atmosphere directly, and secondary – formed in the atmosphere as a result of chemical reactions. (Akhter, 1985; Igor, 2010;, Seinfeld and Pandis, 2006).

Table 1.1: main sources of aerosols

Primary Aerosols	Secondary Aerosols
Natural	**Natural**
Mineral aerosol	Sulfates from biogenic gases
Sea salt	Sulfates from volcanic SO_2
Volcanic dust	Organic aerosols from VOCs
Organic aerosols	Nitrates from NO_x
Anthropogenic	**Anthropogenic**
Industrial dust	Sulfates from SO_2
Soot	Organic aerosols from VOCs
Biomass burning	Nitrates from NO_x

(**Source:** Seinfeld and Pandis, 1998)

1.3 Radiative effects of Aerosols

The radiative properties of aerosol particles is a complicated function of their chemistry, shape, and size spectra. Moreover, if the aerosol particles are hygroscopic, their radiative properties change with the relative humidity of the air. At relative humidities (RH) greater than 70%, the hygroscopic particles (called haze) take on water vapor molecules and swell in size, thus changing their radiative properties not only because of size effects but also because of changes in their complex indices of refraction as the water solution particle mixture changes in relative amounts. At RH greater than about 78%, hygroscopic particles begin taking on water vapor and expand abnormally.

Changes in the amount of radiatively active atmospheric constituents (polarizabilities) can perturb the balance between solar radiation coming into the atmosphere and radiation going

out (radiative forcing). A positive radiative forcing tends to warm the atmosphere, and negative forcing tends to cool the atmosphere.

1.4 Aim and Objectives of the Research

1.4.1 Aim

The aim of this work is to determine the Polarizabilities and radiative forcing for six types of atmospheric aerosols modelsextracted from Optical Properties of Aerosols and Cloud (OPAC), and their impact in variations with relative humidities and wavelengths.

1.4.2 Objectives

The objectives of this research work are:

i. To examinethe consistency of the mixing rules suitable in aerosol science to calculate the polarizability of aerosols.
ii. To compare the impacts of Polarizabilityamong other aerosol models.
iii. To determine the resonance frequencydependence of atmospheric aerosols with polarizabilities and its impacts in variations with wavelength and relative humidities.
iv. To justify the importance of polarizability to get deeper understanding of aerosol particles.

1.5 Justification

The Earth's atmosphere is a natural laboratory, in which wide varieties of physical processes take place. Various atmospheric phenomena have been of interest to man

from time immemorial. The life of people and other representatives of the fauna and flora has depended greatly on the weather and climate on our planet and on illumination conditions. The dependence of the humanity on the weather and climate is still very considerable. Fluctuations of precipitation, anomalous temperatures and winds have the controlling effect on the life of people, (Agranovsk, (2010),.

Long-term droughts result in the deaths of tens and hundreds of thousands of people, regardless of the help provided by various international and charitable organizations and funds. Tens and hundreds of people die during flooding, cyclones and storms. Most of these are strongly influenced bythe impact of atmospheric aerosols because of interactions with light and hence the polarizabilities.

Despite the vast literature and experience, the optical properties of atmospheric aerosols are not well understood, hence, leaving a gap in our understanding of the optical properties of aerosols, consequently, leading to major uncertainties in assessing their current and future impacts on interactions with light.It is therefore necessary to perform detailed computational approaches on the polarizabilities for properties of aerosols.

Over 2000 data wereretrieved for the various polarizabilities of atoms, molecules, compound metals and other substances (David, 2003). Nevertheless, to the best of our knowledge, no data available for the polarizability of atmospheric aerosols. Despite the fact that, aerosols are tiny particles with big impact on atmospheric phenomena.

1.6 Motivation

Aerosol particles as they are transported through the atmosphere interact with existing gases which leads to products with new chemical and physical properties (normally referred to as aging). Aging of aerosols can change their molecular weight, the new products can have higher oxidation states, which will therefore modify the polarizability, hygroscopicity, and change the optical properties (Grieken, 1995). Hence, investigating the polarizability effect of atmospheric aerosols optical processes is of great importance.

Aerosol science does not belong to the group of sciences that are based on one equation or principle, like, for example, classical mechanics (Newton's equation), quantum mechanics (Schrodinger's equation), classical electrodynamics (Maxwell's equations), and so on. Rather, aerosol science applies the results and methods adopted from all other sciences. In particular, Newton's equation applies in aerosol mechanics, Maxwell's equations are used in the theory of light scattering by aerosols, quantum-mechanical approaches are needed for studying the structure of small clusters, and even quantum field ideas have been used in aerosol science.This rather speckled structure of aerosol science makes it difficult to write a review enveloping all branches of aerosol science.Hence, investigating the polarizability effect of atmospheric aerosols optical processes is of great importance.

The complexity, heterogeneity, and strong variability of their global distribution make aerosols a very difficult object of study. Because of unavoidable gaps in spatial and temporal coverage, the data collected with satellite, in situ, and ground based instruments will never be sufficient for a direct global assessment of the long-term aerosol effect on optical radiation and climate.

Most satellite remote sensing techniques of tropospheric aerosols rely upon radiance measurements;some of the retrievals ignore polarizability effects of the radiation. This often is a reasonable approximation, but considering polarizability can offer additional information and improve retrievals (Deschamps et al; 1994,Deuzé et al, 2000; Duforet et al., 2007, Natraj et al., 2007).

1.7 Scope and limitation of the Research

Here in this research, we have limited ourselves to the problems of determinations of effective polarizabilities and its impacts in the radiative processes and the radiation field as a source of information on the optical and physical characteristics of the aerosols and the atmosphere.

The research covers wide range of six types of atmospheric aerosols models within the spectral wavelengths of 0.25μm to 40μm. (i.e IR, near UV to far IRspectral regions)see figure 1.1 and RH 00, 50, 70, 80, 90, 95, 98 and 99%. They are:

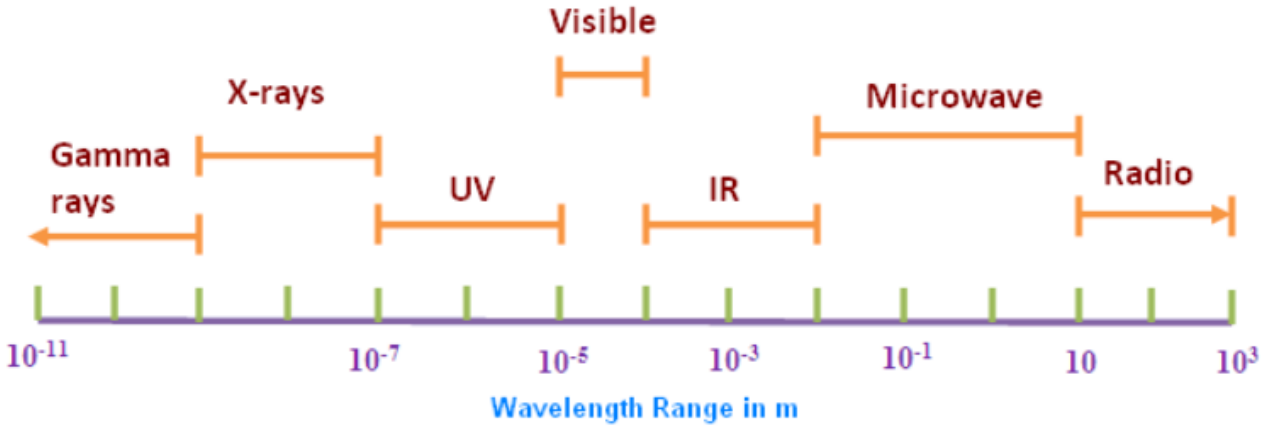

Figure 1.1 Wavelength range of Electromagnetic spectrum. *(Source: http://physics.tutorvista.com).*

The research does not covers the following components:

i. Radioactive aerosols.

ii. Higher order polarizabilities. e.g. hyperpolarizability.

iii. Tensor treatment of polarizability.

iv. Magnetic polarizability.

v. Quantum effects

vi. Relativistic effect.

CHAPTER TWO

LITERATURE REVIEW

2.1 Introduction

Electric and magnetic polarizabilities are general response function for atoms, aerosols and solids in general. An experimentalist might impose an external field upon the sample under investigation. The sample could be a collection of atoms in a gas, liquid, or solid. The sample develops an induced moment in response to the field. In this research, we are concerned for the theoretical determination of polarizabilities for ambient aerosols. For aspherically ambientaerosol light wave or any electromagnetic wave develops an induced electric field **E.**The aerosol would develop an induced dipole moment **p** in response to an external electric field (Buckingham, 1967).

$$p = \alpha\varepsilon + \frac{\gamma}{3!}\varepsilon^3 + ..., \qquad (2.1)$$

where α is linear and γ nonlinear polarizabilitiesrespectivelyand ε is the electric field. Linear and nonlinear polarizabilities are calculated for atoms, liquids, solids, and surfaces.

However, no exact methods are available for aerosols and many-electron systems. Two different theoretical methods are widely used to calculate polarizabilities for many-electron systems. One is mostly used by Chemists, and is called the Time-Dependent Hartree-Fock Approximation. This title is a bit misleading, since the equations are not time dependent! The second method of solving systems with many electrons is called

the Local Density Approximation. The calculation of polarizabilities represents a small fraction of the worldwide activity.

In this work, we will present a new computational techniquethat provides accurate and relatively easy technique for calculating the linear polarizabilities of ambient aerosols using Lorentz – Lorentz relation.

This technique for the calculation of the polarizability can be applied to many systems. e.g., for atoms, ionic solids, metal spheres and metal surfaces (Mian, 2009).

2.2 Dipole

Within a dielectric, positive and negative charges are impelled to move in opposite directions by an applied electric field. As a result, electric dipoles are generated. The product of charges and the separation distance of positive and negative charges is refer as the dipole moment, which, when divided by the unit volume, is referred to as polarization P.

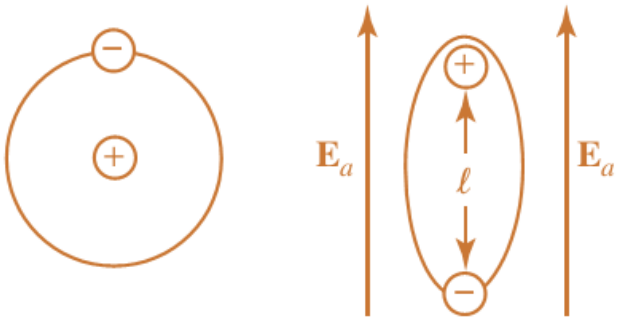

$$d\vec{p} = Q\vec{l}_i \quad (2.2)$$

Figure 2. 1 A typical atom. (a) Absence of applied field. (b) Under applied field.

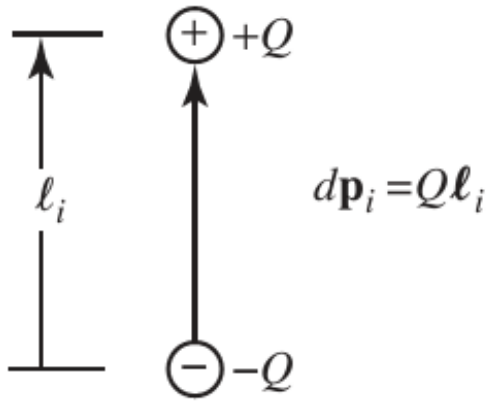

Figure 2. 2 Formation of a dipole between two opposite charges of equal magnitude Q.

When a material is subjected to an electric field, the polarization dipoles of the material interact with the applied electromagnetic field. For aerosols material, this interaction provides the material the ability to store electric energy, which is accomplished by the shift against restraining forces of their bound charges when they are subjected to external applied forces. The presence of these dipoles can be accounted for by developing a microscopic model in which each individual charge and dipole (equation 2.2) is considered. Instead, in practice, the behavior of these dipoles and bound charges is accounted for in a qualitative way by introducing an electric polarization vector $\vec{P}$ using a macroscopic scale model involving thousands of atoms , molecules or particles.

The total dipole moment $\vec{p}_i$ of a material is obtained by summing the dipole moments of all the orientational polarization dipoles, each of which is represented by equation (2.2). For a volume ΔV, where there are N_e electric dipoles per unit volume, or a total of $N_e \Delta V$ electric dipoles, we canwrite that:

$$\vec{p}_t = \sum_{i=1}^{N_e \Delta V} d\vec{p}_i \qquad (2.3)$$

Assuming an average dipole moment of $d\vec{p}_i = d\vec{p}_{av}$ per molecule, the electric polarization vector of (2.3) can be written, when all dipoles are aligned in the same direction, as

$$\vec{p} = \lim_{\Delta V \to 0} \left[\frac{1}{\Delta V} \sum_{i=1}^{N_e \Delta V} d\vec{p}_i \right] = N_e d\vec{p}_{av} = N_e Q \vec{l}_{av} \qquad (2.4)$$

Electric polarization for dielectrics can be produced by any of the following three mechanisms,as demonstrated in Figure2.3.

2.2.1 Dipole or Orientational polarization

This polarization is evident in materials that, in theabsence of an applied field and owing to their structure, possess permanent dipole momentsthat are randomly oriented. However when an electric field is applied, the dipoles tend toalign with the applied field.

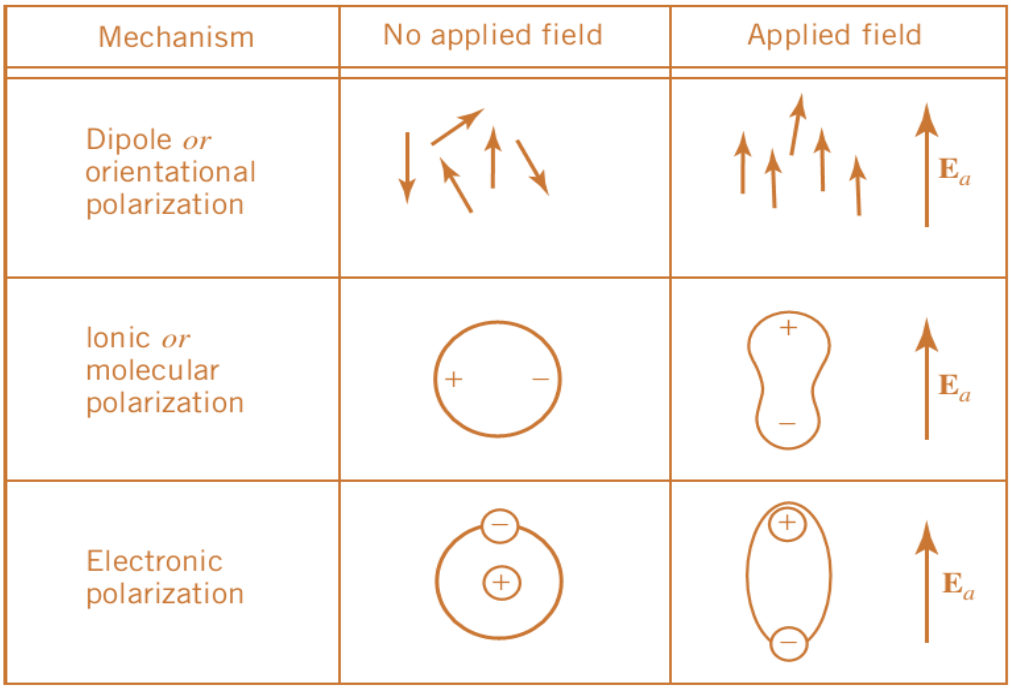

Figure 2. 3 Mechanisms producing electric polarization in dielectrics.

2.2.2 Ionic or Molecular polarization

This polarization is evident in materials, that possess positive and negative ions and that tend to displace themselveswhen an electric field is applied.Such as sodium chloride (NaCl).

2.2.3 Electronic polarization:

This polarization is evident in most materials, and it exists whenan applied electric field displaces the electric cloud center of an atom relative to the centerof the nucleus. If the charges in a material, in the absence of an applied electric field $\mathbf{E}_a$, are averaged in such a way that positive and negative charges cancel each other throughout the

entire material, then there are no individual dipoles formed and the total dipole moment of (2.1) and the electric polarization vector $\vec{p}$ of (2.2) are zero. However, when an electric field is applied, it exhibits a net nonzero polarization. Such a material is referred to as nonpolar, and it is illustrated in Figure 2.4a. Polar materials are those whose charges in the absence of an applied electric field E_a are distributed so that there are individual dipoles formed, each with a dipole moment $\vec{p}_i$ as given by (2.1) but with a net total dipole moment $\vec{p}_t = 0$ and electric polarization vector $\vec{p} = 0$. This is usually a result of the random orientation of the dipoles as illustrated in Figure 2.4b. When an electric field is applied to a nonpolar or polar dielectric material, as shown in Figures 2.4aand 2.4b, the charges in each medium are aligned in such a way that individual dipoles with nonzero dipole moments are formed within the material.

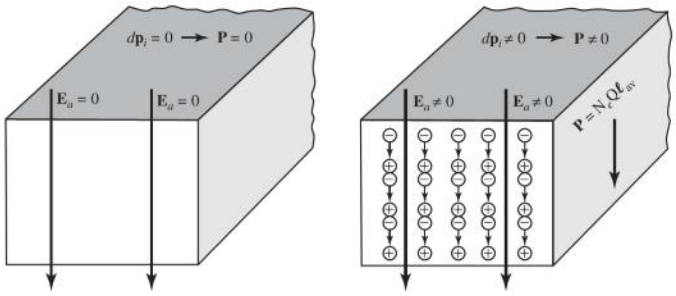

(a) Nonpolarmaterials

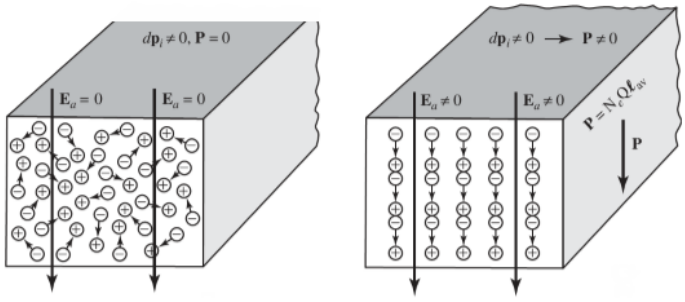

*(b) polar*materials

Figure 2. 4 (a) Macroscopic scale models of materials (a) Nonpolar (b) polar

2.3 Aerosol Background

An “aerosol” is a suspension of finely divided matter (liquid or solid) dispersed in a gaseous medium such as air. The suspended particles are called “aerosol particles” or “aerosols.” Particle sizes range from about 2 nm to more than 100 µm.

Although attempts to give a strict definition of aerosol have appeared from time to time, to date no commonly acceptable and concise definition of an aerosol exists. Aerosol science studies the properties of particles suspended in air or other gases, or even in vacuum, and the behavior of collections of such particles. Although the particles may be suspended in some other gaseous medium, not just air. The term cosmosol is used for a collection of particles suspended in vacuum.

Aerosol particles that occur naturally in the atmosphere are called “atmospheric aerosols;” those, which are produced in the laboratory or field space by fabricated chemical, thermal, or mechanical means are called “artificial aerosols”, or anthropogenic aerosols.

In this work, the term atmospheric aerosols will cover aerosols derived from both natural and anthropogenic sources; the anthropogenic source being those generated as by-products of human activity, such as burning of fossil fuels and are often referred to as “anthropogenic aerosols (Winiwarter, 2009).

Atmospheric aerosols may be formed as the result of wind action at the earth’s surface (land or ocean), or formed insitu by condensation from the gaseous phase. Gaseous precursors may in turn, be formed by the action of sunlightand chemical action on other naturally or anthropogenically produced gases.

Aerosols are subject to changes insize and composition by processes of condensation, evaporation, and coagulation. Water-soluble aerosols mayalso change size in response to changes in atmospheric humidity. Aerosols, particularly those in the troposphere,are often mixtures of different chemical components. Such mixtures may be external, in which different particleswithin the same air mass have differing compositions, or "internal," in which individual particles are of mixedcomposition. An example of a relatively simple homogeneous aerosol is that found in the stratosphere, which,except just after a volcanic eruption, consists of a solution of sulfuric acid in water that is in equilibrium with itssurroundings. The marine boundary layer aerosol is an example of an external mixture, in which aerosols ofdifferent compositions (sea salt and sulfates) occupy different parts of the size distribution spectrum. Internal mixtures are often formed within the atmosphere, as for example, when a solid desert aerosol passes through anindustrial plume and the individual particles acquire a layer of sulfuric acid.

Atmospheric aerosols are also subjectto modification by cloud processes, where aerosols becomes integrated into the cloud droplets and may be laterregenerated, often in modified form, as a result of evaporation. Cloud processes are also responsible for theremoval of much of the aerosol from the atmosphere within rain or snow.Aerosol concentrations and compositions depend on location relative to source regions, production and removalrates, transport, and altitude. It is possible to classify aerosols according to their sources and to describe theirapproximate chemical composition and size distribution.

The most significant sources for atmospheric aerosols liewithin the planetary boundary layer, and it is here that the largest concentrations are normally to be found. Sourcesare

not only localized but may also vary in time. These variations may be seasonal, such as in the formation ofdesert dust plumes by springtime surface wind erosion or in the annual cycle of biomass burning and smokeproduction in tropical countries. Examples of sporadic aerosol production are those formed as a result of volcanicactivity or forest fires.

2.4 Aerosol Properties

We distinguish different types of aerosols based on their methods of generation, the size of the particles, and whether the particles are solid or liquid. Typical particle size ranges and other properties are illustrated in Figure 2.5.

2.5 Aerosol Size Distributions

2.5.1 Characterization of atmospheric Aerosols

Aerosols are characterized by their physical and chemical properties, namely, size, shape, and material composition. The properties of atmospheric aerosols not only vary within a unit volume of the atmosphere, but also vary considerably over the global atmosphere. Of these, traditionally the most commonly used aerosol property is the particle size (Ulrich, 2012). It is assumed that the shape of atmospheric aerosols is spherical, which is a valid assumption for most applications of interest, so that the sizecan be represented by the parameter, r, for the particle radius. (Thenon-sphericity of atmospheric particles becomes important in dealing with snowflakes, ice crystals, raindrops,volcanic ash, etc.)

When neither the shape, size, nor the constitution of the aerosol particles is uniform, it is referred to as Polydisperse aerosol. (Deirmendjian, 1969).However, if a Polydisperse suspension has particles that are uniform in physical constitution and shape butvary in number concentration depending on the size only, it is referred to as a "polydispersion;" and, if all particleshave the same size or a very narrow range of sizes, then the aerosol is referred to as "monodisperse aerosol" or"monodispersion."

2.5.2 Aerosol size distribution functions

It is convenient to characterize the polydispersity of atmospheric aerosols by a distribution function, called the sizedistribution, which gives the variation of the particle size in terms of either number concentration or surface area, orvolume, with size being represented by either radius (r) or logarithm (natural or to the base 10) of the radius.

Suppose the entire range of possible radii of aerosol particles is divided into subintervals Δr_i and each subinterval we determine the number of particles $N(r_i, r_i + \Delta r_i)$.

To compare the concentrations of different subintervals, we shall normalize them. We denote $n(r_i) = \frac{N(r_i \Delta r_i)}{\Delta r_i}$ the concentration of particles in the range of the radii 0 to r_i will be:

$$N(r_i) = \sum_{i}^{M} n(r_i)\Delta r_i \qquad (2.5)$$

Where n is the number of subintervals. Moreover, the Function n(r) is the function of the size distribution of aerosol particles. i.e. it shows the number of particles with specific radii. The total concentration of all aerosol particles, according to equation (2.5) (Hinds, 1999) is

$$n(r) = \frac{dN(r)}{dr} \quad (2.6)$$

2.6 Aerosols Compositions

The chemical composition of aerosols in the troposphere strongly depends on location, such as urban, rural, maritime, and desert. In other words, it depends on the surface character of the earth for a particular region. In addition, all regions have some level, of water vapor content. Many aerosols are hygroscopic or act as condensation nuclei and therefore will contain water at some level, depending on the relative humidity. Dryer particles exist during the winter and wetter particles exist during the summer.

Regions of high humidity (near 100%) lead to the formation of fog (near ground level) and clouds (higher altitude regions), which are particles dominantly composed of water. High altitude clouds, such as cirrus, exist at subfreezing altitudes and are composed of ice .

2.7 Particle Absorption and Scatter

Maritime aerosols are wet, and contain the salts that are in the ocean, although this can change as chemical reactions occur. Desert aerosols are typically composed of dry silica (SiO_2). Urban particles are composed of sulfate, nitrate, and ammonium

compounds. A greater diversity of particle composition for urban areas exists because of anthropogenic sources. The burning of fossil fuels produces soot or carbon-based particles, for example. Rural and urban areas include organic particles such as pollen. Small organic aerosols such as spores, viruses, and bacteria exist in rural and urban environments as well. Such particles are a concern for public health.

2.8 Types of Aerosol

The main aerosol types are:

2.8.1 Sea - Salt Aerosol (SSA): SSA Originates from the oceanic surface due to wave breaking phenomena. The largest droplets fall close to their area of origin. Only the smallest aerosol particles with sizes from approximately 0.1 to 1μm (e.g., those formed by the bursting of bubbles at the ocean surface) are of a primary importance to the large-scale atmospheric aerosol properties. These particles can exist in the atmosphere for a long time. They have been identified over continents as well.

The shape of sea-salt aerosol particles depends on the humidity. Cubic particles are found at low humidity. This is due to the cubic structure of sodium chloride. NaCl, the main constitute of SSA is easily dissolved in water. Therefore, cubic forms transform into spherical shapes in high-humidity conditions. SSA is extremely dynamic with respect to the modification of its shape. It is difficult to construct the universal optical model of SSA because of the considerable influence of shapes on the processes of light interaction with particles. At least two optical models of SSA are needed (i.e., for low and high humidity conditions). Yet another problem is associated with the fact that sea salt is not distributed uniformly in the aerosol particle formed by the attraction of water

molecules in the field of high humidity. The concentration of NaCl molecules is larger close to the center of a particle as compared to its periphery. This leads to the necessity to account for the inhomogeneity of a particle in theoretical studies of its optical characteristics.

The optical properties of SSA aerosol particles are largely determined by the ratio a/λ, where λ is the wavelength of incident light and a is the characteristic size of a particle (e.g., the radius of a droplet or the side of a cubic crystal). Clarke et al. (2003) found that dry sizes of sea-salt particles are in the range 0.1 to 10 μm.

2.8.2 Dust Aerosol (DA):The DA Originates from the land surface. It is composed of solid particles. Most of particles (e.g., composed of Si) are not soluble in water. Therefore, dramatic changes of the aerosol particle shape and structure in the humidity field are rare events as compared to sea-salt aerosols. However, a water or ice shell in high humidity conditions can cover the mineral core. This will modify the optical properties of the particle. Wet solid particles generally have lower refractive indices as compared to particles in dry conditions.

2.8.3 Secondary Aerosol (SA): SA Originates in the atmosphere due to gas-to-particle conversion. This aerosol is composed of mostly sulfates and nitrates. Also various organic substances (originating, for example, from gases emitted by plants) can make a large contribution in the total aerosol mass (Seinfeld and Pandis, 1998). In particular, SO_2 is oxidized to H_2SO_4 and the rate of conversion is influenced by the presence of heavy metal ions (e.g., Fe, Mn,V). Some of proposed reactions are given below

$$SO_3 + H_2O \rightleftharpoons H_2SO_4,$$

$$NO + O_2 + H \rightarrow HNO_3,$$

$$SO_2 + C_2H_2 + \text{allene} \rightarrow C_3H_4S_2O_3,$$

$$NO_2 + \text{hydrocarbons} + \text{photochemistry} \rightarrow \text{organic nitrates},$$

$$SO_2 + \text{alkanes} \rightarrow \text{sulfinilic acid},$$

$$O_3 + \text{olefines} \rightarrow \text{organic particles}.$$

The generated particles are mostly of spherical shape with parameters of the lognormal distribution.

The parameters mentioned above can vary considerably depending on the humidity. This aerosol is found at all locations. Therefore, it plays an important role in the global aerosol budget (Lacis andMischenko, 1990).

2.8.4 Biological Aerosols (BA):BA Are characterized by the extreme particle size range and enormous heterogeneity. Biological material is present in the atmosphere in the form of pollens, fungal spores, bacteria, viruses, insects, fragments of plants and animals, etc. The volumetric concentration of bioaerosols depends on the season, location, and height of the sampling volume with smaller values at higher altitudes and in winter time (e.g., at high latitudes).

Bioaerosols can occupy up to 30%of the total atmospheric aerosol volume at a given location (especially in remote continental areas). Clearly, the impact of inland biological matter and dust is of a great importance for oceanic life forms.

Bioaerosols (e.g., viruses and bacteria) can be attached to other particles (e.g., dust, pollen, spores) and travel large distances using other particles, including cloud droplets, as a means of transportation (Nevalienen, 1985).

Table 2.1 Size Of Biological particles

Biological particles	**radius (μm)**
Viruses	0.05 – 0.15
Bacteria	0.1 – 4.0
Fungal spores	0.5 – 15.0
Pollen	10.0 – 30.0

(Source: liou 2002)

2.8.5 Smoke Aerosols (SA): Originate due to forest, grass, and other types of fires. However, it has important local effects (e.g., as a cause of human, animal, and plant diseases; the reduction of visibility; and the changing of the heat balance) and an effect on global climate due to generally larger values of light absorption by smoke aerosol (e.g., black carbon) as compared to other aerosol species. In particular, it has been found that aerosols transported to the Arctic from highly polluted areas in Europe can lead to a decrease in the planetary albedo (e.g, due to atmospheric absorption effects and also due to increased absorption of polluted snow and ice). (Hansen and Travis, 1974), argued that dirty snow modifies planetary albedo and makes an important contribution to the global warming of the planet. Smoke aerosols may lead to a number

of spectacular optical atmospheric effects such as the blue Moon and Sun (van de Hulst, 1969).

Combustion processes produce tremendous numbers of small particles with radii below 0.1lm. They also produce particles in the accumulation mode (0.1–1μm, and 'giant' particles with radii above 1μm. particles of smoke can easily penetrate the respiratory system of humans leading to various health problems. Smoke aerosol has a large content of soot.

2.8.6Volcanic Aerosols (VA):VA originate due to emissions of primary particles and gases (e.g., gaseous sulfur) by volcanic activity. Most of the particles ejected from volcanoes (dust and ash) are water insoluble mineral particles, silicates, and metallic oxides such as SiO_2, Al_2O_3 and Fe_2O_3, which remain mostly in the troposphere. Volcanic eruptions can have a large impact on stratospheric aerosol loads.

2.8.7Anthropogenic Aerosols(AA):AA consists of both primary particles (e.g., diesel exhaust and dust) and secondary particles formed from gaseous anthropogenic emissions. Secondary liquid particles are quite small and their shapes can be approximated by spheres.Anthropogenic aerosols contribute about 10% of the total aerosol loading. However, these emissions did not occur in the pre-human era.

2.9 Aerosol Models

It follows from the discussion above that the microphysical characteristics of aerosols change considerably depending on the aerosol type, the season, etc. In particular, the sea-salt aerosol is divided into two fractions: fine mode and coarse mode. The coarse

mode is of importance only for rough oceanic surface conditions occurring at high wind speed. Far from the oceans and also over calm water, the fine mode prevails. The desert dust aerosol is composed of three fractions with the behavior of the fractions similar to that of sea salt. In addition, the nucleation mode with very small particles is added. Only the spherical model of scatterers is considered, which is very remote from reality for mineral aerosols and dry sea salt.

All other aerosol particles are subdivided into two broad categories: water-soluble aerosol (e.g., sulfates and nitrates) and water-insoluble aerosol (e.g., soil). In addition, the soot component is introduced. This component is used to represent absorbing black carbon. Soot only weakly influences light scattering in atmospheric air, but black carbon is of primary importance for light absorption processes, especially in urban areas.

2.10 Interaction of radiation with a medium

2.10.1 Aerosol optical properties

Whenever electromagnetic radiation passes through a medium composed of particles and molecules, its intensity always decreases during transit (Sun et al, 2010). The loss of intensity is due to either scattering or absorption or both by the medium constituents. In the absorption process, the light radiation actually disappears (the energy being converted into the heat motion of the particles). During the scattering process, some of the incident radiation is re-radiated in all directions at different rates, with a change in its state of polarization but with no change in wavelength (λ). The sum of lost contributions due to “scattering” and “absorption” is called “extinction”.

The medium in which both “scattering” and “absorption” processes are present is often called a “turbid” medium. The angular scattering and polarization change, absorption, and extinction are generically called the “optical” properties of aerosols, independently of the wavelength of radiation. These aerosol optical properties are dependent on variations in particle size, shape, and refractive index (Nakajima et al, 1989).

In the propagation of electromagnetic radiation in vacuum, the intensity of radiation does not change. In actual media, (in particular in the atmospheres of planets and on their surface) different complicated processes of interaction of radiation with the medium take place and change its intensity. The main mechanisms of interactions of radiation with the medium are:

i. Extinction
ii. Scattering
iii. Absorption
iv. Reflection
v. Refraction

The generation of radiation by the medium,it should be added to these processes.The interaction of radiation with matter results in attenuation (extinction) of the radiation as a result of the absorption ofradiation by the matter and its scattering to the sides away from the direction of propagation. From the physical viewpoint, the nature of absorption is related to the transition of radiation energy to the internal energy of the atoms and the molecules of atmospheric airand aerosol particles. The scattering of

radiation is associated with the diffraction of electromagnetic waves on aerosol particles and on fluctuations of air density.

If the interaction of radiation with a molecule or particle is not accompanied by any change in the internal energy of the latter, this process is referred to as scattering (simple or elastic scattering). The intensity of interaction of radiation with the molecule depends on the type of internal energy of the molecule with which radiation interacts. If radiation interacts with matter whose internal energy is determined only by translational motion, the appropriate coefficients of interaction are very small under the conditions in the atmospheres of planets. All components of the atmosphere (atoms, molecules, aerosols) have electronic, vibrational, rotational, etc., internal energies.

An illustration of the possible interactions between an incident electromagnetic wave of wavelength $\lambda_o$with a particle is shown in Figure 2.6. Even though Raman scattering and fluorescence occur in atmospheric aerosols, only elastic scattering will be addressed in this thesis, and it will be referred to as „scattering“ . Elastic scattering encompasses the combined effect of reflection, refraction, and diffraction. In elastic scattering, the scattered photons have the same energy (frequency) and wavelength as the incident photons. If absorption of the incident light occurs, the absorbed energy can be re-emitted as thermal energy or fluorescence.

The combined effects of absorption and elastic scattering cause a net loss of energy from an incident light beam of irradiance I_o (in units of W/m^2), and it is referred to as extinction.

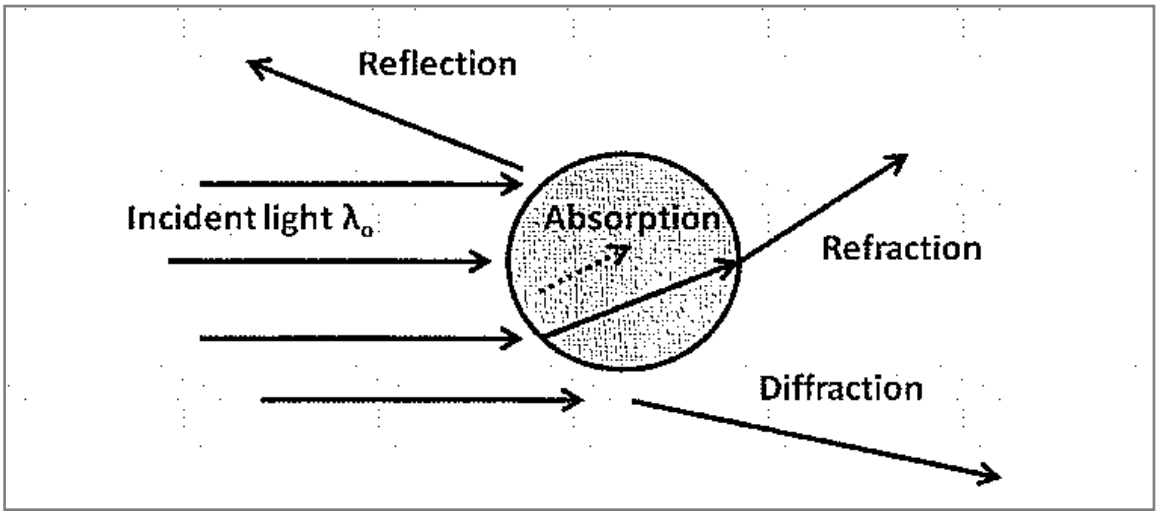

Figure 2. 6 Representation of the possible optical interactions between an incident electromagnetic wave of wavelength λ_o and a particle. Raman scattering and fluorescence are not depicted.

In short, aerosol optical extinction is the sum of the effects of absorption and scattering. The total energy removed (expressed in W/m^2) from an incident beam by a single particle can be expressed as:

$$I_{ext} = I_0 \sigma_{ext} \quad (2.7)$$

where σ_{ext} is the optical extinction cross-section (normally expressed in m^2) and is defined as:

$$\sigma_{ext} = \sigma_{abs} + \sigma_{sca} \quad (2.8)$$

where σ_{abs} and σ_{sca} represent the optical absorption and scattering cross-sections, respectively.

The optical cross-sections are defined as:

$$\sigma_{ext/abs/sca} = \sigma_{ext/abs/sca} \cdot \sigma_{geometric} \quad (2.9)$$

where $\sigma_{geometric}$ is the geometric cross-section, r is the particle radius, and the σ terms are the extinction, absorption, or scattering efficiencies respectively.

For a collection of particles the extinction absorption and scattering coefficients describe the amount of light removed, absorbed, and scattered, respectively. The optical coefficients are expressed as the sums of the individual optical cross-sections of each substance present in a population of particles divided by the total volume (V) filled by this population. For the same type of particles the expression simplifies to the product of the cross-sections by the particle number concentration N.

$$\sigma_{ext/abs/sca} = \sum_{i=1}^{n} \sigma_{ext_i/abs_i/sca_i} = N\sigma_{ext/abs/sca} \quad (2.10)$$

where $N = \rho / V$ and N is the number mix ratio of the aerosols.

The single scattering albedo (SSA) ω for a single particle is defined as the ratio of the scattering cross-section by the extinction cross-section or their corresponding Q terms:

$$\omega = \frac{\sigma_{sca}}{\sigma_{ext}} = \frac{\sigma_{sca}}{\sigma_{sca} + \sigma_{abs}} \quad (2.11)$$

For an ensemble of particles the SSA is defined as the ratio of the scattering coefficient and the extinction coefficient, which, in the same way as the cross-sections equation (2.11).

Hence, the SSA values range between $0 \leq \omega \leq 1$. A value of 1 represents a purely scattering particle (or population), and 0 a purely absorbing one (purely absorbing substances).

All of the optical properties stated above (σ, Q, α, and ω) depend on the wavelength of the incident light, the size of the particle, and the spatial complex refractive index distribution of the surrounding medium. When the material has absorbing properties the refractive index is expressed as a complex number: $n = n' + ik$, where n is the real and k the imaginary part of the refractive index.

The real and imaginary parts express the extent of scattering and absorption, respectively. For most atmospheric particles n' ranges from 1.3 to 2 and k from 0 to 1, depending on the wavelength. The complex refractive index is the only intrinsic optical property of a particle (where size is the intrinsic physical property); therefore, knowing the value of n is of high importance to accurately model the optical properties of aerosols.

Since the interaction of a beam of light of a particular wavelength with particle of a certain size is scale invariant (i.e., micrometer waves interact with micrometer particles in the same way as nanometer waves with nanometer particles), particles sizes are presented as the particle size parameter (x). For spherical particles, the particle size

parameter is given as the ratio of the particles circumference to the wavelength (λ) of the incident light:

$$x = \frac{2\pi r}{\lambda} \quad (2.12)$$

To calculate the various optical properties different theories have been developed depending on the size parameter (x), and the shape of the particle. When particles are "very small" compared to the wavelength (x<<1), it is the Rayleigh regime, and Rayleigh's theory properly models the optical properties.

When particles have approximately the same size as the incident wavelength (x~1), particles are said to be in the Mie regime, and Mie Theory is used. And if the particles have a much larger diameter than the wavelength (x>>1), the particles are said to be in the geometrical optics regime and classical laws of reflection, refraction, and diffraction can be used for the description of the optical properties.

Mie theory can be used to calculate the exact angular redistribution (i.e. the phase function) and absorption of light for any spherical particle at any wavelength if x and m are known, as it is a complete analytical solution of Maxwell's equations for the interaction of infinite electromagnetic plane waves with homogeneous, linear, isotropic, spherical particles.

A detailed mathematical description of Mie theory is provided by Bohren and Hoffman, (Bohren and Hoffman 1983). Even though Mie theory provides solutions for homogeneous spherical particles, it is regularly used for all atmospheric aerosols, regardless of their shape.Since many atmospheric aerosols have, or are close to having,

spherical shapes, they yield reasonable approximations. Furthermore, Mie theory has been extended to coated (core-shell) particles, spheroids, and some approximations of sphere aggregates etc.

2.10.2 Electric Polarization

When a solid is placed in an externally applied electric field, the medium will adapt to this perturbation by dynamically changing the positions of the nuclei and the electrons. We will only consider time-varying fields of optical frequencies. At such high frequencies, the motion of the nuclei is not only effectively independent of the motion of the electrons, but also far from resonance. Therefore, we can assume the lattice rigid.

The reaction of the system to the external field consists of electric currents flowing through the system. These currents generate electromagnetic fields by themselves, and thus the motion of all constituent particles in the system is coupled. The response of the system should therefore be considered as a collective phenomenon. The electrical currents now determine in what way the externally applied electric field is screened. The induced fieldresulting from these induced currents tends to oppose the externally applied field, effectively reducing the perturbing field inside the solid. In metals the moving electrons are able to flow over very large distances, so they are able to completely screen any static (externally applied) electric field to which the system is exposed. For fields varying in time, however, this screening can only be partial due to the inertia of the electrons.

Ininsulators this screening is also restricted since in these materials the electronic charge is bound to the nuclei and cannot flow over such large distances. The charge density then merely changes by polarization of the aerosols.

Tropospheric aerosols are thought to cause a significant direct and indirect climate forcing, but the magnitude of this forcing remains highly uncertain because of poor knowledge of global aerosol characteristics and temporal changes(Hansen, and Lacis 1988). Microphotographs of naturally occurring dust-like aerosols show highly variable shapes and great variability of the particle aspect ratio (ratio of the largestto the smallest particle dimensions), and laboratory and in situ measurements for natural sand and dust particles show that in mostcase, phase function is relatively smooth and featureless, especially at side-scattering angles (Nakajima and Tanaka, 1982) . However, any particle shape, either spherical or nonspherical, produces its own shape-specific scattering pattern.

On the other hand,to retrieve the aerosol properties, such as optical thickness and effective radius, single scattering albedo, etc, most current and proposed satellite remote sensing of tropospheric aerosols relies upon radiance measurement that are interpreted using algorithms that determine the best fitting to precalculated scattered sunlight for one or more "standard" aerosol models, but this can pose a severe uniqueness problems (Mishchenko, and Travis, 1997). Experience and theory have demonstrated that the measurements of polarization as well as the radiance can resolve such a uniqueness problem (Mishchenko, and Travis, 1997). Moreover, measurements of the linear and circular depolarization ratios at the backscattering direction are also a powerful remote sensing technique for characterizing the microphysics of nonspherical

aerosol particles, and for spherical particles both ratios are equal to zero. On theother hand, for nonspherical scatterers, both the linear and circular depolarization ratios can substantially deviate from zero, thus can be considered the indicators of particle nonsphericity (Chiang, et al, 2008. Cloude, 2009).

In 1852, Sir George Gabriel Stokes showed that any state of polarized light could be described completely by reference to four physically observable characteristics, known as the Stokes parameters (Stokes, 1852). The first parameter I describes the total intensity, Q and U the linear polarization, and V the circular polarization of a light beam (van de Hulst, 1969). Stokes also proved that these parameters could not only describe unpolarized light, but also partially polarized and completely polarized light.

Thus,The polarization state of a beam of light is traditionally described by a vector

$I = (I, Q, U, V)^T$ composed of four Stokes parameters (Tmeans transpose) (Van De Hulst, 1969; Li, et al 2001; Kotsis and Roumeliotis, 2007. Li, et al; 2008. Wang and Li,, 2009). The scattering of light by a particle can be described by a 4×4 scattering matrix.

The scattering matrix is a function of the directions of light incidence and scattering and transforms the Stokes parameters I_0, Q_0, U_0, V_0 of the incidence light into those of the scattered light (Zheng and Kobayashi,, 2008).

$$I^{sca} = FI^{inc} \qquad (2.13)$$

Where I^{sca} and I^{inc} are the scattered and incident Stokes parameters, respectively. Electromagnetic scattering most typically produces light with polarization

characteristics different from those of the incidence beam.If the incident beam is unpolarized, the scattered light generally has at least one nonzero Stokes parameter other than intensity, and this phenomenon is often called polarization. When the incident beam is fully linearly (I =Q, U=V = 0) or circularly (I = V, Q=U= 0) polarized, the scattered light may become partially polarized or even totally unpolarized, and this phenomenon is called depolarization (Yalcin, 2009).

Consider single scattering by a small-volume element composed of a collection of sparsely distributed, independently scattering particles. If the particles comprising the small-volume element are randomly oriented and have a plane of symmetry, the scattering matrix has the well-known simplified block-diagonal structure.

$$F(\varphi)=\begin{pmatrix} F_{11} & F_{12} & 0 & 0 \\ F_{21} & F_{22} & 0 & 0 \\ 0 & 0 & F_{33} & F_{34} \\ 0 & 0 & -F_{43} & F_{44} \end{pmatrix} \quad (2.14)$$

and it has only six independent elements. So, the Stokes vector of the scattered light is given by

$$F(\varphi)=\begin{bmatrix} F_{11}I^{inc}+F_{12}Q^{inc} \\ F_{21}I^{inc}+F_{22}Q^{inc} \\ F_{33}U^{inc}+F_{34}V^{inc} \\ F_{34}U^{inc}+F_{44}V^{inc} \end{bmatrix} \quad (2.15)$$

From (2.15), even if the incident beam is unpolarized, i.e., I^{inc} = (I, 0, 0, 0)^T the scattered beam has a nonzero Stokes parameter, unless the (1, 2) element of the scattering matrix is equal to zero.

2.11 Lorentz – Lorentz model

The classical Lorentz model of dielectric dispersion due to polarization is of fundamental importance in the study of aerosol science as it provides a physically appealing, accurate description of both normal and anomalous dispersion phenomena in the extended aerosol and optical region of the electromagnetic spectrum from the far infrared up to the near ultraviolet (Yangang and Peter, 2008). Of equal importance is the Lorentz-Lorenz relation which, as stated in Born and Wolf (Born and Wolf, 2005) "connects Maxwell's phenomenological theory with the atomistic theory of matter." It is typically assumed that, the number density of molecules is sufficiently small so that the Lorentz-Lorenz formula can be simplified to a simple linear relationship between the mean molecular polarizability and the dielectric permittivity. Although the influence of the Lorentz-Lorenz formula on the resulting frequency dispersion can be striking when the number density becomes sufficiently large, the fundamental frequency structure is not altered from that described by the Lorentz model alone; a frequency band of anomalous dispersion with high absorption surrounded by lower and higher frequency regions exhibiting normal dispersion with small absorption. The fact that the Lorentz model is a strong and powerful instrument in the correlating the polarizabilityand refractive indices of aerosols.

The purpose of this research is to establish accurate computational techniques for determination of polarizabilities forseveral aerosol components.

2.12 Complex Index of Refractionand Lorentz–Lorenz Formula

Within a dielectric, positive and negative charges are impelled to move in opposite

directions by an applied electric field. As a result, electric dipoles are generated. The product of charges and the separation distance of positive and negative charges is called the dipole moment, which, when divided by the unit volume, is referred to as polarization $\vec{P}$. The displacement vector $\mu \square \mu_0$ (charge per area) within a dielectric is defined by (Liou, 2002).

$$\vec{D} = \varepsilon \vec{E} = \vec{E} + 4\pi \vec{P} \qquad (2.16)$$

where ε is the complex permittivity of the medium. Thus,

The velocity of light in terms of ε and the permeability μ is given by

$$c = \frac{1}{\sqrt{\mu_0 \varepsilon_0}} \qquad (2.17)$$

The permeability μ in air or water is nearly equal to the permeability μ_0 in vacuum, in amedium is not a vacuumthe speed of light is given by $v = \frac{1}{\sqrt{\mu\varepsilon}}$

But $\mu\varepsilon = \varepsilon_0 \varepsilon_r \mu_0 \mu_r$, therefore, $v = \frac{1}{\sqrt{\varepsilon_0 \varepsilon_r \mu_0 \mu_r}} = \frac{1}{\sqrt{\varepsilon_0 \mu_0}} \frac{1}{\sqrt{\varepsilon_r \mu_r}} = \frac{c}{\sqrt{\varepsilon_r \mu_r}}$

That is $\mu \square \mu_0$, The index of refraction n is defined as the ratio of the velocity of light invacuum to that in the medium and may be expressed by (Liou, 2002).

$$n = \frac{c_0}{c} \square \sqrt{\varepsilon} \qquad (2.18)$$

The expression $n = \sqrt{\varepsilon}$ is called the Maxwell relationship for complex refractive index and its permittivity.

The Lorentz force acting on a bound electron in a material depends upon the local or effective electromagnetic field present at that molecular site. The effective electric field E_{eff} acting on an aerosol or molecule at space-time position in a polarizable medium with polarization **P** is given by

$$\vec{E}_{eff} = \vec{E} + \frac{4\pi}{3}\vec{p} \quad (2.19a)$$

Consider aerosol as a system of molecules that react to an incident electric field like electric dipoles. From the microscopic perspective, when a piece of dielectric is placed in an applied electric field, the electric polarization p (average electric dipole moment per unit volume) is given by:

$$\vec{p} = \rho\alpha\varepsilon_0\vec{E}_{loc} \quad (2.119b)$$

Where ρ is the number density of the material molecules, α is the mean molecular polarizability, ε_0 is the vacuum permittivity, and $\vec{E}_{loc}$ is the local electric field experienced by an individual molecule. From the macroscopic perspective, the electric polarization is related to the applied electric field $\vec{E}$ by

$$\vec{p} = (\varepsilon - 1)\varepsilon_0\vec{E} \quad (2.19c)$$

where ε is the complex dielectric constant (also called complex relative permittivity) of the material. Combining Equations. (2.19b) and (2.19c) yields;

$$\varepsilon = 1 + \alpha\rho \frac{\vec{E}_{loc}}{\vec{E}} \quad (2.19d)$$

Elimination of $\mathbf{E}_{loc}$ and $\mathbf{E}$ using the Lorentz expression for the local electric field

$$\vec{E}_{loc} = \vec{E} + \frac{\vec{p}}{3\varepsilon_0} = \frac{1}{3}(\varepsilon + 2)\vec{E} \quad (2.20)$$

Gives the Clausius–Mossotti relation

$$\frac{(\varepsilon - 1)}{(\varepsilon + 2)} = \frac{\rho\alpha}{3} \qquad (2.21)$$

Applying the Maxwell relation $\varepsilon = n^2$ in to the equation (2.21) gives the well known Lorentz - Lorentz relation for the refractive index (n).

$$\frac{(n^2 - 1)}{(n^2 + 2)} = \frac{\rho\alpha}{3} \quad (2.22)$$

This implies

$$\alpha = \frac{3}{4\pi N} \frac{(n^2 - 1)}{(n^2 + 2)} \qquad (2.23)$$

2.13Basic principles for mixing rules: Dielectric mixing rules of Aerosols components

This section will provide theoretical background for understanding and prediction of macroscopic dielectric properties of aerosols component. Optical properties of aerosol components are not of direct practical use, since aerosol particles in the atmosphere

always exist as mixtures of several components. In this research, they are handled in that way with the possibility to combine them as mixed components so that, the optical properties could be accurately handled.

To reproduce an exact electromagnetic descriptionfor the structural complexity of aerosol component is of course impossible. Mixing rulesare an attempt to perform this task approximately. The approach in analytical mixing formulasis to idealize to the geometry and model the microstructure using simple forms, like spheres andellipsoids. It is encouraging that, quite often, this turns out to lead to mixing rules that approximatethe real world to such an extent that the mixing predictions can be used in practical computational study of polarizability of ambient aerosol.

Dielectric mixing rules are algebraic formulas with which the effective permittivity of the mixture can be calculated as a function of the constituent permittivity, their fractional volumes, andpossibly some other parameters characterizing the microstructure of the mixture. The concept of effective, or macroscopic permittivity, implies that the mixture responds to electromagnetic excitation as if it werehomogeneous. It may, however, be proper to remind that the dielectric constant (which term isoften used synonymously with permittivity) of a material very seldom is constant with respect totemperature, frequency, or any material property.This view to the homogenization of heterogeneous media is obviously not exact because byusing electromagnetic waves of higher and higher frequency one can always “see” more accuratelyinto the medium and probe its structural details. Therefore, a quantity such as effective permittivityis only meaningful in the longwavelength limit. This limit corresponds to low frequencies andindeed, the mixing rules are very often derived

using static or quasi-static arguments. The size ofthe aerosols in the mixture and the spatial correlation length of the permittivity function need tobe small with respect to the wavelengths.

The effective permittivity can be complex, " $\varepsilon_{eff} = \varepsilon'_{eff} + \varepsilon''_{eff}$, where the real and imaginary parts are certain averages of the real and imaginary parts of the components materials. To some extent, the validity of the effective permittivity can be generalized to include the first-order scattering effects of the aerosols. because scattering entails losses, its effect gives a contribution to the imaginary part of the effective permittivity, which can be estimated by calculating the energy that the electric dipoles radiate which are induced within the inhomogeneities of the mixture.

When an aerosol that is exposed to an electromagnetic field is small it can be safely assumed that its momentary internal field is the same as in the problem with a static excitation. The aerosols creates a perturbation to the field which to the lowest order is that of an electric dipole. The polarizability of the aerosols can be enumerated by solving the Laplace equation for the field inside the scatterer, in other words neglecting the dynamic wave processes altogether.

It is not easy to give an exact upper frequency limit for the validity of the concept of effective permittivity. However, the following rule of thumb is often used: the size of an inclusion in the mixture must not exceed a tenth of the wavelength in the effective medium.

2.14Polarizability of particles

The polarizability of an aerosol is a measure to its response to an incident electric field. In general, the polarizability of a particle α is the relation between the dipole moment **p** that is induced in the particle by the polarization, and the external electric field $\mathbf{E}_e$.related by (Sun et al, 2010).

$$\vec{p} = \alpha \vec{E}_e \qquad (2.24)$$

For a sphere the polarizability is easy to calculate. It is proportional to the internal field within the aerosol or mixture, its volume, and the dielectric contrast between the aerosol and the environment. Since the electric field $\mathbf{E}_i$ induced in a sphere in a uniform and static external field $\mathbf{E_e}$ is also uniform, static, and parallel to the external field

$$\vec{E}_i = \frac{\varepsilon_e}{\varepsilon_i + 2\varepsilon_e} \vec{E}_e \quad (2.25)$$

The polarizability α can be written as:

$$\alpha = V(\varepsilon_i - \varepsilon_e) \frac{3\varepsilon_e}{\varepsilon_i + 2\varepsilon_e} \quad (2.26)$$

where the permittivity of the aerosol and its environment are denoted by ε_i *and* ε_c respectively, and the volume of the aerosol is V .

2.15Clausius–Mossotti relation

From the polarizability of a single sphere, the effective permittivity of a mixture can be calculatedas a function of the number density of the spheres in the background medium

with permittivity "ε_e.

The effective permittivity is the relation between the external field and the average electric fluxdensity $<\Phi>$:

$$<\Phi>=\varepsilon_{eff}\vec{E}_e \quad (2.27)$$

where the average polarization $<P>$ is connected to the dipole moment density in the mixture:

$$<\vec{P}>=n\vec{p} \quad (2.28)$$

and here n is the number density of dipole moments **p** in the mixture. In a mixture of aerosols, especially when it is dense, one cannot assume the field exciting one component tobe the external field $\mathbf{E_e}$. The surrounding polarization increases the field effect and has to be taken into account (Mossotti, 1850, Sihvola, 1999; Sihvola, , 1991). The field that excites one aerosol $\mathbf{E_L}$ is often called as the local field or Lorentzian field. It is dependent on the shape of the aerosol and for a sphere it is given by equation (2.20).

where the coefficient $\frac{1}{3}$ corresponds to the depolarization factor of the sphere. Combining this equation with $p = \alpha\vec{E}_e$ gives us the average polarization, and then the effective permittivity can be written:

$$\varepsilon_{eff} = \varepsilon_e + \frac{n\alpha}{1-\frac{n\alpha}{3\varepsilon_e}} = \frac{n\alpha}{3\varepsilon_e} \quad (2.30)$$

Rearranging equation(2.30), we have:

$$\frac{\varepsilon_{eff} - \varepsilon_e}{\varepsilon_{eff} + 2\varepsilon_e} = \frac{n\alpha}{3\varepsilon_e} \qquad (2.31)$$

This relation is known as Clausius–Mossotti formula, although it deserves the label Lorenz– Lorentz formula as well.

$$\varepsilon_{eff} \approx \varepsilon_e + n\alpha \quad (2.32)$$

In practical applications, quantities like polarizabilities and scatterer densities are not alwaysthose most convenient to use. Rather, one prefers to play with the permittivities of the componentsof the mixture. When this is the case, it is advantageous to combine Clausius–Mossotti formulawith the polarizability expression (2.26). Then we can write

$$\frac{\varepsilon_{eff} - \varepsilon_e}{\varepsilon_{eff} + 2\varepsilon_e} = f\,\frac{\varepsilon_i - \varepsilon_e}{\varepsilon_i + 2\varepsilon_e} \qquad (2.33)$$

where $f = nV$ (2.34)

is a dimensionless quantity, the volume fraction of the ith aerosol in the mixture.This formula is called Rayleigh mixing formula (Sihvola, 1991).

2.16 Common Mixing Rules For Aerosol Particles

2.16.1 Effective Medium Theory Mixing Rule

Ambient aerosol particles are generally mixtures of different chemical constituents. A common approach to treating such inhomogeneous mixtures is the so-called effective

medium theory where by a mixture is considered a homogeneous material with the effective quantities that are calculated from some mixing rules (Heller, 1965; Ossenkopf, 1991).

2.16.2 Volume and polarizability additivity

Volume additivity states that the total mass of the mixture equals to the sum of all the components:

$$V = \sum_{I} f_i V_i \quad (2.35)$$

Dividing Equation (2.35) by (2.36) yields the volume mixing rule to calculate the effective mass density

$$\rho_{me} = \frac{m}{V} = \frac{\sum_i V_i \rho_{m_i}}{V} = \sum_{I} f_i \rho_{mi} \quad (2.36)$$

where f_i is the volume mixratio.

Polarizability additivity states that the total of polarizability of a mixture equals to the sum of themolecular polarizability of each component:

$$P = N\alpha_e = \sum_i N_i \alpha_i \quad (2.60)$$

There fore,

$$\alpha_e = \sum_i \frac{N_i}{N} \alpha_i \quad (2.61)$$

Where $\frac{N_i}{N}$ is the number mix ratio.

2.17 Concept of Radiative Forcing (RF)

The Earth receives a continuous influx of energy from the Sun. Some of this energy is absorbed at the Earth's surface or by the atmosphere, while some is reflected back to space. At the same time, the Earth and its atmosphere emit energy to space, resulting in an approximate balance between energy received and energy lost. Knowledge of the natural and anthropogenic processes that affect this energy balance is critical for understanding how Earth's climate has changed in the past and will change in the future, IPCC (2007).

Climate change is driven by perturbations to the energy balance of the Earth system. These perturbations are called "climate forcings" and have been the subject of considerable scientific inquiry both for understanding Earth's history and for projecting future change.

Radiative forcing is a way to quantify an energy imbalance imposed on the climate system either externally (e.g., solar energy output or volcanic emissions) or by human activities (e.g., deliberate land modification or emissions of greenhouse gases, aerosols, and their precursors). The concept of radiative forcing has been central for guiding climate research and policy over the past two decades.

New studies on climate forcing agents not conventionally considered have, however, raised doubts as to the continued viability of the Radiative forcing concept. For example, the

climatic effects from light absorbing aerosols and land use changes do not lend themselves to quantification using the traditional Radiative forcing concept.

Polarizability effects due to Aerosol on clouds are difficult to describe in terms of simple Radiative forcing. These challenges have raised the question of whether the Radiative forcing concept has outlived its usefulness and, if so, what new climate change metrics should be used? In this research, we will examine the impacts of how the energy balance regulating Earth's climate is modified by "forcings" of aerosols due to polarizability.

Factors that drive climate change are usefully separated into forcings and feedbacks (Figure 2.7). A climate forcing is an energy imbalance imposed on the climate system either externally or by human activities. Examples include changes in solar energy output, volcanic emissions, deliberate land modification, or anthropogenic emissions of greenhouse gases, aerosols and their precursors.

A climate feedback is an internal climate process that amplifies or dampens the climate response to a specific forcing. An example is the increase in atmospheric water vapor that is triggered by an initial warming due to rising carbon dioxide (CO_2) concentrations, which then acts to amplify the warming through the greenhouse properties of water vapor. Climate forcings are usefully subdivided into direct radiative forcings, indirect radiative forcings, and non radiative forcings.

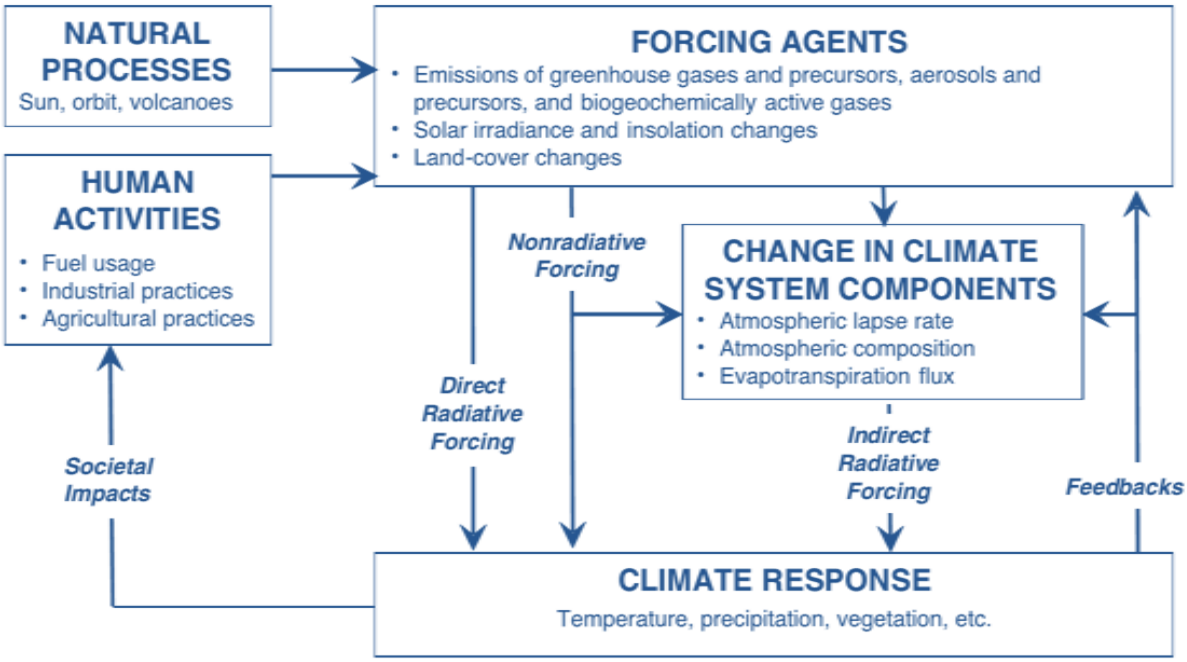

Figure 2. 7Conceptual framework of climate forcing, response, and feedbacks under present day climate conditions. Examples of human activities, forcing agents, climate system components, and variables that can be involved in climate response are provided in the lists in each box. (IPCC (2007).

2.17.1 Direct radiative forcings:Directly affect the radiative budget of the Earth; for example, added CO_2 absorbs and emits infrared (IR) radiation.

2.17.2 Indirect radiative forcings:Create an energy imbalance by first altering climate system components (e.g., precipitation efficiency of clouds), which then lead to changes in radiative fluxes; an example is the effect of solar variability on stratospheric ozone.

2.17.3 Non radiative forcings:Create an energy imbalance that does not directly involve radiation; an example is the increasing evapotranspiration flux resulting from agricultural irrigation.

Studies of long term changes in climate have emphasized global mean surface temperature as the primary index for climate change. The concept of "radiative forcing" provides a way to quantify and compare the contributions of different agents that affect surface temperature.

2.18Expanding the radiative forcing concept

Radiative forcing traditionally has been defined as the instantaneous change in energy flux at the tropopause resulting from a change in a component external to the climate system. The radiative forcing concept has been used extensively in the climate research literature over the past few decades and has also become a standard tool for policy analysis endorsed by the Intergovernmental Panel on Climate Change.

Despite all these advantages, the traditional global mean (TOA) radiative forcing concept has some important limitations, which have come increasingly to light over the past decade. The concept is inadequate for some forcing agents, such as absorbing aerosols, polarizabilities and land use changes, that may have regional climate impacts much greater than would be predicted from TOA radiative forcing. Also, it diagnoses only one measure of climate change global mean surface temperature response while offering little information on regional climate change or precipitation. These limitations can be addressed by expanding the radiative forcing concept and through the introduction of additional forcing metrics. In particular, the concept needs to be extended to account for the effect of: polarizabilities due to absorbing aerosols.

2.19Better quantify the direct radiative effects of Aerosols

Aerosols have direct radiative effects in that they scatter and absorb both shortwave and long wave radiations. Knowledge of direct radiative forcing of aerosols is limited to a large extent by uncertainty about the global distributions and mixing states of aerosols. Mixing states have major implications on aerosol optical properties that are not well understood and are difficult to parameterize in climate models. Small scale variability of humidity and temperature, which has a major impact on aerosol optical properties, is also difficult to represent in models. Mechanisms of aerosol production are not understood, so the effects of future changes in emissions and climate are highly uncertain. Removal of aerosols from the atmosphere occurs mainly by wet deposition, but model parameterizations of this process are highly uncertain and rudimentary in their coupling to the hydrological cycle.

Radiative forcing is used to :

2.19.1 Improve understanding and parameterizations of aerosol cloud thermodynamic interactionsand land-atmosphere interactions in climate models in order to quantify the impacts of these nonradiative forcings on both regional and global scales.

2.19.2 Develop improved land-use and land-cover classifications at high resolution for the past and present, as well as scenarios for the future.

2.19.3 Encourage policy analysts and integrated assessment modelers to move beyond simple climate models based entirely on global mean radiative forcing and

incorporate new global and regional radiative and nonradiative forcing metrics as they become available.

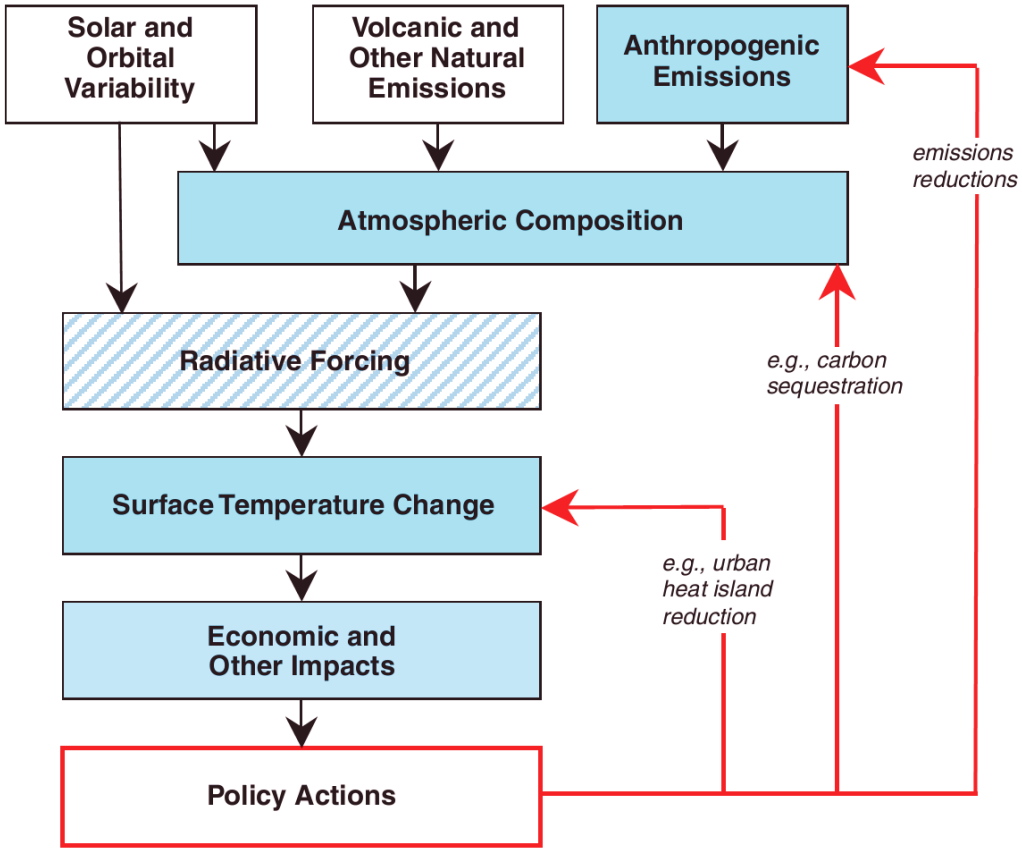

Figure 2. 8 Conceptual policy framework for how radiative forcing fits into the climate IPCC (2007).

Radiative forcing is thus one of the more highly quantified methods of determining how the climate system is forced.

This research will adequately describe fully the radiative effects of several anthropogenic influences including:

2.19.3.1,Absorbing aerosols, which lead to a positive radiative forcing of the troposphere with little net radiative effect at the top of the atmosphere;

2.19.3.2, Effects of aerosols on cloud properties (including cloud fraction, cloud microphysical parameters, and precipitation efficiency), which may modify the hydrological cycle without significant radiative impacts;

2.19.3.3, Surface modification due to deforestation, urbanization, and agricultural practices and surface biogeochemical effects.

Land surface modification of heat fluxes and aerosol induced changes to the precipitation efficiency modify not only the radiative fluxes but also the dynamical (turbulent heat flux) and thermodynamical fluxes (evaporation). These modifications to the climate system fall under the broader umbrella of climate forcings, which include radiative and nonradiative fluxes. Broadening the concept of radiative forcing in this way allows consideration of climate variables that may have more direct societal impacts, such as changes in precipitation.

Indeed, the computational radiative forcing concept is appropriate to predict the sign or the magnitude of the global mean precipitation changes due to both scattering and absorbing aerosols, which affect precipitation differently in summer and winter.

CHAPTER THREE

METHODOLOGY AND COMPUTATIONAL TECHNIQUES

3.1 The software package (OPAC)

The software package OPAC is intended to serve as a tool to scientists who need to describe the optical properties of the atmosphere for climate-modeling purposes, which assumes that theparticles are spherical and homogeneous. It therefore consists of datasets of optical properties of cloud and aerosol components that describe average conditions in combination with easy to use software, which allows calculation of any mixtures of these components. Since real aerosol in the atmosphere always is a mixture of different components. Thus, in OPAC it is made possible to get optical properties of any mixtures of the basic components and to calculate optical depths on the base of exponential aerosol height profiles.

OPAC consists of two parts. The first part is a dataset of microphysical properties and the resulting optical properties of cloud and aerosol components at different wavelengths and for different humidity conditions. The other part is a FORTRAN program that allows the user to extract data from this dataset, to calculate additional optical properties, and to calculate optical properties of mixtures of the stored clouds and aerosol components. The

radiative properties in OPAC are modeled on the basis of components of aerosols and clouds, from which weighted sums of these data are used to describe radiative properties of the total amount of aerosol particles, water droplets, and ice crystals in the atmosphere. Each component is described by an individual particle size distribution and spectral refractive index. The refractive index of humid aerosols changes as the dry particulate matter is mixed with water.The software package OPAC is freely available on the http://www.meteo.physik.unimuenchen.de/strahlung/aerosol/aerosol.html(Hess et al, 1998).

3.2 Methodology

The aerosols model extracted from the (OPAC). The dataset extracted give the microphysical properties for six types of aerosol model. These constituted 20 components of the atmospheric aerosols.The Six aerosol models are chosen in this research to span the range of climatologically important aerosols. They are given both to represent average conditions and also to consider extreme conditions for sensitivity studies. The aerosol types and the component that composed them are specify in Table 3.1

In this research, they are handled in that way with the possibility to combine them as much as we like. The components can be mixed and thus the optical properties for an atmospheric layer can be calculated.

The model are available at 61 wavelengths between 0.25 and 40 µm. The data are given in each case for 1 particle cm^{-3}, which describes the effective properties of the mixture of all particles in the size distribution.For practical use, In the case of those

aerosol components that are able to take up water, the models are treated for eight values of relative humidity (0%, 50%, 70%, 80%, 90%, 95%, 98%, 99%) .

Table 3.1(a) Composition of aerosol types components and concentration at 50% relative Humidities (Hess et al, 1998).

S/N	Aerosol Model	TotalComponent	Concentration N_i (cm^{-3})
1	Continental Clean	water soluble (WASO)	2600
		insoluble (INSO)	0.15
2	Antarctic	sea salt accumulate(SSAM)	0.0047
		mineral tropical (MITR)	0.0053
		sulfate(SUSO)	42.9
3	Arctic	insoluble (INSO)	0.01
		water soluble (WASO)	1300
		soot (SOOT)	1.9
		sea salt accumulate (SSAM)	5300
4	Maritime tropical	water soluble (WASO)	590
		sea salt accumulate (SSAM)	10
		sea salt coarse (SSCM)	0.00013
5	Desert	water soluble (WASO)	2000
		mineral nucleation (MINM)	269.5
		mineral accumulate (MIAC)	30.5
		mineral coarse (MICM)	0.142
6	Urban	insoluble (INSO)	1.5
		water soluble (WASO)	28000
		soot (SOOT)	130000

Table 3.1(b) Composition of aerosols components and mixing at 00% relative humidities.

Aerosol model	Aerosol Comp	NUMBER [1/cm^3]	VOLUME []	MASS [ug/m^3]	DENSITY [g/cm^3]	NUM.MIX RATIO	VOL.MIX RATIO	MASS.MIX RATIO
	INSO	1.00E-02	1.19E+05	2.37E-01	2.0	1.52E-06	5.66E-02	6.21E-02
	WASO	1.30E+03	9.69E+05	1.74E+00	1.8	1.97E-01	4.62E-01	4.56E-01
	SOOT	5.30E+03	3.17E+05	3.17E-01	1.0	8.03E-01	1.51E-01	8.30E-02
ARCTIC	SSAM	1.90E+00	6.92E+05	1.52E+00	2.2	2.88E-04	3.30E-01	3.99E-01
	SSAM	4.70E-02	1.71E+04	3.77E-02	2.2	1.09E-03	2.74E-02	3.42E-02
	MITR	5.30E-03	3.24E+04	8.42E-02	2.6	1.23E-04	5.18E-02	7.65E-02
ANTARTIC	SUSO	4.29E+01	5.76E+05	9.79E-01	1.7	9.99E-01	9.21E-01	8.89E-01
	WASO	2.00E+03	1.49E+06	2.68E+00	1.8	8.70E-01	1.71E-02	1.19E-02
	MINM	2.70E+02	2.88E+06	7.49E+00	2.6	1.17E-01	3.31E-02	3.33E-02
	MIAM	3.05E+01	6.49E+07	1.69E+02	2.6	1.33E-02	7.47E-01	7.51E-01
SAHARA	MICM	1.42E-01	1.77E+07	4.60E+01	2.6	6.17E-05	2.03E-01	2.04E-01
	INSO	1.50E-01	1.78E+06	3.56E+00	2	5.77E-05	4.79E-01	5.05E-01
CC	WASO	2.60E+03	1.94E+06	3.49E+00	1.80	1.00E+00	5.21E-01	4.95E-01
	WASO	1.50E+03	1.12E+06	2.01E+00	1.80	9.87E-01	1.28E-01	1.07E-01
MARITIME	SSAM	2.00E+01	7.29E+06	1.60E+01	2.20	1.32E-02	8.35E-01	8.55E-01
TROP	SSCM	3.20E-03	3.26E+05	7.18E-01	2.20	2.11E-06	3.74E-02	3.82E-02
URBAN	INSO	1.50E+00	1.78E+07	3.56E+01	2.00	9.49E-06	3.83E-01	4.40E-01
	WASO	2.80E+04	2.09E+07	3.76E+01	1.8	1.77E-01	4.49E-01	4.64E-01
	SOOT	1.30E+05	7.78E+06	7.78E+00	1	8.23E-01	1.68E-01	9.61E-02

3.3Description of the Aerosols components

3.3.1 The water-insoluble (INSO) : Component, consisting mainly of soil particles with a certain amount of organic substances.

3.3.2 The water-soluble (WASO) : Component that mainly originates from gas-to-particle conversion and consists of various kinds of sulfates (of anthropogenic origin, with mass density equal to only about half that of the water-soluble component), nitrates, and other (mainly organic) substances mixed together, for which the optical effects of the dimethyl sulfide-related aerosol forming in the oceanic regions were also modeled.

3.3.3 The soot (SOOT): Component, mainly containing black carbon (BC), which strongly absorbs the solar radiation and is assumed to be insoluble. Several assumptions were made in defining this component:

3.3.3.1 The particles do not grow with increasing RH;

3.3.3.2 The density of soot is equal to 1 g cm^{-3}, because the soot particles sampled on filters and used to determine aerosol weight per air volume are in general fluffy particles with space inside;

3.3.3.3 The optical propertieswere evaluated by neglecting the chainlike character of these particles, while the size distribution contains a significant amount of very small particles, with particulate matter density $\rho=2.3 g cm^{-3}$; and no coagulation of soluble aerosol and soot was considered in the formation of the soot particle component.

3.3.4The two Sea-Salt particles(accumulate and coarse): Components, both consisting of various kinds of salt contained in sea-water, and presenting the first a sea-salt accumulation particle mode (SSAM), and the second a sea-salt coarse particle mode (SSCM), as originated by different wind-speed dependent effects on the particle number density in the various size ranges (Koepke et al. 1997).

3.3.5 The three mineral Aerosols(nucleation, accumulation, coarse): Components, consisting of mixtures of quartz and clay minerals and modeled using three different monomodal curves for the nucleation (MNM), accumulation (MAM) and coarse

(MCM) particle components, which present relative amounts of large particles varying with the atmospheric turbidity conditions.

3.3.6 The mineral Particle (MTR) : Component of desert origin, used to describe the properties of desert dust transported over long distances, and consisting mainly of (i) mineral aerosol particles not growing with increasing RH, and (ii) a reduced amount of large particles.

3.3.7 The Sulphate (SDR): Component, consisting of 75% H_2SO_4 and used to describe the sulfate particles found in the Antarctic aerosol and in the stratospheric background aerosol layers consisting mainly of sulphuric acid droplets.

3.4Descriptions of the Aerosols models

The six OPAC aerosol models chosen were determined using the above 10 aerosol components. Their optical composition and microphysical characteristics, and assuming the presence of soot particles (SOOT) in the polluted aerosol models only:

3.4.1The Continental clean (CC): aerosol model represents the aerosol polydispersion monitored in remote continental areas, with very low anthropogenic influences and, consequently, a very low mass concentration of soot substances ($<0.1 \mu gm^{-3}$). The composition assumed inTable 3.1(a) does not contain soot substances thus constituting a lower benchmark with respect to absorption in the solar spectral range.

3.4.2 The Urban (UR): Aerosol model represents cases of strong pollution in urban areas, with the soot mass concentration assumed to be relatively high ($\sim 7.8\ \mu gm^{-3}$)

and the mass concentrations of both water soluble and insoluble substances about twice those assumed in the continental polluted aerosol, as it was often found in aerosol samples collected in central urban areas.

3.4.3 The Desert (DE): aerosol model is used to describe aerosol suspended over the desert areas of the world, consisting of the mineral aerosol components in a combination that is representative for average atmospheric turbidity conditions, together with a certain mass fraction of the water-soluble (WASO) component.

3.4.4 The Maritime tropical (MT): aerosol model was assumed to have a very low mass concentration of water-soluble (WASO) substances and was defined for a lower wind speed ($5ms^{-1}$) than those assumed in the previous two models and, hence, a lower number concentration of sea-salt particles.

3.4.5 The Arctic (AR): aerosol model represents the airborne particles found in the Arctic region at latitudes higher than 70^0N, and describes atmospheric turbidity conditions characterized by the presence of a relatively high amount of soot (SOOT) particles transported from the mid-latitude continental areas to the Arctic. This model is therefore particularly suitable for representing the aerosol characteristics during springtime, while it is less appropriate for representing the Arctic aerosol radiative properties during the other seasons, when single scattering albedo was found to range on average between about 0.93 and 0.95 (Tomasi et al., 2012).

3.4.6 The Antarctic (AN): Aerosol model represents the airborne particles found over the Antarctic continent, and consists mostly of sulfate droplets, containing also lower concentrations of mineral and sea-salt particles (typical of the coastal sites) and rather

high number concentrations of nss sulfate aerosols (typical of the inner region), these composition features being valid especially for summer conditions, when average values of ω of around 0.96–0.98 were found (Tomasi et al., 2012).

In this research, we presentnew efficient and flexible computational approaches that provides accurate and relatively easy technique for calculating the linear polarizabilities of ambient aerosols using Lorentz – Lorentz relation.This technique for the calculation of the polarizability can be applied to many systems. e.g., for atoms, ionic solids, metal spheres and metal surfaces.

3.5 Relative Humidity (RH)

More commonly we find the water vapor content expressed as relative humidity, which is the ratio of the amount of water relative to its saturation value, at the temperature under consideration. It is usually expressed as a percentage. When the relative humidity becomes so large that particles absorb water their size will increase drastically and so will the scattering especially for water soluble aerosols or compounds like sulfates and nitrates. The number of particles in Urban air is typically highest in the morning and afternoon, not only be-cause of rush hours, but also because of a low lying mixing layer. At the same time, the humidity may be high.

With increasing Relative Humidity values, atmospheric water vapor condenses onto the particles and alters their size and refractive index. This may be applied to hygroscopic particles such as water- soluble or sea-salt components, but makes no significant contribution for insoluble particles such as all mineral components that form desert aerosol classes.

3.6Variations of the size of Aerosol Particles as a function of the relative humidity

The size distribution of aerosol particles varies as a function of the relative humidity (RH) because of the presence of water-soluble materials in the particulate matter. Consider a single water-soluble particle consisting of a given substance. The particle, with radius (r) is in a dry state, that is, in an environment containing no water vapour. If the RH of the particle's environment is increased the radius initially remains the same, disregarding the adsorption process which is of little importance (see Fig. 3.1). At a relative humidity determined by the nature of the substance (and also somewhat by the particle size) the radius of the particle suddenly changes to a larger value. This phenomenon is due to the fact that the particle has changed to a solution. (Meszaros , 1981).

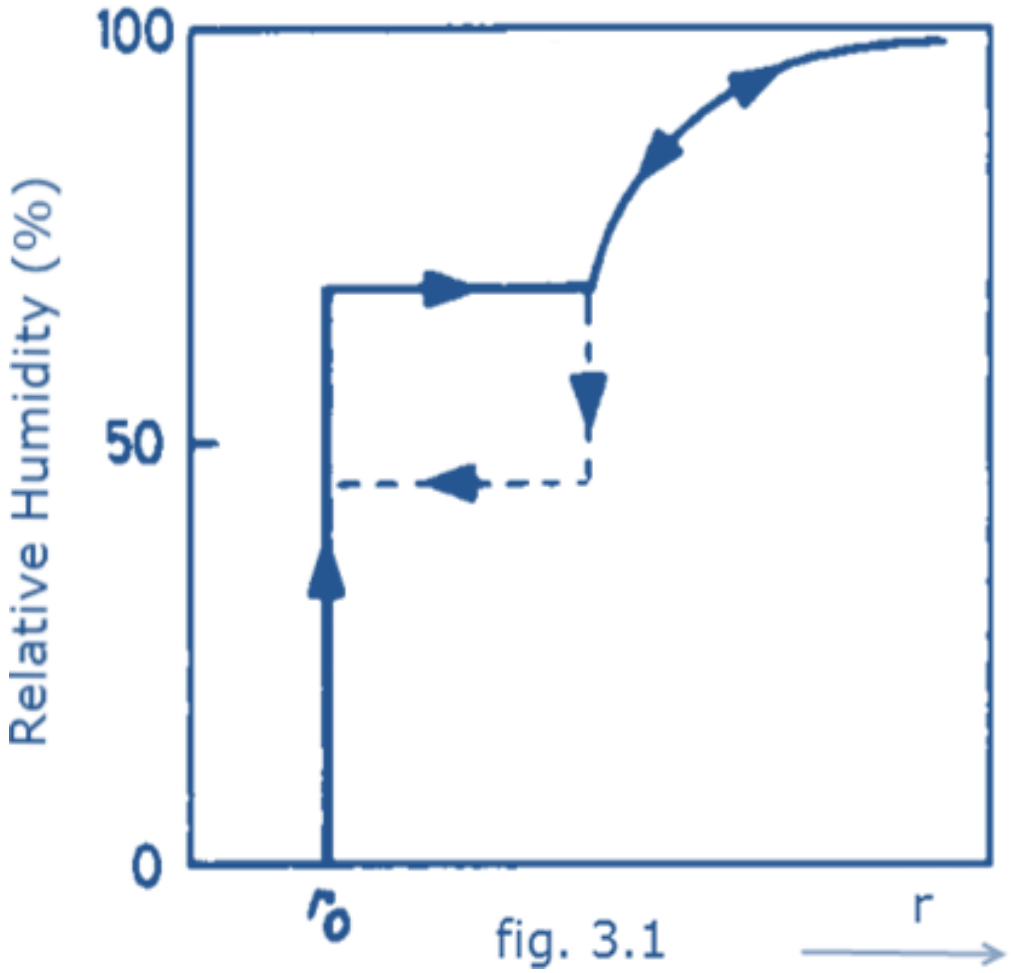

Figure 3.1shows a schematic variation of the radius (r) of a soluble particle as a function of RF of the air (r_0): dry air droplet. (Source: E. Meszaros, 1981, p. 128).

The phase change takes place at the relative humidity at which a saturated solution of the substance considered is in vapour equilibrium with its environment. If we further raise the relative humidity after the phase change (see Fig. 3.1); the radius of the droplet increases and the solution becomes weaker and weaker. This means that at higher relative humidity a more dilute solution is in dynamic equilibrium with the vapour environment.

Variations of the size distribution of aerosol particles as a function of relativehumidity can be observed in situ in the air. Changes in particle size distributions are detected by optical counters (Laktionov and Bogomolov, 1972).

3.7 Mixing Types

In this research, we have the opportunity to mix the components internally or externally. In an internal mixture, the individual particle consists of mixed components, whereas in the external mixture, pure particles of various chemical compounds exist side by side. It is currently thought that aerosols often exist initially as external mixtures near aerosol sources and that the aerosols gradually tend toward an internal mixture as they age. An internal mixture is characterized by airborne particles with a heterogeneous chemical composition.

In view of the difficulty of specifying the refractive index of internal mixtures, aerosol models usually deal only with external mixtures. Here the approach adopted is to compute the refractive index of an internally mixed class by use of the volume-weighted average of refractive indices of the components. The computation of volume mixing ratios is derived from number-density mixing ratios and size distributions.

External mixing implies that each component of a given aerosol class is represented by a different substance with its own size distribution and complex refractive index.

3.8 Radiative Forcing (RF)

Although a fully exact radiative transfer model is difficult, so in this work we used the approach of Chylek and Wong (1995), where they show that the direct aerosol radiative

forcing at the top of the atmosphere can be approximated by:

$$\Delta F_R = -\frac{S_0}{4} T_{atm}^2 (1 - N_{cloud}) 2\tau\{(1 - A)^2 \beta\omega - 2A(1 - \omega)\} \quad (3.3)$$

where

S_0 =1368Wm^{-2} is a solar constant,

T_{atm} =0.79 is the transmittance of the atmosphere above the aerosol layer,

N_{cloud}=0.6 is the fraction of the sky covered by clouds, the global averaged albedo

A=0.22 over land,

β is the fraction of radiation scattered by aerosol into the atmosphere and

τ the optical thickness (Penner et al, 1992). The above expression gives the radiative forcing due to the change of reflectance of the earth-aerosol system. The upscattering fraction is calculated using an approximate relation (Sagan and Pollack, 1967):

$$\beta = \frac{1}{2}(1 - g) \quad (3.4)$$

where g is the asymmetry parameter. Although the model is simple but was used to provide reasonable estimates for the Radiative forcing by both sulfate aerosols (Charlson et al., 1992) and absorbing smoke aerosols Chylek and Wong (1995).

The spectral behavior of the aerosol optical thickness, with the wavelength of light (λ) is expressed as inverse power law (Angstrom, 1961):

$$\tau(\lambda) = \beta\lambda^{-\alpha} \qquad (3.5)$$

where β is the turbidity and α is the Angstom exponent (Liou,2002; O'Neill and Royer, 1993). The formula is derived on the premise that the extinction of solar radiation by aerosols is a continuous function of wavelength, without selective bands or lines for scattering or absorption (Ranjan et al., 2007). The wavelength dependence of $\tau(\lambda)$ can be characterized by the Angstron parameter, which is a coefficient of the following regression:

$$\ln\tau(\lambda) = -\alpha\ln(\lambda) + \ln\beta \qquad (3.6)$$

The Angstrom exponent itself varies with wavelength, and a more precise empirical relationship between aerosol extinction and wavelength is obtained with a second-order polynomial (King and Byrne, 1976; Eck et al., 1999; Eck. et al., 2001a, b, 2003; Kaufman, 1993;O'Neill et al., 2001a, 2003) as:

$$\ln\tau(\lambda) = \alpha_2(\ln\lambda)^2 + \alpha_1\ln(\lambda) + \ln\beta \qquad (3.7)$$

Here, the coefficient α_2 accounts for a "curvature" often observed in sunphotometry measurements. In case of negative curvature ($\alpha_2 > 0$, convex type curves) the rate of change of α is more significant at the longer wavelengths, while in case of positive curvature ($\alpha_2 < 0$, concave type curves) the rate of change of α is more significant at the shorter wavelengths (Kaufman, 1993; Eck et al., 1999; Eck. et al, 2001b; Reid et al., 1999). Eck et al, (1999) reported the existence of negative curvatures for fine-mode aerosols and positive curvatures for significant contribution by coarse-mode particles in the size distribution.

3.9Vibrational polarizabilities

We may also determine the angular frequency of oscillation for an aerosol known as Vibrational polarizability using a simple dynamical model. Suppose that the electron is bound to the aerosol by a spring, so that, if displaced from equilibrium, it feels a restoring force.

$$\vec{F}_{restore} = -m\omega_0^2 x \qquad (3.8)$$

where m is the aerosol mass, and ω_0 the angular frequency of oscillations.

If we apply an external electric field **E**, the displacement x of the aerosols from equilibrium will grow until $F_{restore}$ is equal and opposite to the electronic force on the aerosol.

$$-(-e\vec{E}) = -m\omega_0^2 x, \quad so \quad x = \frac{-e\vec{E}}{m\omega_0^2}. \qquad (3.9)$$

The induced dipole moment is then

$$\vec{p} = -ex = \frac{e^2}{m\omega_0^2}\vec{E} = \alpha\vec{E} \qquad (3.10)$$

So that the effective Polarizability α is

$$\alpha = \frac{e^2}{m\omega_0^2}$$

Hence,

$$\omega_0 = \frac{e}{\sqrt{m\alpha}} \qquad (3.11)$$

Or

$$\omega_0 \ \alpha \frac{1}{\sqrt{\alpha}} \qquad (3.12)$$

CHAPTER FOUR

RESULTS AND DISCUSSION

4.1 Results

The results of polarizability and radiative forcing for six types of atmospheric aerosol models extracted from OPAC were obtained by computational approaches using the Microsoft Office excel for each component of the six aerosols models. The effective polarizability was obtained using the number mix ratio rule. The details procedure is summarized in flowchart, figure 5.1.

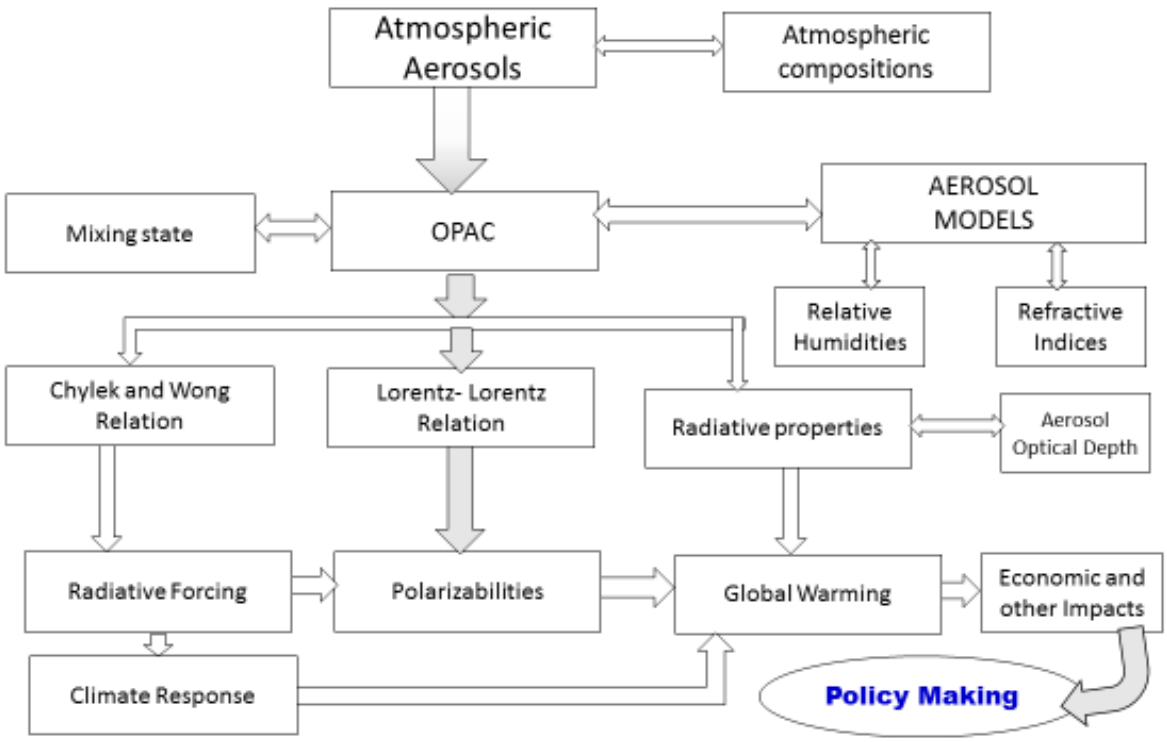

Figure 4.1.A flowchart for the details procedure and scope for the research.

4.1.1. For the polarizabilities (α),I applied Lorentz –Lorentz relation (equation 2.23)

4.1.2. For the Radiative forcing (RF), I appliedthe Chylek and Wong relationequation (3.3)

4.1.3. For the angular frequency (ω),I appliedequation (3.11).

4.1.4. For the optical depth (τ),I appliedequation (3.5).

The effective components were computed for each model within sixty one (61)λ ranges (0.25 - 40μm) and eight (8 RH (00%, 50, 70, 80, 90, 95, 98, and 99%).

The results are categorized into three main different spectral λ ranges:

Part I : Near UV region to visible range. **(**0.25 to 0.8 μm).

Part II Near infrared to medium spectral range (0.8 to 6.0 μm)

Part III: Far Infrared region (6.0 to 40.0 μm).

4.2 Part I: Near UV to visible spectral range (0.25- 0.8 μm)

4.2.1 AntarcticAerosols

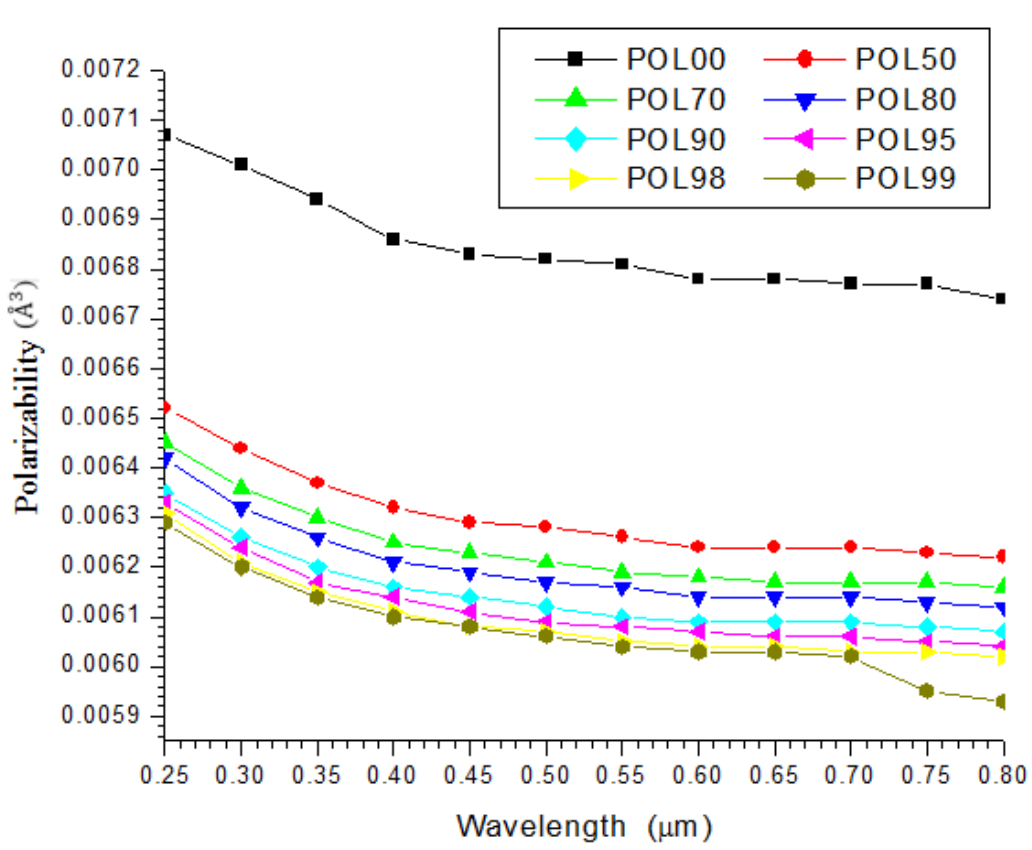

*Figure 4.2*A plot of polarizabilities of Antarctic aerosols against wavelength near UV to visible spectral region.

Fig.4.2, shows that, The polarizabilitiesdecrease with respect to the increase in wavelengths and decrease with increases in RH.

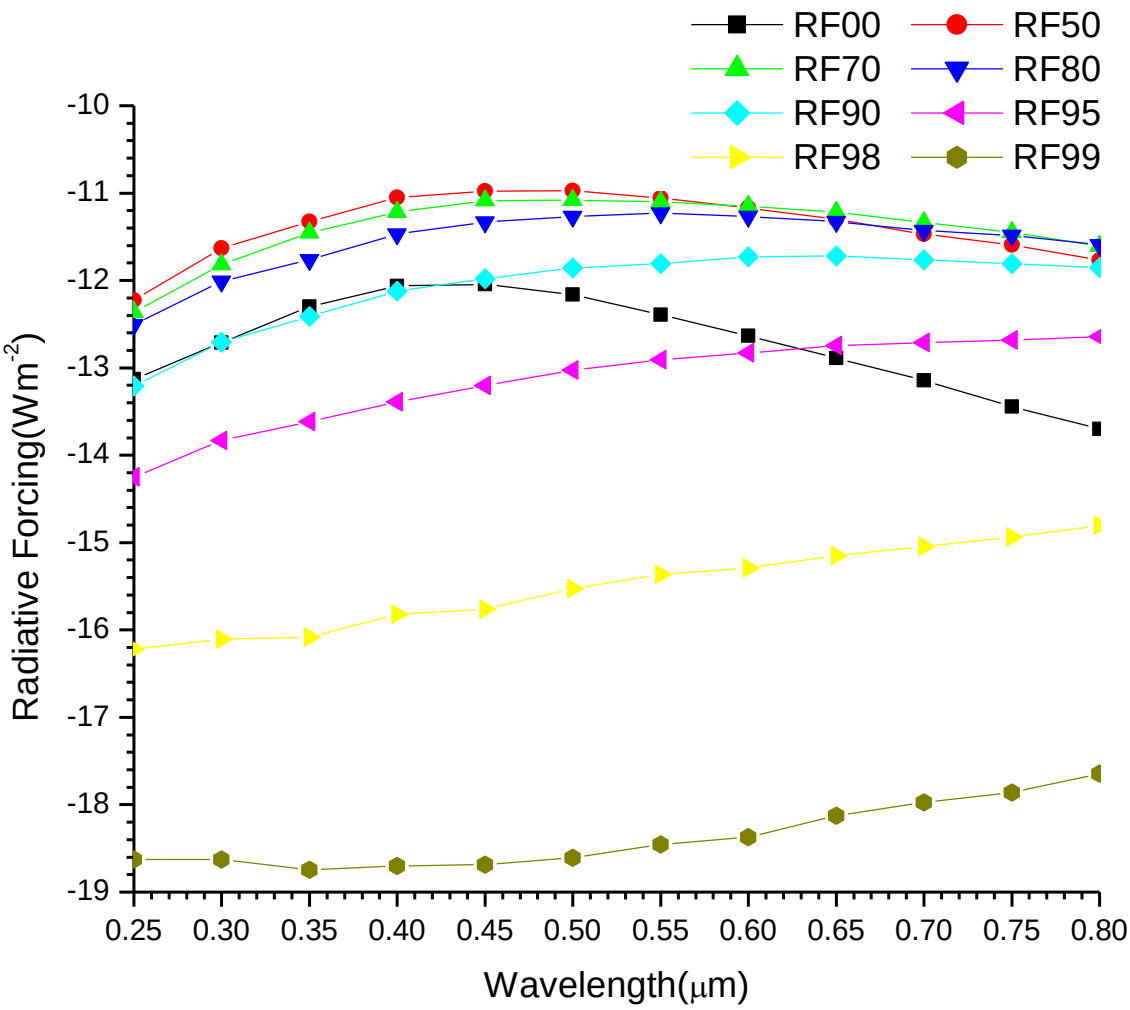

Figure 4. 3, A graph of Radiative forcing (RF) of Antarctic aerosols against wavelength near ultra-violet to visible range.

From figure 4.3, the nature of the graph shows coolingeffect with increase of RH. At 00 % RH, the RF shows quadratic relations with λ. As the RH increases to 50% the RF decreases. i.e increase in warming Subsequently, as the RH increases.

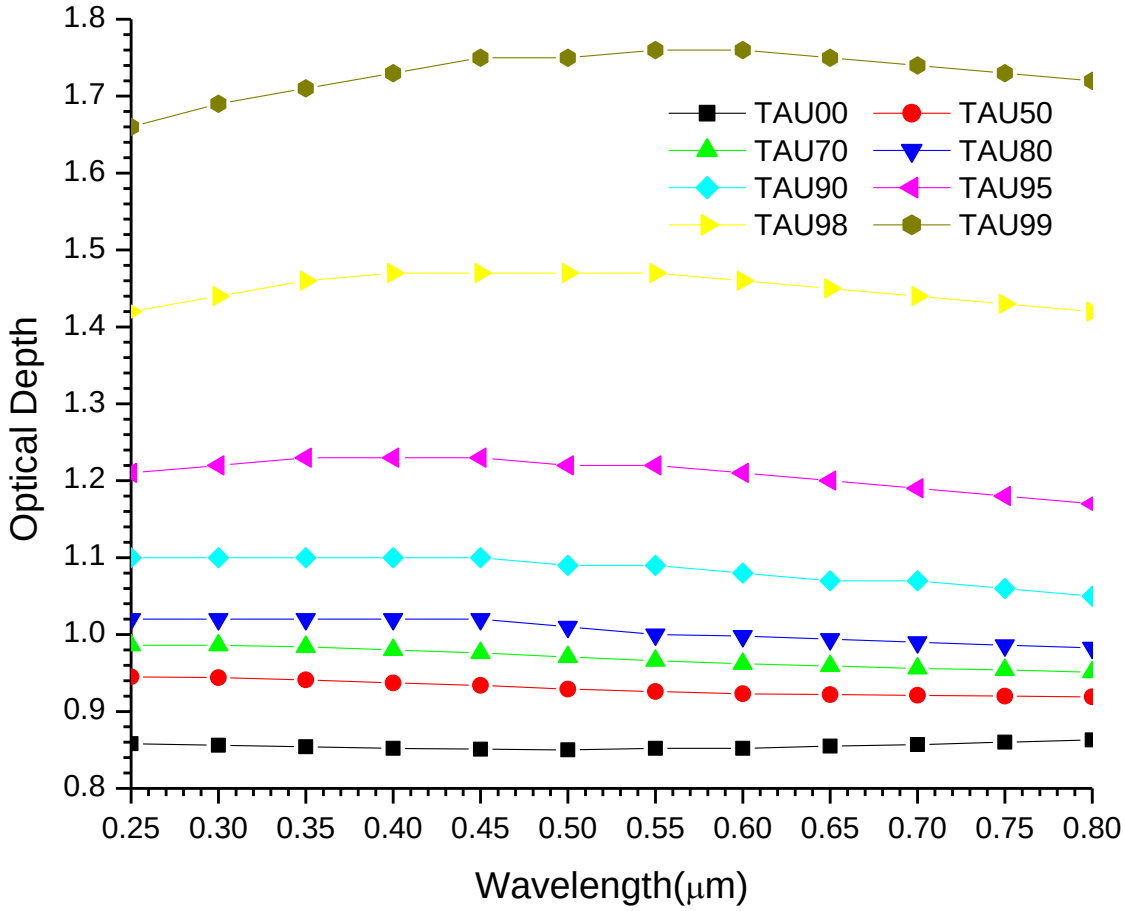

Figure 4. 4A graph of variations of Aerosol Optical Depth (AOD) with λ for Antarctic Aerosol near UV to visible spectral range.

From figure 4.4, In relation to RH, it shows that aerosol optical depths (AOD) increase with increase in RH. As the RH increases the AOD continue to increase due to the increase in concentration of fine mode particles as a result of the continue sedimentation of coarse particles due to the increase in RH.

It can be observe that at 0% RH the AOD does not obey inverse power law (equation 3.5) with respect to λ. As the RH increases from 50 to 90% RH, they can be approximate the power law with very small alpha. At 95 to 99% RH, they do not satisfy power law. The AOD increases with increase in RH.

Table 4. 1 Regression analysis of Aerosol Optical Depth(AOD) for Antarctic aerosol near UV to Visible wavelength range.

Ultraviolet to Visible (0.25 -0.80)							
	Linear			**Quadratic**			
RH (%)	**α**	**β**	**R^2**	**α_1**	**α_2**	**β_1**	**R^2**
0	-0.00342	0.85721	0.07624	-0.05689	-0.03419	0.87131	0.90210
50	0.02749	0.91221	0.97588	0.03255	0.00324	0.91080	0.97734
70	0.03466	0.94574	0.94840	0.06825	0.02148	0.93609	0.98783
80	0.03779	0.97888	0.89410	0.09704	0.03790	0.96134	0.99146
90	0.03869	1.05415	0.78277	0.13508	0.06164	1.02360	0.99787
95	0.03484	3.26428	0.48885	0.20398	0.10817	3.10006	0.99910
98	-0.00073	1.44980	0.00043	0.16657	0.10699	1.37764	0.98260
99	-0.03357	1.76910	0.49428	0.10061	-0.52246	1.68618	0.97485

From table 4.1 at 0% RH, it can be observe that, the alpha at the linear part is negative, this shows the dominance of large particles suspended in the atmosphere. As the RH increases to 50%, it can be observe that, the values of become positive , this shows the particles size decreases up to 90% RH. As from 95% , the alpha decreases with increase in RH. This shows the increase in particles sizes. The values of R^2 is very small, this signifies also the dominance of large particles. As from 50 to 90% RH, the R^2 is large, i.e. the particles obey the inverse power law, while from 95 to 99% RH, the power law is not obeyed.

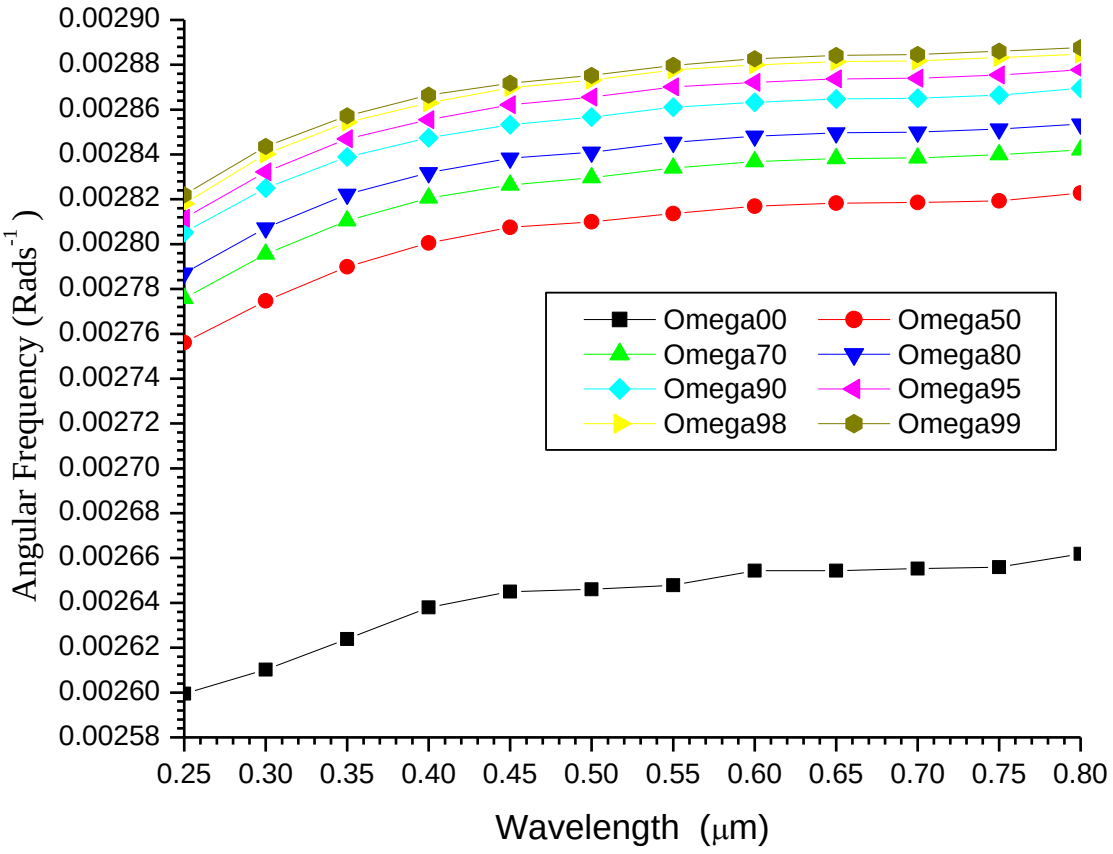

Figure 4. 5. A graph of variations of angular frequency (ω) with λ for Antarctic Aerosol near UV to visible range

4.2.2 ArcticAerosols

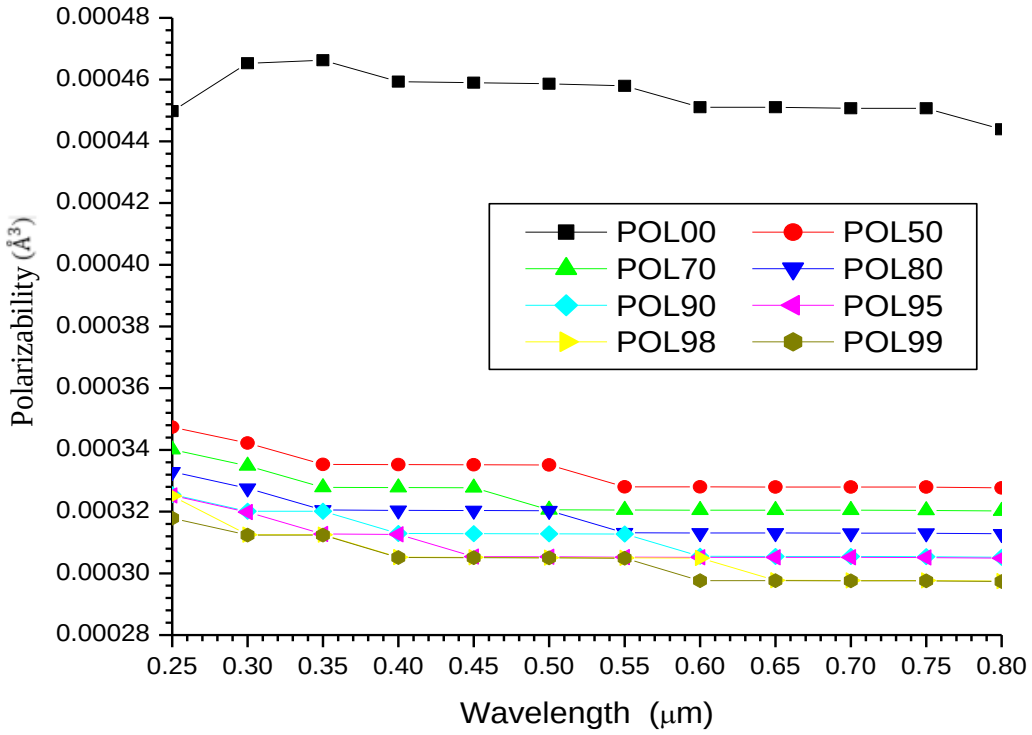

Figure 4. 6.The graph shows the variations of polarizabilities against wavelength of Arctic aerosols near ultra-violet to visible region.

From figure 4.6, the polarizabilities decreases with increase in RH and wavelength.

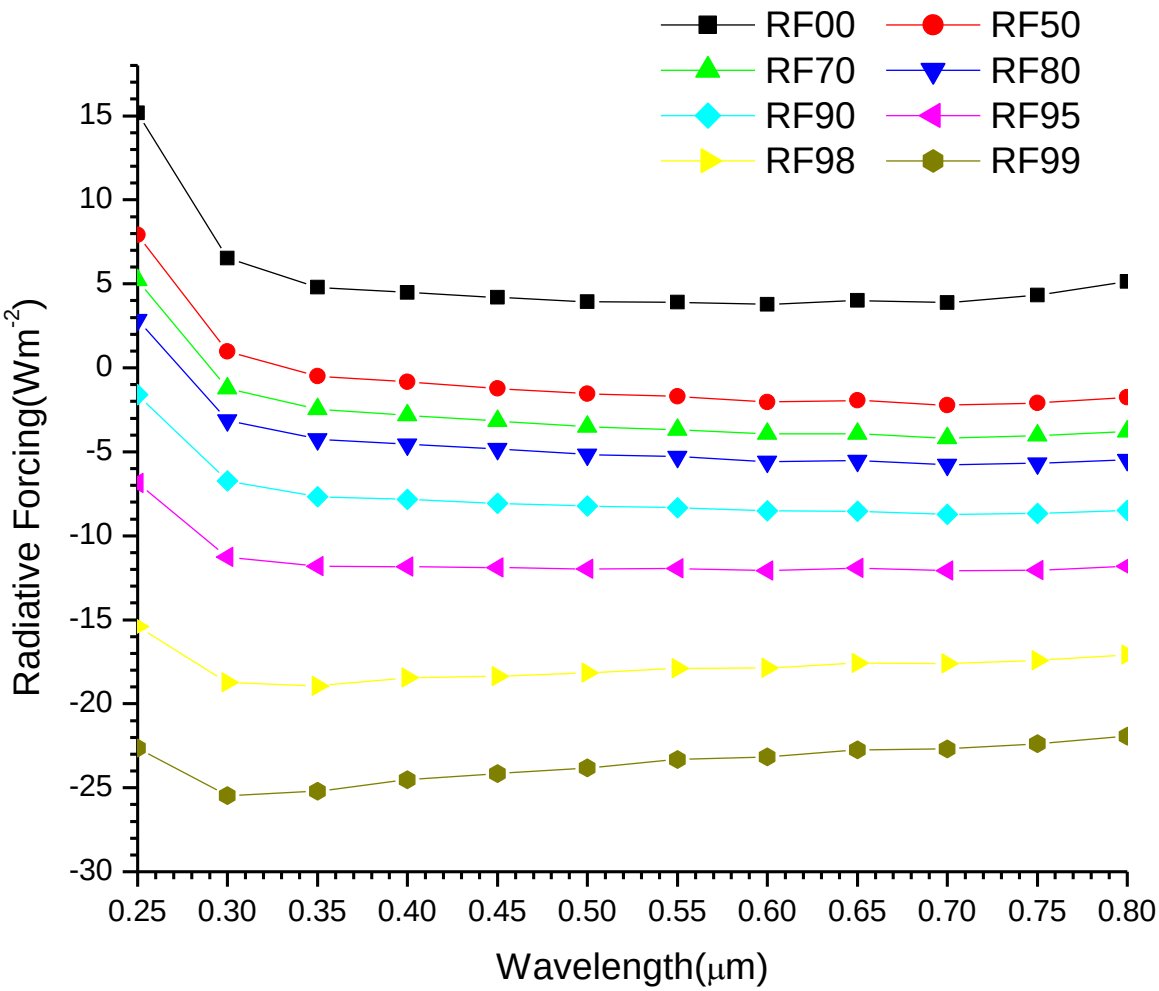

Figure 4. 7. A graphof variations of Radiative forcing of Arctic aerosols withwavelength near ultra-violet to visible range.

Fig. 4.7, shows increase in cooling with the increase in RH.

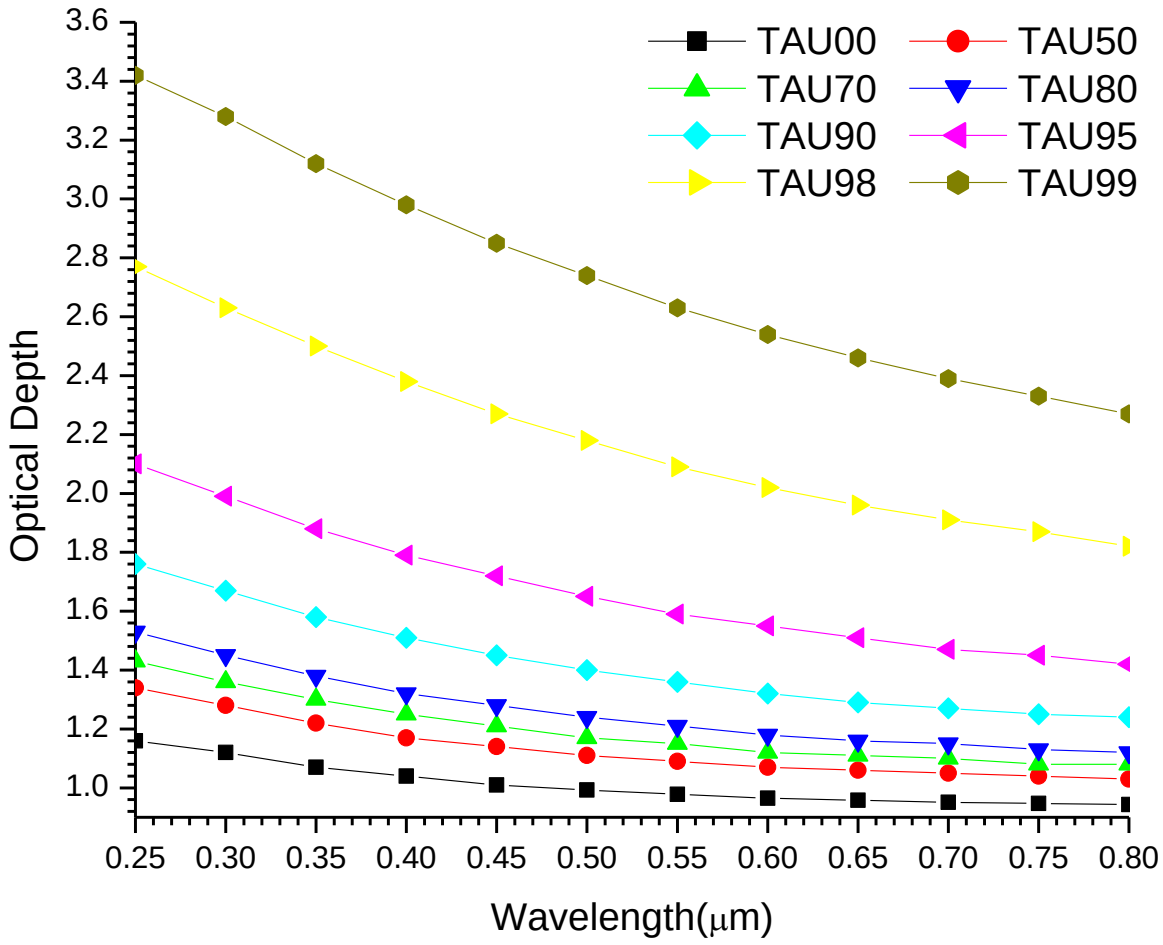

Figure 4. 8.A graph of variations of AOD with λ for Artic Aerosol near UV to visible spectral range.

From figure 4.8, the AOD increases with increase in RH but decays exponentially with increase in λ.

Table 4. 2Regression analysis of AOD for Arctic aerosol near Ultraviolet to Visible wavelength range.

Ultraviolet to Visible (0.25 to 0.80)							
	Linear			**Quadratic**			
RH(%)	α	β	R^2	α_1	α_2	β	R^2
0	0.18064	0.88831	0.97092	0.03952	-0.09025	0.92740	0.99715
50	0.22789	0.96061	0.98230	0.09083	-0.08765	1.00164	0.99803
70	0.25173	0.99728	0.98656	0.12131	-0.08340	1.03777	0.99828
80	0.27323	1.03629	0.99008	0.15436	-0.07602	1.07458	0.99838
90	0.31213	1.13565	0.99502	0.22402	-0.05635	1.16660	0.99853
95	0.34740	1.30193	0.99817	0.31182	-0.02276	1.31614	0.99863
98	0.37173	1.67829	0.99802	0.42523	0.03421	1.65111	0.99894
99	0.36457	2.11034	0.99499	0.47624	0.07141	2.03964	0.99912

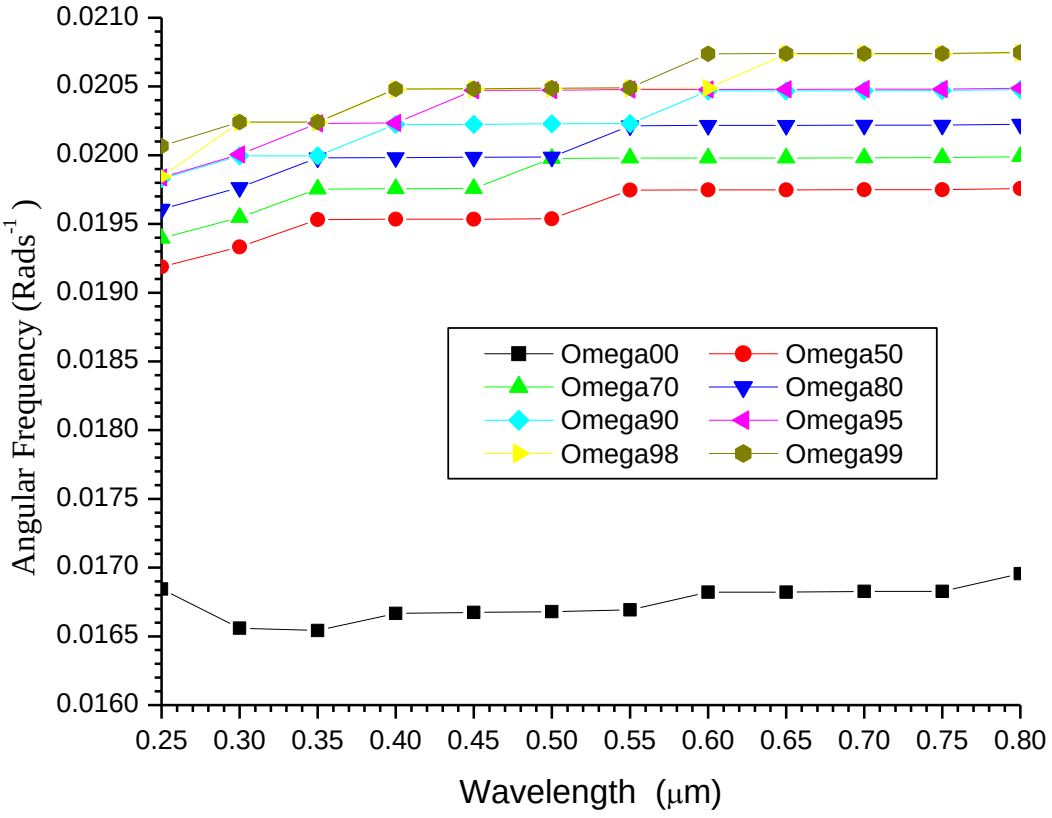

Figure 4. 9.A graph of variations of angular frequency (ω) with λ for Arctic Aerosol near UV to visible range.

4.2.3 Continental cleanAerosol

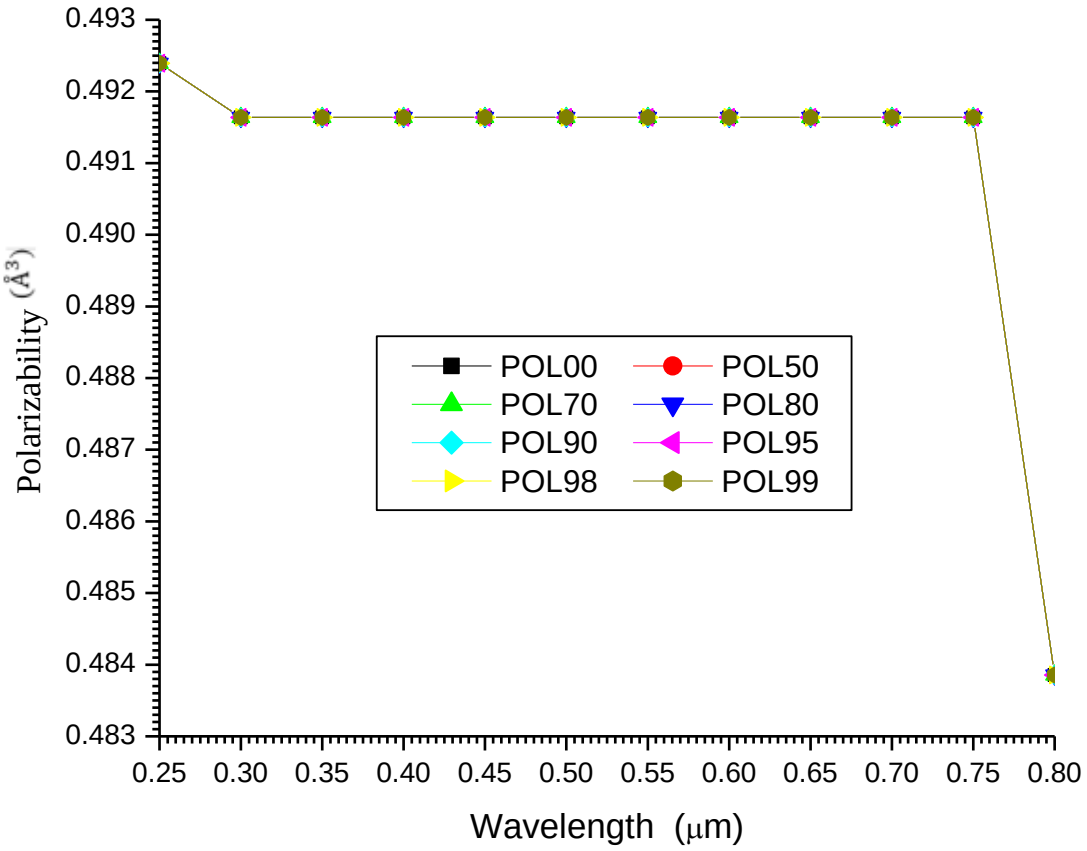

Figure 4. 10. A plot of polarizabilities of continental clean aerosols against wavelength.

Fig. 4.10, shows that, RH has negligible effect on polarizabilities with respect to the λ. It shows decreases from 0.25 to 0.30 μm and remains constant up to 0.77 μm but suddenly decreases sharply from 0.77 to 0.80 μm.

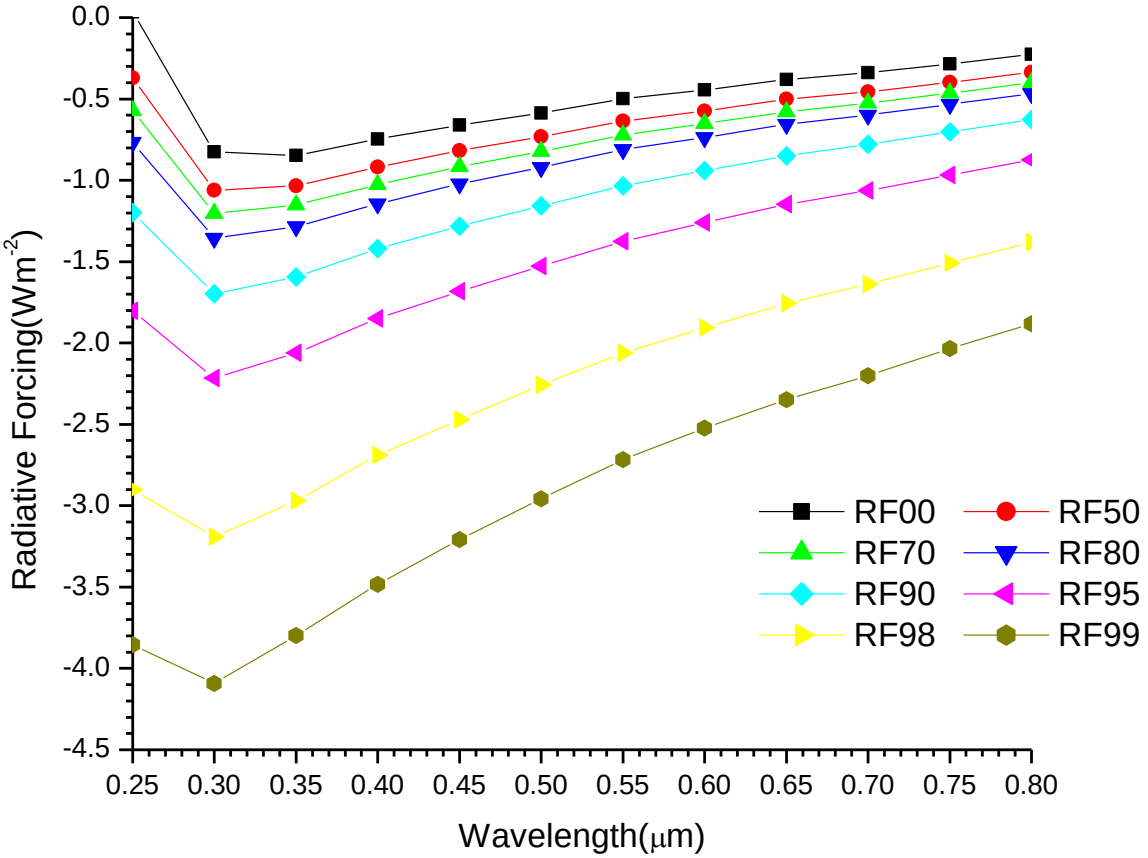

Figure 4. 11.The variations of RF of continental clean aerosols with λnear UV to visible.

Fig. 4.11, the cooling effect increases from 0.25 to 0.30 μm and increase with the increase in λ and decrease in RH. From 0.30μm the cooling effects begin to decrease with respect to the increase in λ and RH respectively.

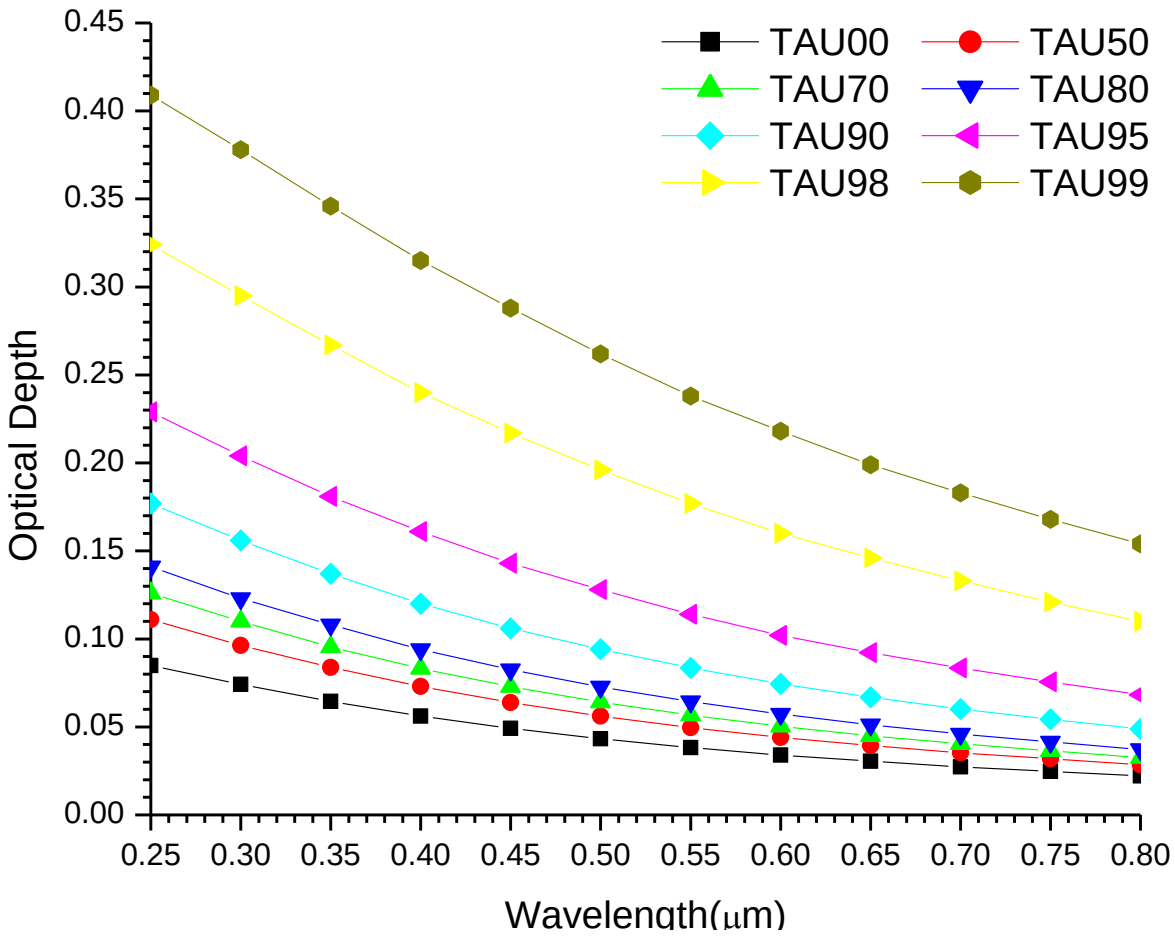

Figure 4. 12.A graph of variations of AOD with λ for Continental Clean Aerosol near UV to visible Spectral Range .

From figure 4.12, the AOD decreases with increase in λ and increase with increase in RH.

Table 4. 3 Regression analysis of AOD for Continental Clean aerosol near Ultraviolet to Visible wavelength range.

Ultraviolet to Visible (0.25 to 0.80 um)							
	Linear			**Quadratic**			
RH(%)	α	β	R2	α_1	A_2	β_1	R^2
0	1.1756	0.0183	0.9881	1.7864	0.3906	0.0152	0.9999
50	1.1843	0.0235	0.9880	1.8042	0.3964	0.0195	1.0000
70	1.1764	0.0270	0.9875	1.8039	0.4013	0.0223	1.0000
80	1.1626	0.0309	0.9870	1.7968	0.4056	0.0255	1.0000
90	1.1216	0.0410	0.9856	1.7649	0.4114	0.0337	1.0000
95	1.0556	0.0583	0.9834	1.7069	0.4165	0.0478	1.0000
98	0.9426	0.0967	0.9791	1.5963	0.4181	0.0792	1.0000
99	0.8578	0.1370	0.9750	1.5099	0.4170	0.1122	1.0000

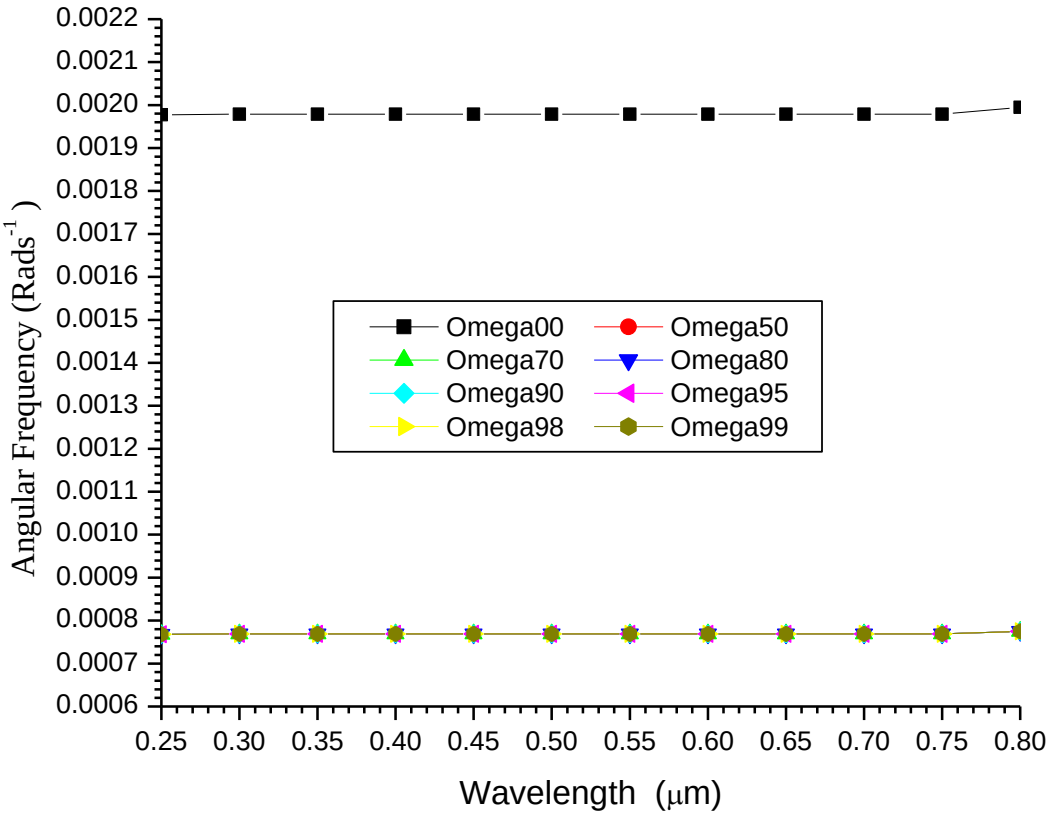

Figure 4. 13.A graph of variations of angular frequency (ω) with λ for continental clean Aerosol near UV to visible range.

4.2.4 Maritime tropical aerosol

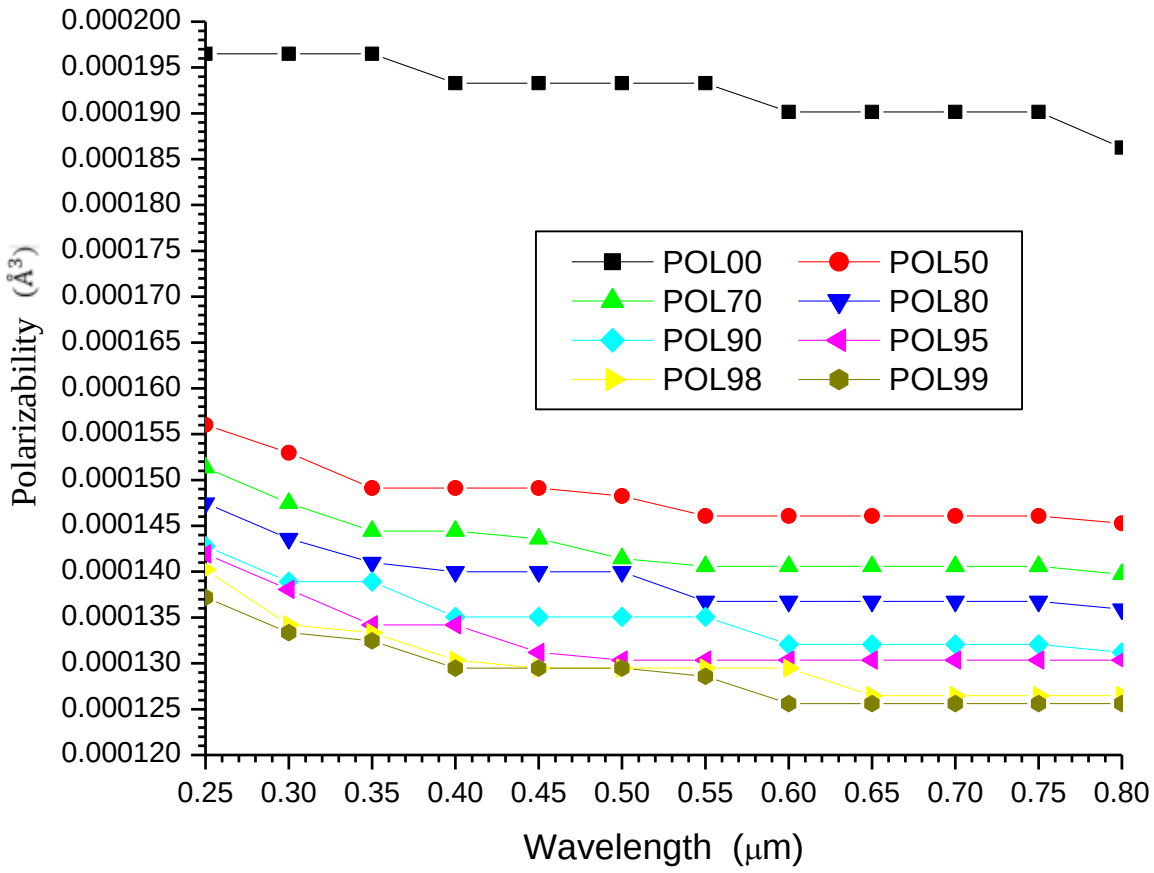

Figure 4. 14. The effect of polarizabilities of Maritime tropical aerosols with λ near Ultra-violet to visible.

From fig. 4.14,the polarizabilities decrease with increase in RH and λ.

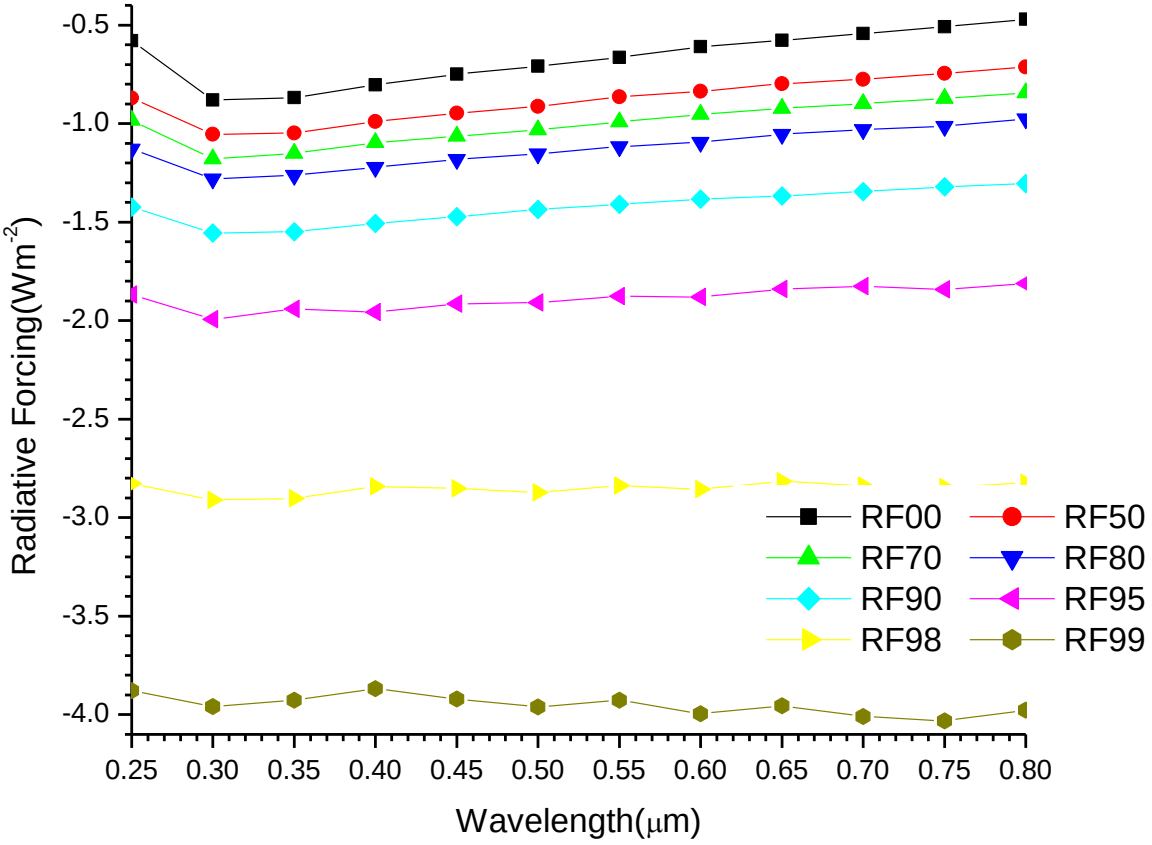

Figure 4. 15.A graph of variations of Radiative forcing of maritime tropical aerosols with λ near ultra-violet to visible .

From figure. 4.15, there are generally cooling effects with the respect to the increase in λ and decrease in RH from 0.25 to 0.30 μm, then it remains constants with the increase in λ.

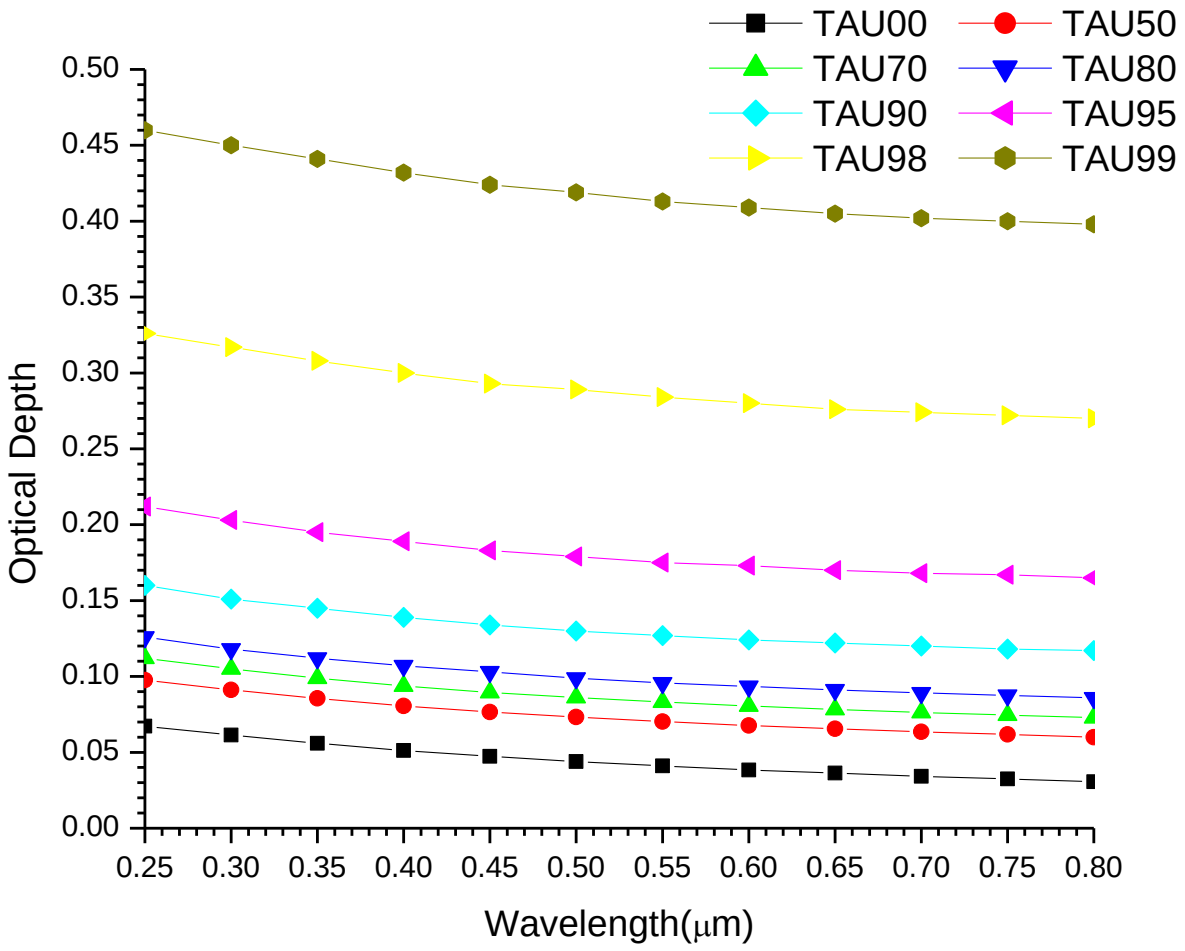

Figure 4. 26.A graph of variations of AOD with λ for Maritime tropical Aerosol near UV to visible range.

Table 4. 4Regression analysis of OD for Maritime Tropical Aerosol near Ultraviolet to Visible wavelength range.

Ultraviolet to Visible (0.25 to 0.80)							
	Linear			Quadratic			
RH(%)	α	β	R^2	α_1	α_2	β_1	R^2
0	0.6847	0.0270	0.9956	0.8962	0.1352	0.0253	0.9998
50	0.4232	0.0546	0.9997	0.4389	0.0101	0.0543	0.9998
70	0.3724	0.0668	0.9994	0.3392	-0.0212	0.0674	0.9998
80	0.3310	0.0791	0.9986	0.2795	-0.0330	0.0804	0.9997
90	0.2725	0.1086	0.9952	0.1906	-0.0524	0.1114	0.9992
95	0.2177	0.1553	0.9907	0.1250	-0.0592	0.1597	0.9986
98	0.1669	0.2580	0.9949	0.1229	-0.0282	0.2615	0.9980
99	0.1291	0.3840	0.9947	0.0963	-0.0210	0.3879	0.9975

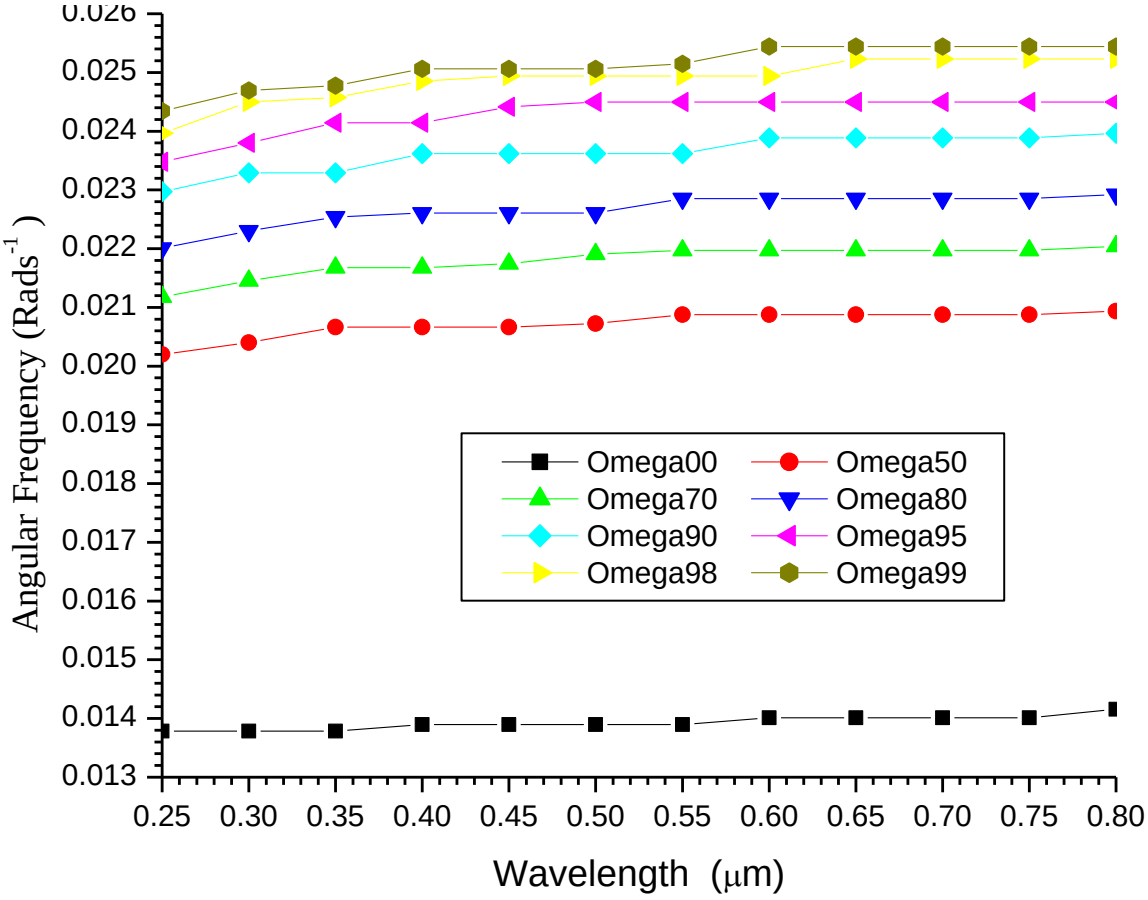

Figure 4. 17.A graph of variations of angular frequency (ω) with λ for maritime Aerosol near UV to visible range.

4.2.5 Sahara / Desert Aerosol

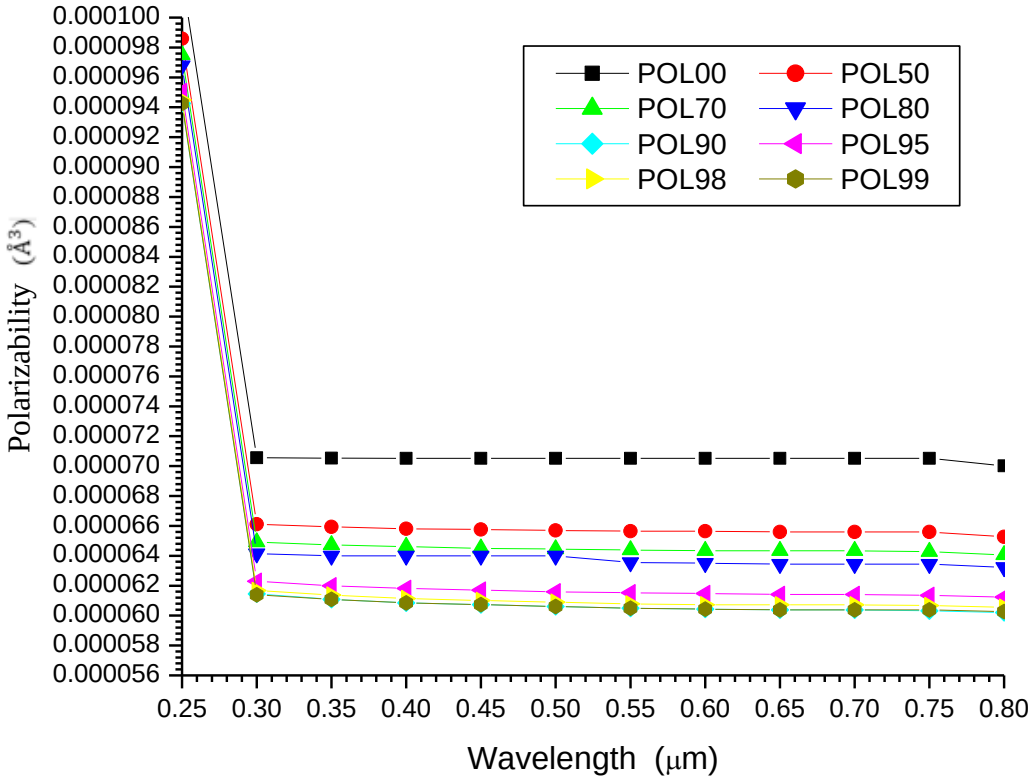

Figure 4. 18.A graph of variation of polarizabilities of Sahara aerosols with λ near UV to visiblespectral λrange .

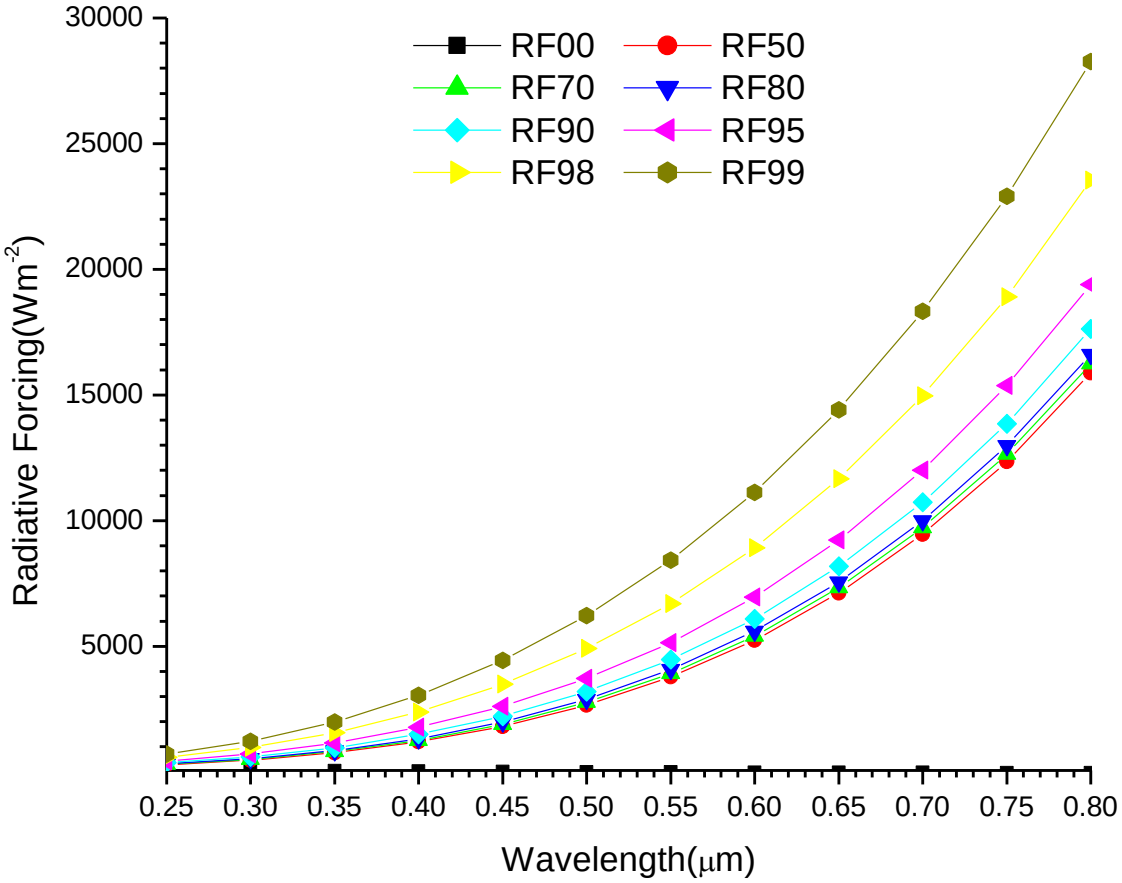

Figure 4. 19. A plot of Radiative forcing of Sahara aerosols againstλ.

From fig. 4.19, The warming effects rapidly increase with the increase in RH and λ respectively. At 00% RH, the neutral point occurred and remains constant with increase in λ.

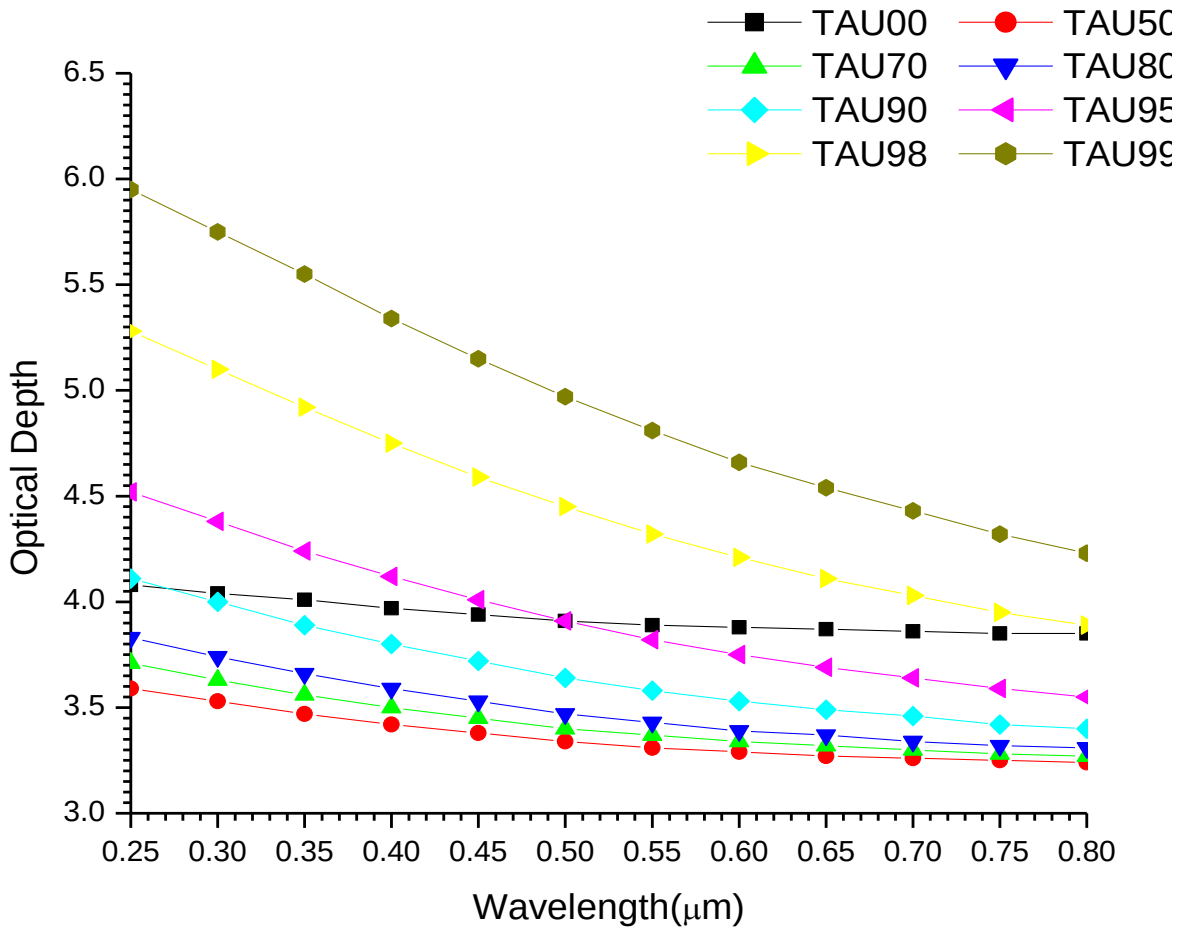

Figure 4. 20.A graph of variations of AOD with λ for Sahara Aerosol near UV to visible range.

Table 4. 5Regression analysis of AOD for Sahara aerosol near Ultraviolet to Visible wavelength range.

Ultraviolet to Visible (0.25 to 0.80							
	Linear			Quadratic			
RH(%)	α	β	R^2	α_1	α_2	β_1	R^2
0	0.0527	3.7858	0.9781	0.0220	-0.0196	3.8215	0.9929
50	0.0920	3.1490	0.9885	0.0523	-0.0253	3.1874	0.9967
70	0.1115	3.1662	0.9916	0.0713	-0.0257	3.2053	0.9973
80	0.1303	3.1877	0.9939	0.0921	-0.0244	3.2250	0.9977
90	0.1691	3.2508	0.9971	0.1425	-0.0170	3.2774	0.9982
95	0.2149	3.3721	0.9985	0.2162	0.0008	3.3707	0.9985
98	0.2737	3.6655	0.9962	0.3403	0.0426	3.5917	0.9988
99	0.3055	3.9864	0.9915	0.4315	0.0805	3.8358	0.9991

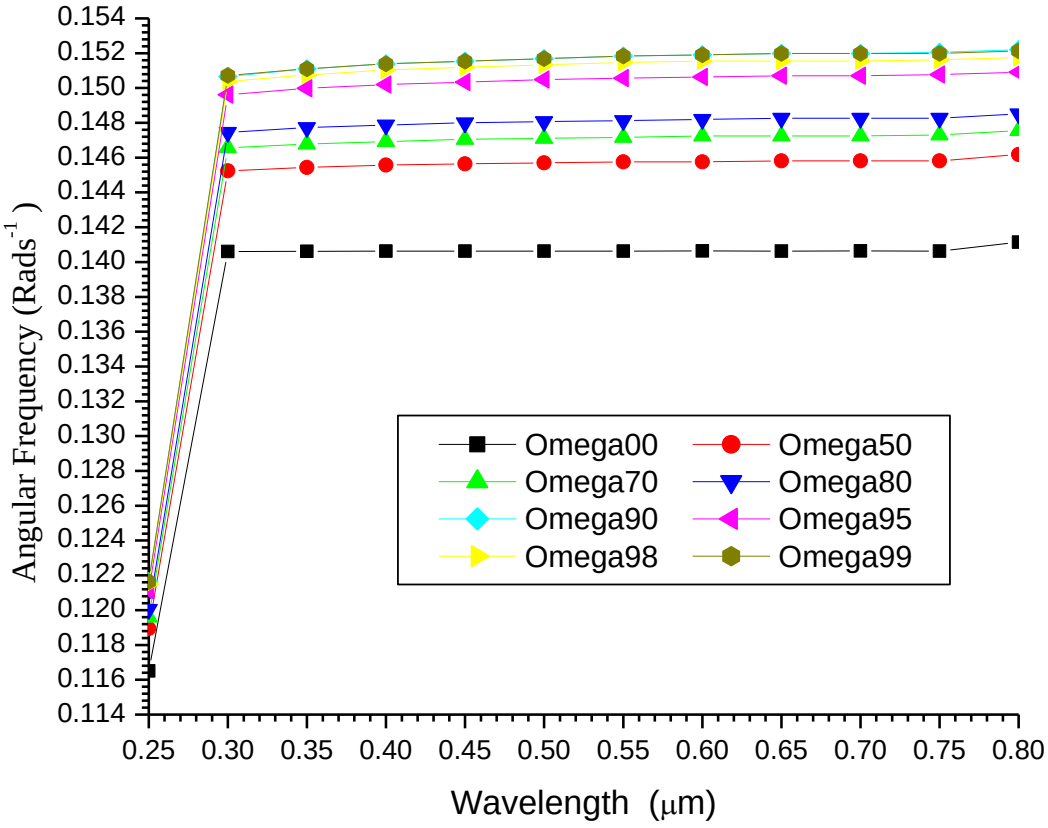

Figure 4.21.A graph of variations of angular frequency (ω) with λ for Sahara Aerosol near UV to visible range.

4.2.6 UrbanAerosol

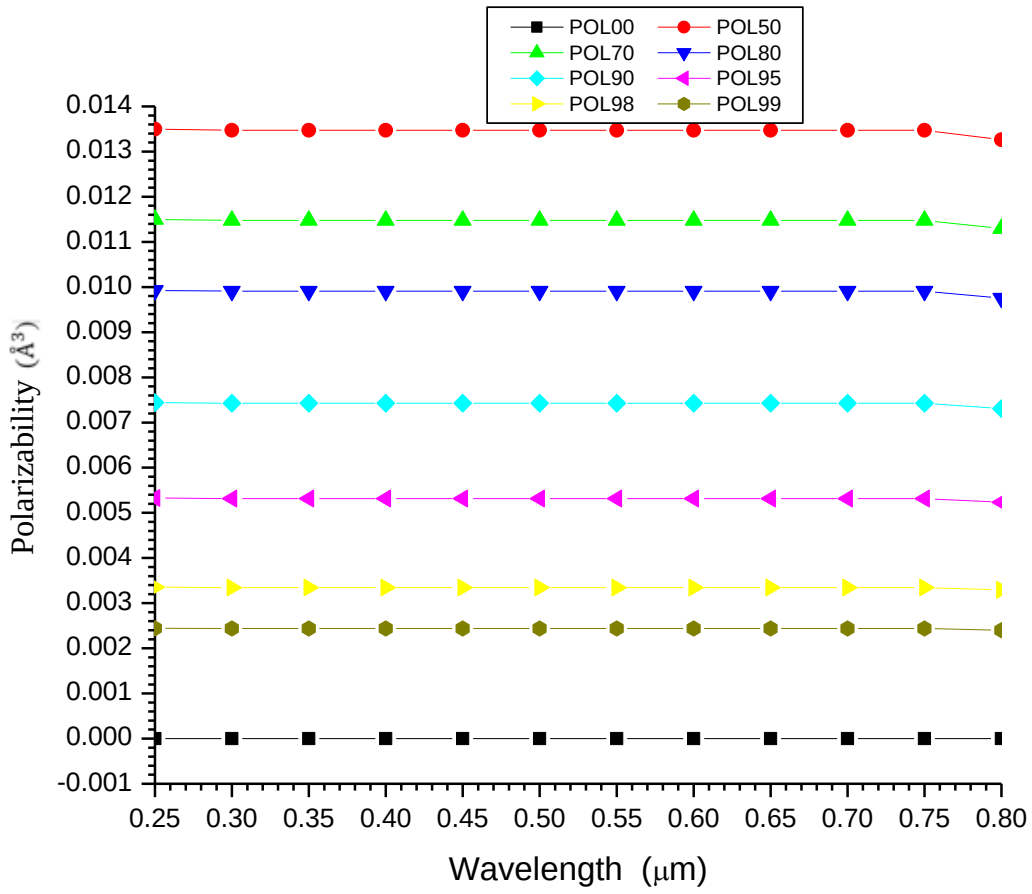

Figure 4.22.Shows the effect of RH with polarizabilities of Urban aerosols against λnear Ultra-violet to visible.

From figure. 4.22, the polarizability is minimum at dry state (0% RH) then decreases with increase in RH and nearly constant withincrease in λ.

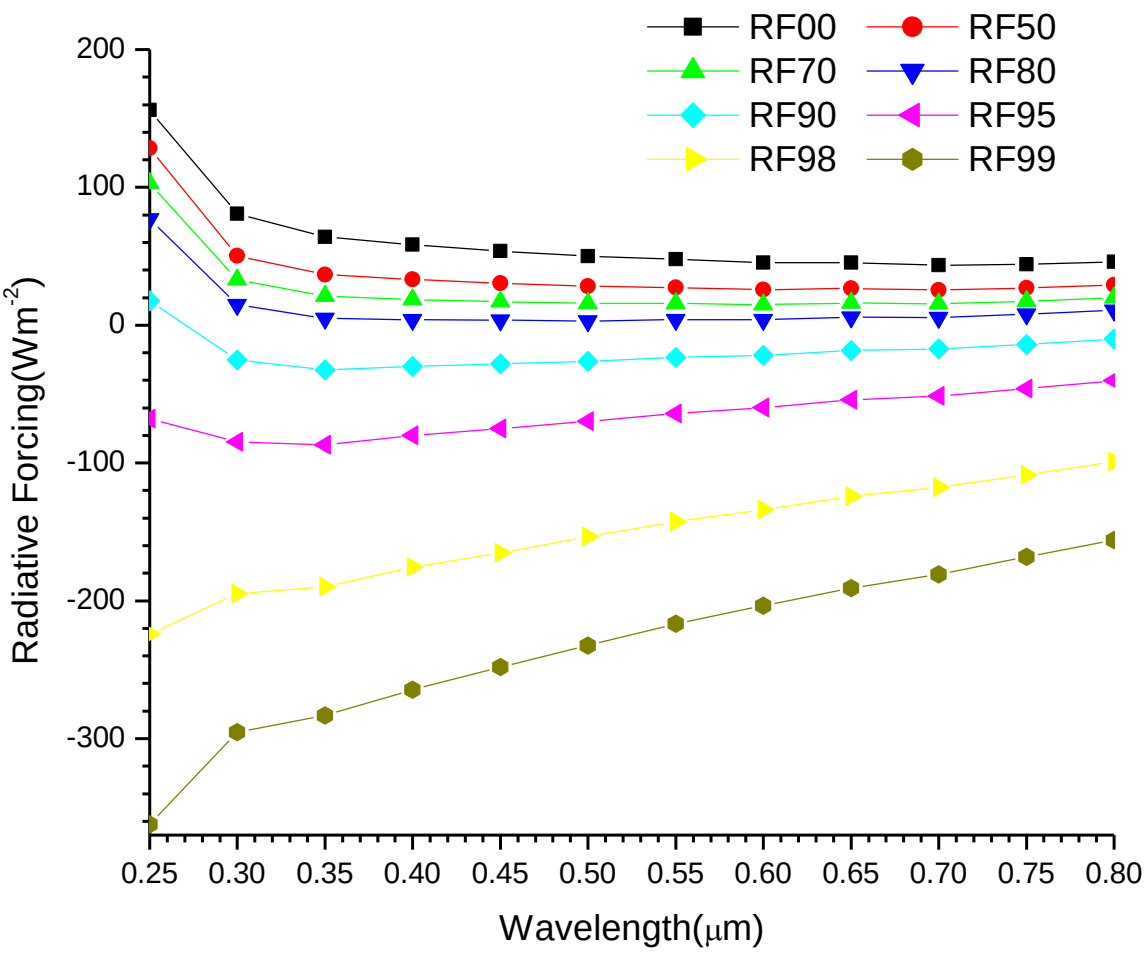

Figure 4.23. Shows a graph of Radiative forcing for Urban aerosols with λ near ultra-violet to visible.

From fig. 4.23, at RH 0% to 90%, there were warming effect which cools with increase in λ from 0.25 to 0.30μm, while the cooling effect occurred at RH from 85 to 99% from 0.25 to 0.30μm and decrease with the increase in λ. From 0.30 to 0.80μm, the warming effect begins to increases with the increase in λ and RH respectively.

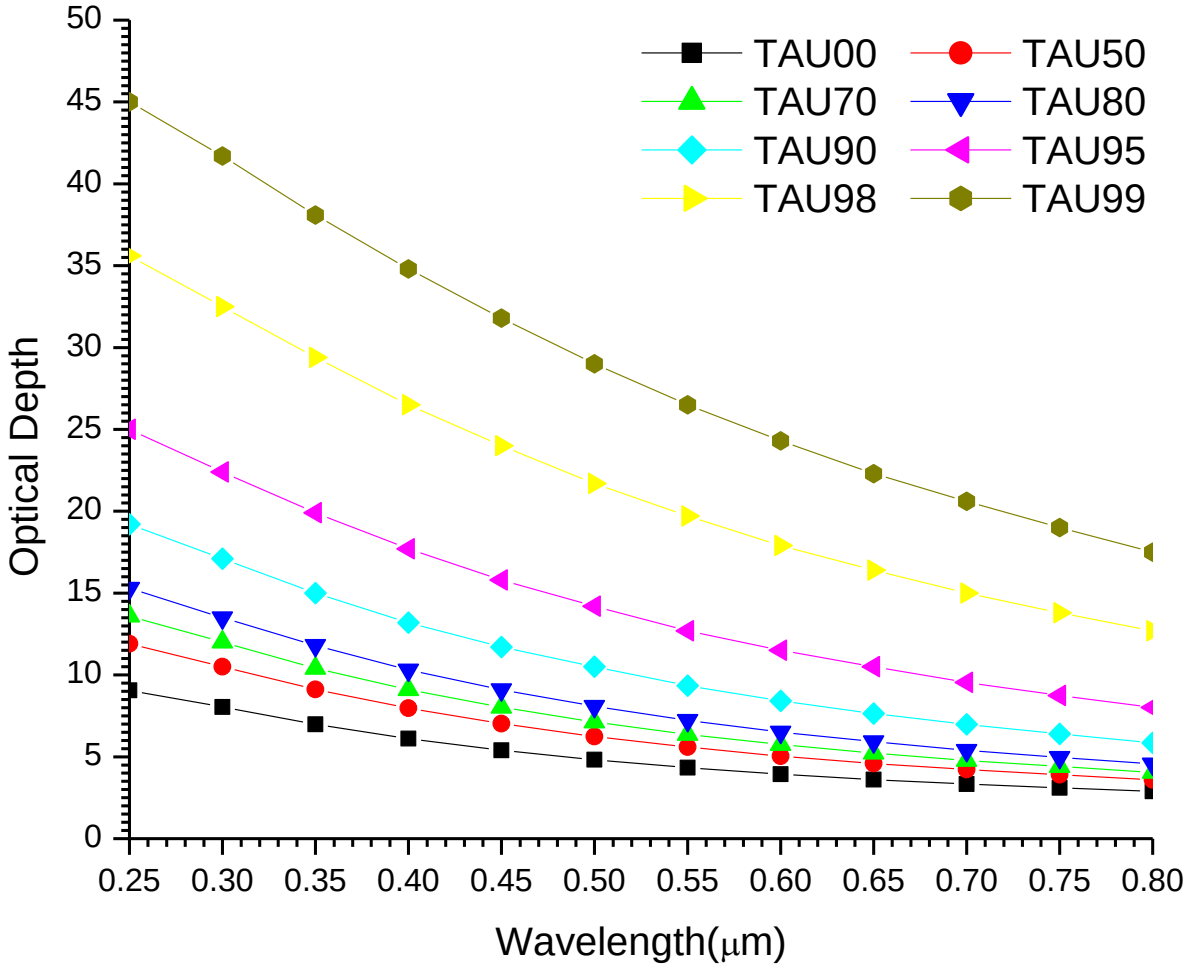

Figure 4.24.A graph of variations of AOD with λ for Urban Aerosol near UV to visible range.

Table 4. 6.Regression analysis of OD for Urban aerosol near Ultraviolet to Visible wavelength range.

Ultraviolet to Visible (0.25 to 0.80							
	Linear			Quadratic			
RH(%)	α	β	R^2	α_1	α_2	β_1	R^2
0	1.0159	0.8520	0.9962	1.2792	0.1684	0.7717	0.9991
50	1.0598	1.0731	0.9949	1.4041	0.2202	0.9680	0.9995
70	1.0667	1.1975	0.9939	1.4520	0.2464	1.0799	0.9996
80	1.0659	1.3205	0.9929	1.4858	0.2686	1.1923	0.9997
90	1.0466	1.5837	0.9906	1.5259	0.3065	1.4375	0.9998
95	1.0005	1.9156	0.9875	1.5343	0.3414	1.7527	0.9999
98	0.9071	2.4035	0.9820	1.4895	0.3725	2.2257	1.0000
99	0.8317	2.7434	0.9773	1.4339	0.3851	2.5596	1.0000

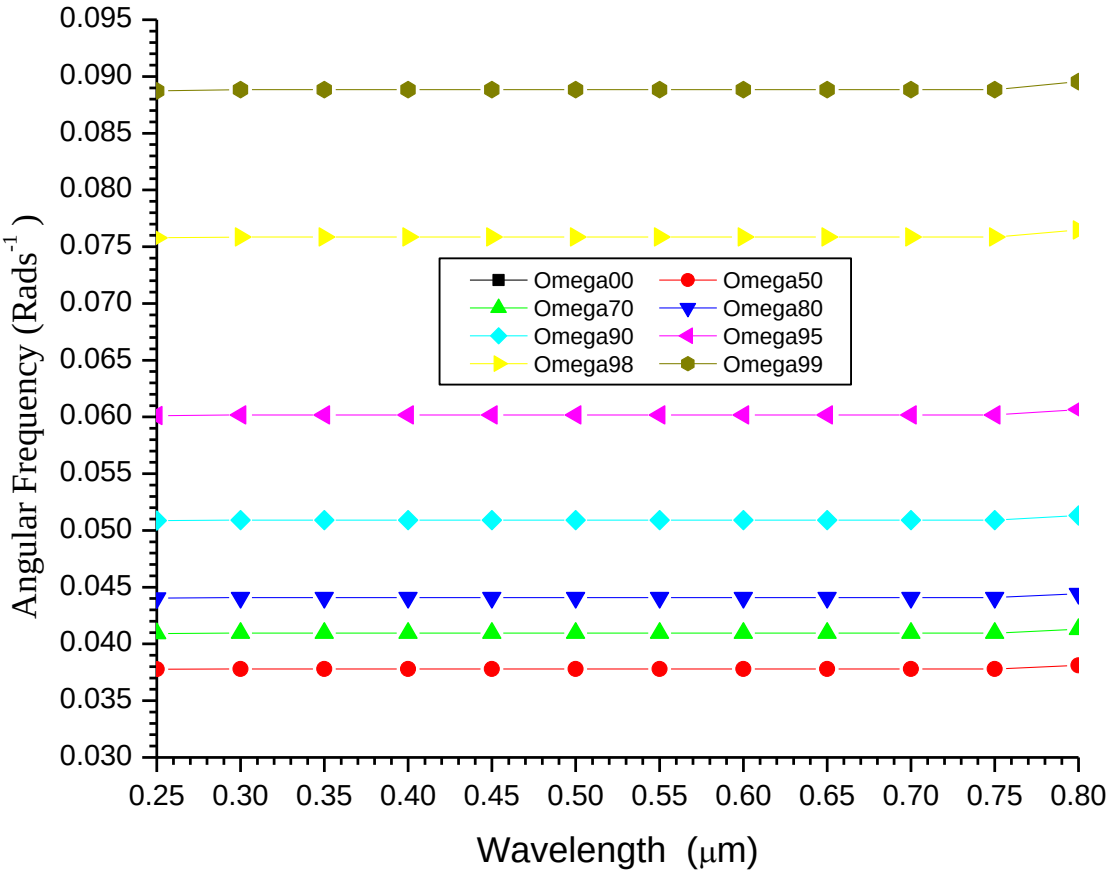

4Figure 4. 35.A graph of variations of angular frequency (ω) with λ for Urban Aerosol near UV to visible range.

4.3 PART II: Near infrared to medium spectral range (0.8 to 6.0 μm)

4.3.1 AntarcticAerosol

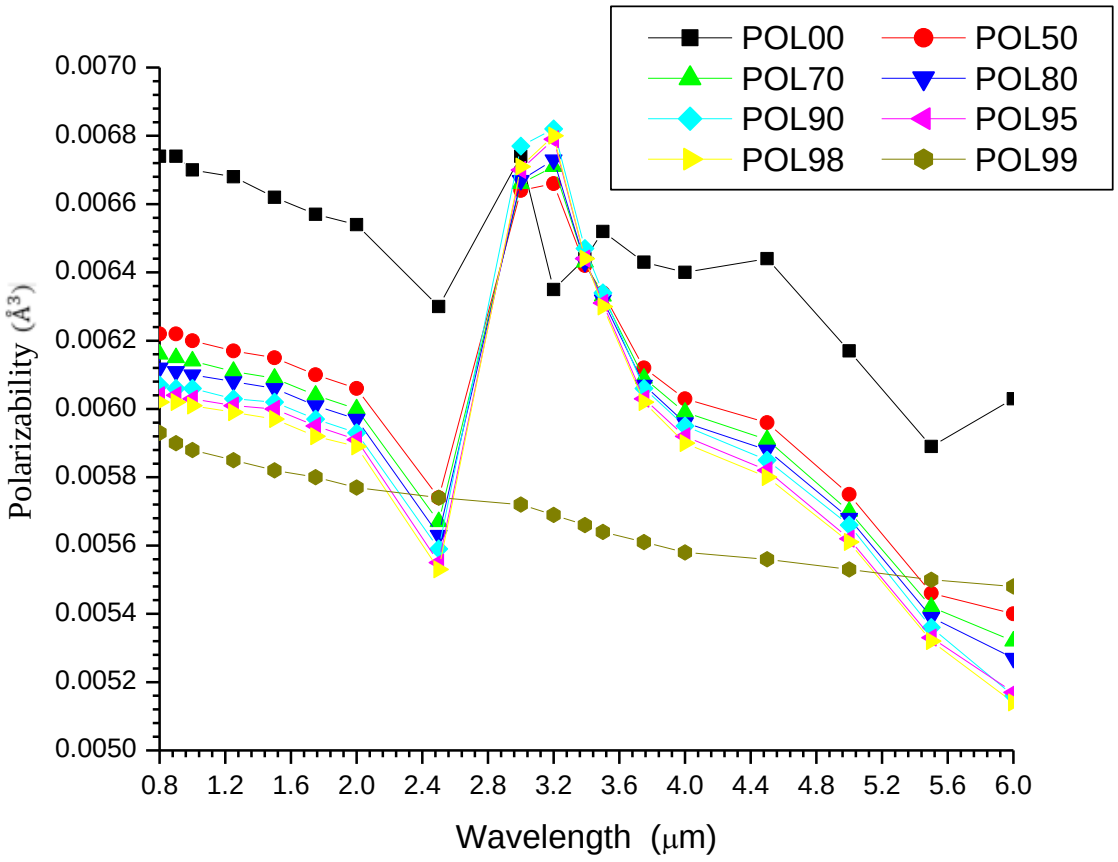

Figure 4. 26. A graph of variations of polarizabilities of Antarctic aerosols against λ near infrared to medium spectral range.

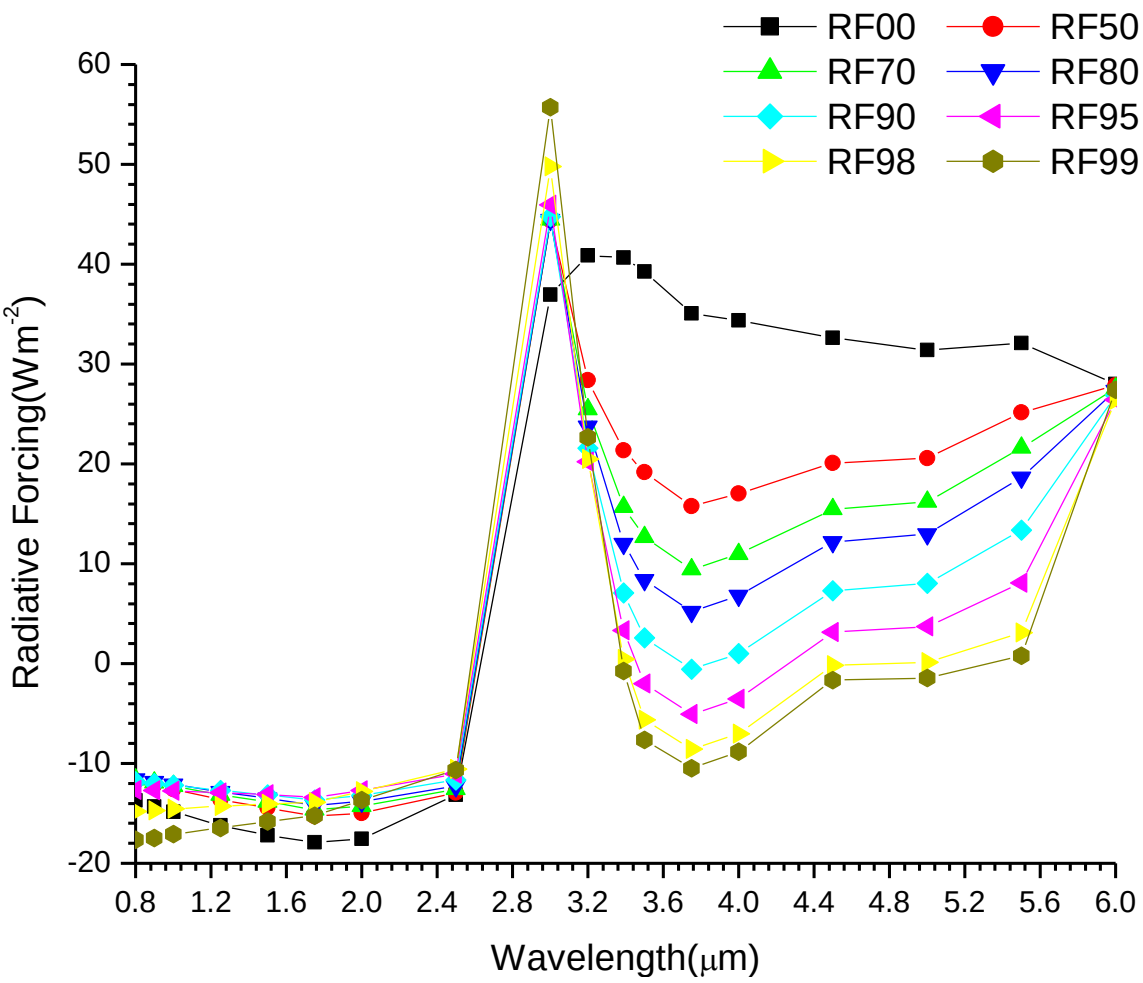

Figure 4. 4A graph of the effect of Radiative forcing of Antarctic aerosols with λnear infrared to medium spectral range.

From fig. 4.27, The cooling effect occurred from 0.8 to 2.5μm. the atmospheric window occurred from 2.5μm to 3.5μm where the maximum warming effect was sharply recorded which increases with the respect to the increase in RH.

This effect decreases with the increase in λ and decrease in RH. As the λ increases, all the line graphs converged at a point (6.0μm).

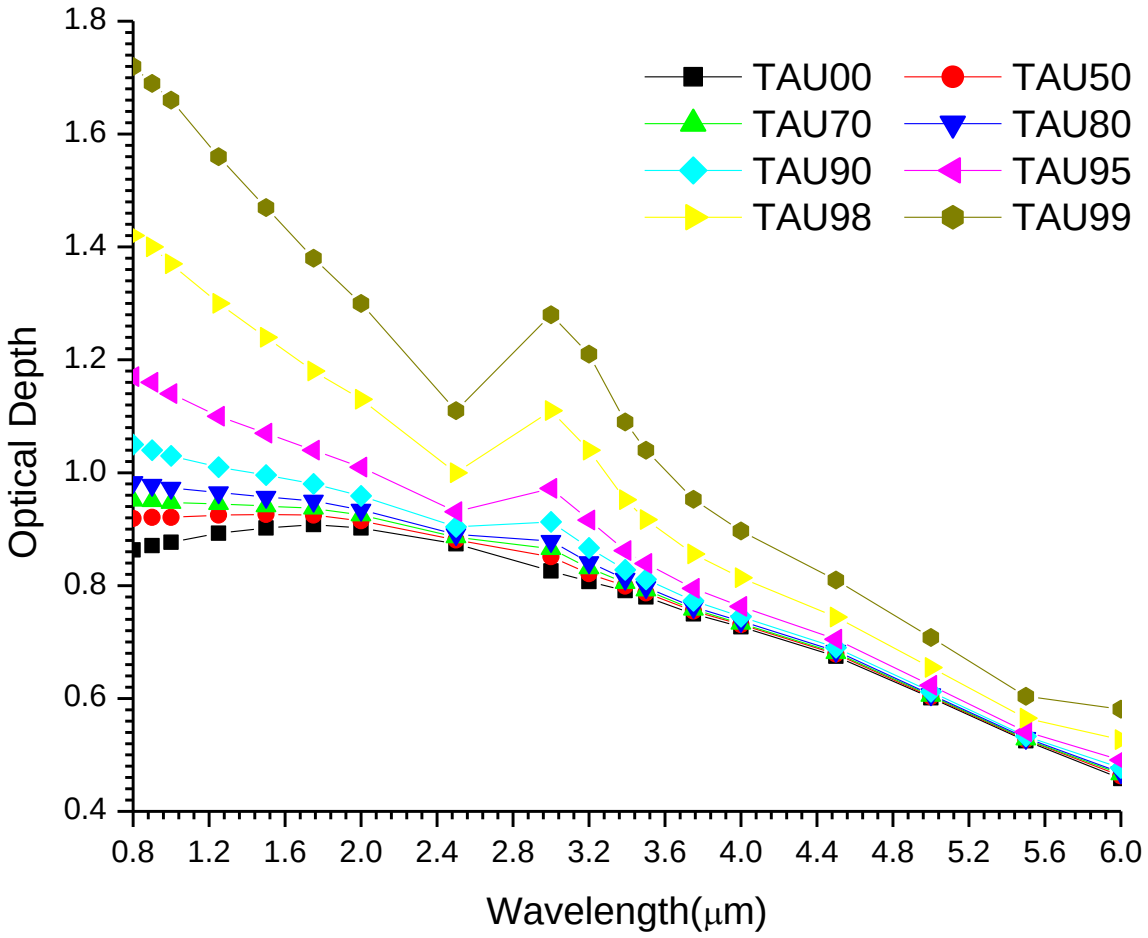

Figure 4. 58.A graph of variations of AOD with λ for Antarctic Aerosol near IR.

Table 4. 7Regression analysis of AOD for Antarctic aerosol near Infrared wavelength region.

Near Infrared (0.8 to 6.0)							
	Linear			Quadratic			
RH(%)	α	β	R^2	α_1	α_2	β_1	R^2
0	0.23709	0.95260	0.58954	-0.31013	0.35034	0.88741	0.95538
50	0.26318	0.99612	0.65746	-0.25743	0.33330	0.93116	0.95716
70	0.27773	1.02226	0.68914	-0.23067	0.32548	0.95710	0.95814
80	0.29128	1.04803	0.71538	-0.20682	0.31889	0.98254	0.95907
90	0.32043	1.10844	0.76179	-0.15933	0.30715	1.04165	0.96072
95	0.32043	1.10844	0.89022	-0.15933	-0.30715	1.04165	0.97741
98	0.43678	1.44987	0.85422	-0.01717	0.29062	1.36707	0.96170
99	0.49679	1.75302	0.86677	0.02291	0.30339	1.64865	0.95864

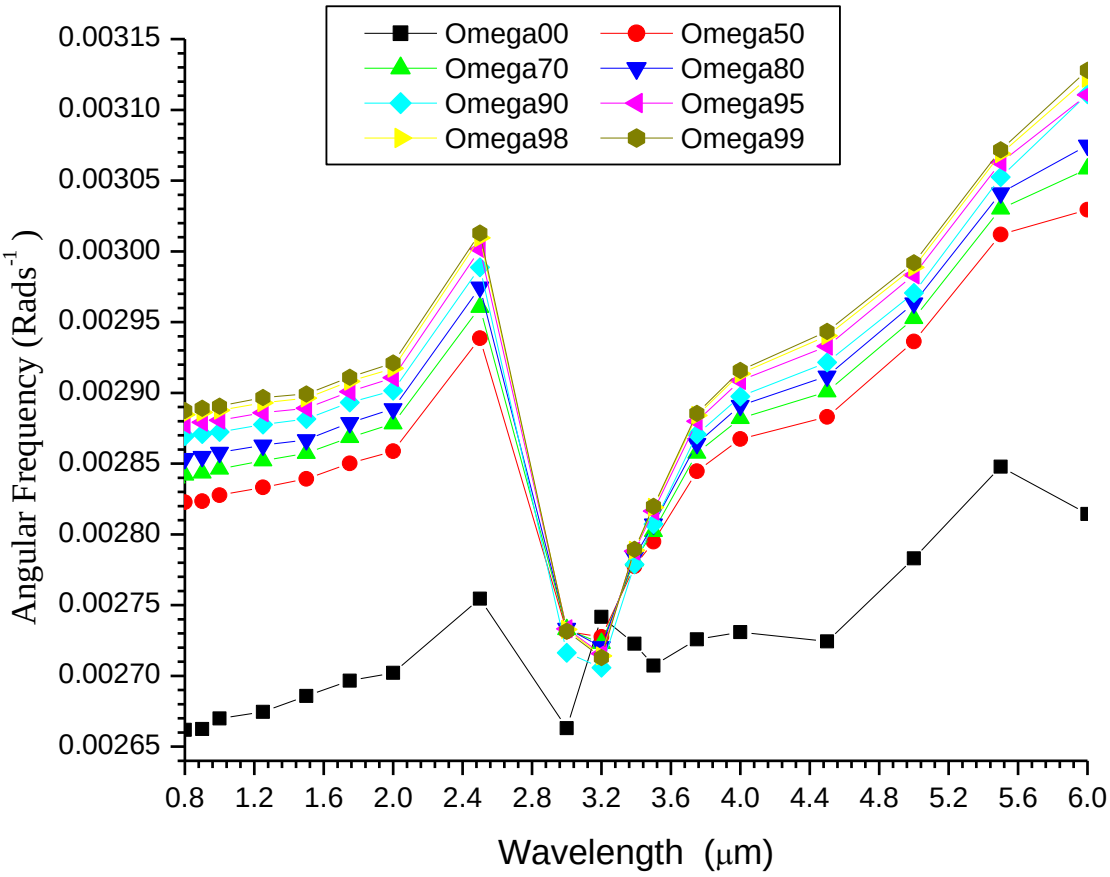

Figure 4. 69.A graph of variations of angular frequency (ω) with λ for Antarctic Aerosol at IR range.

4.3.2 Arctic Aerosols

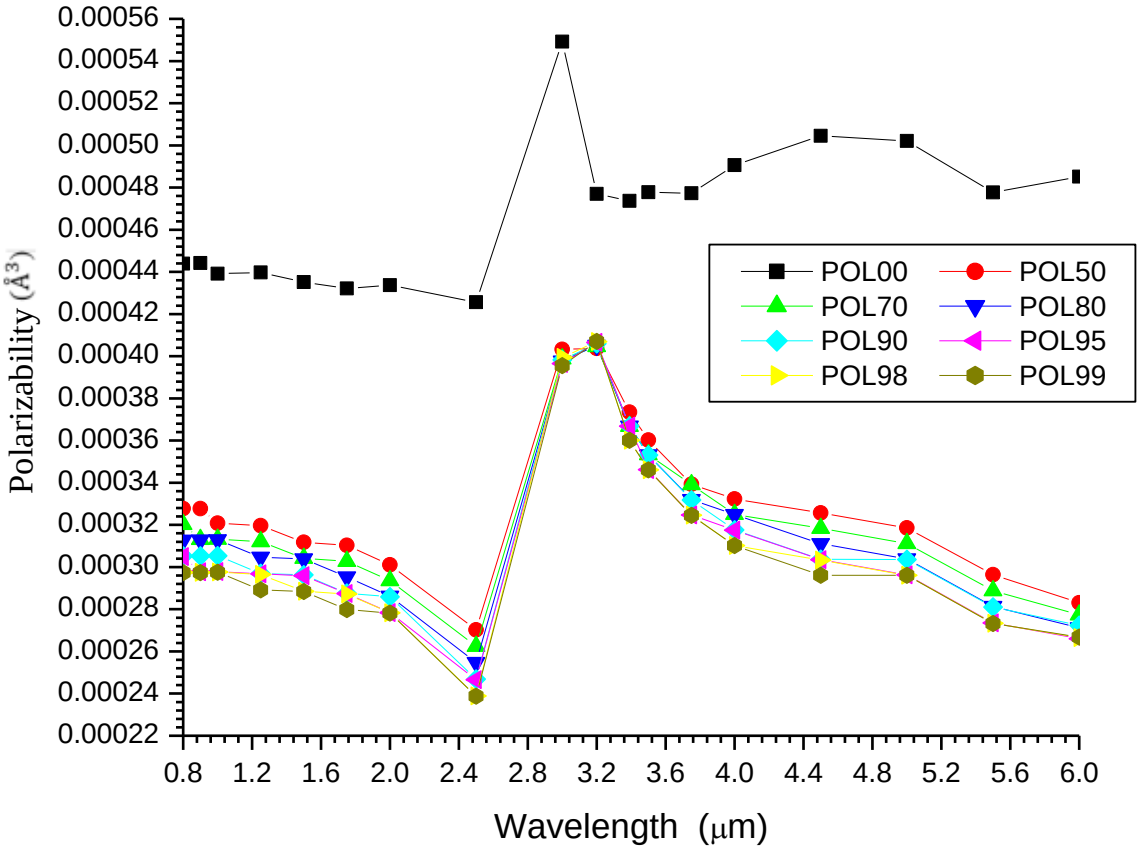

Figure 4. 30.A Plot of polarizabilities of Arctic aerosols with λ near infrared to medium spectral range.

From fig. 4.30, The polarizabilities decreases suddenly with the increase inλ and RH respectively. These effects fluctuate sinusoidally as λ increases.

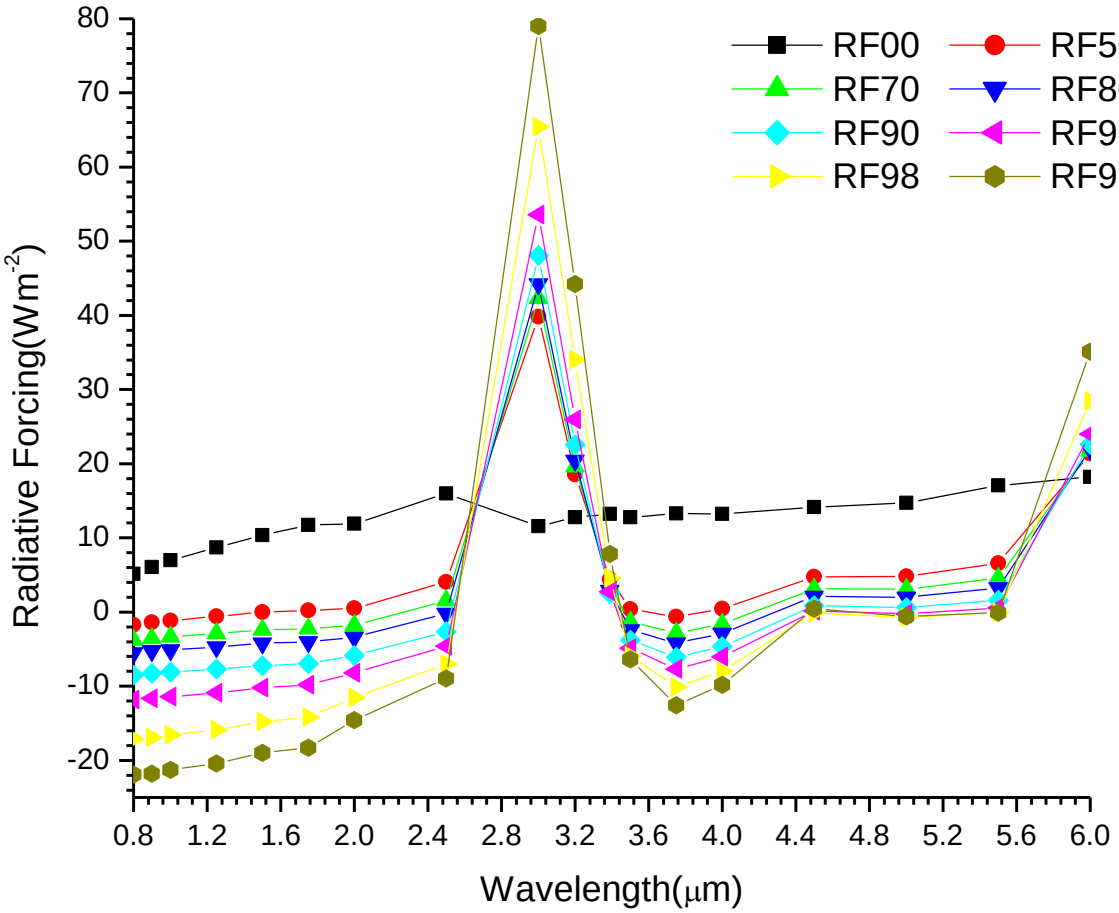

Figure 4. 31.A graph of Radiative forcing of arctic aerosols against wavelength near infrared to medium spectral range.

From figure 4.31, the warming effect occurred at 0% RH while the cooling effect begins to occurred at 50% RH, this effect increases with increase in RH from 0.8 to 2.4 μm of wavelength. The atmospheric window occurred between 2.4 to 3.5 μm except at 0% RH.The warming effect increases with decrease in RH.

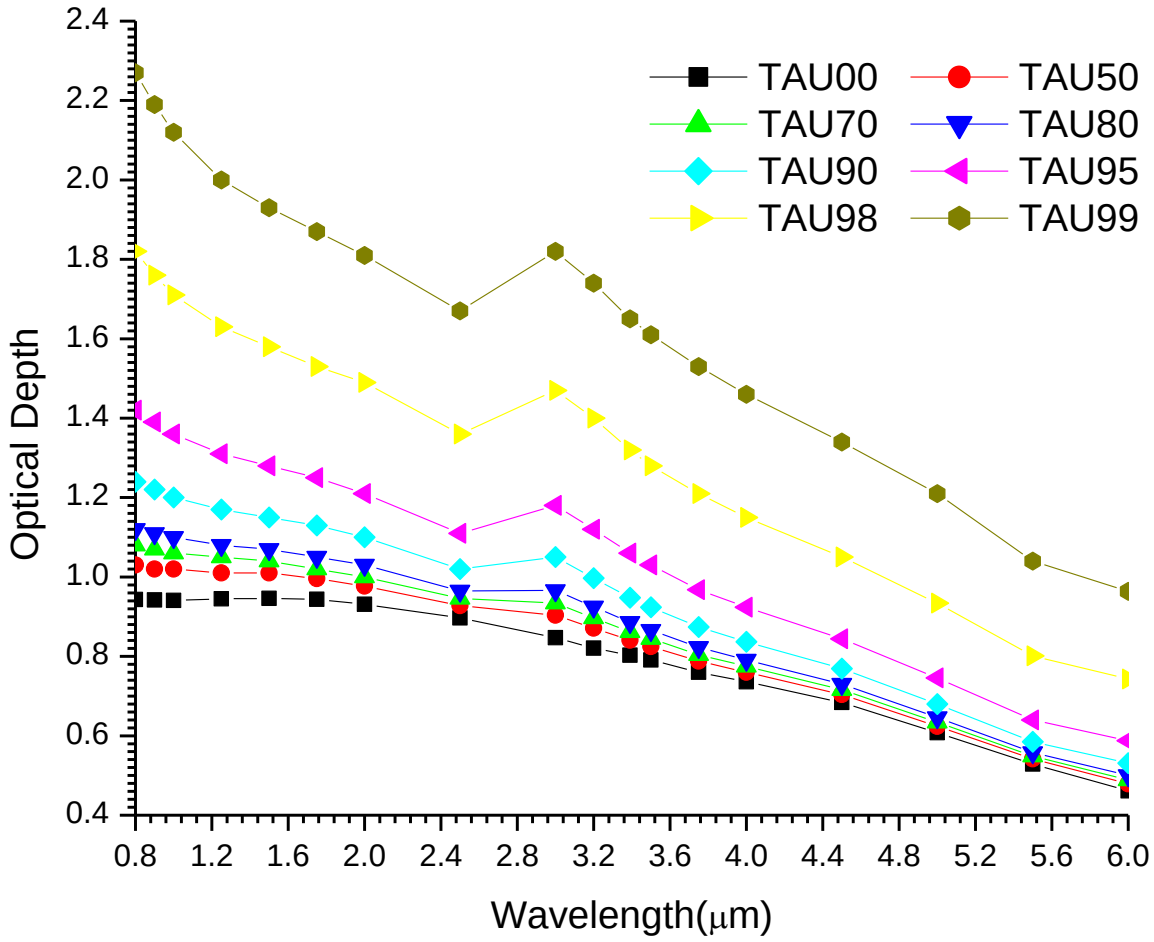

Figure 4. 32.A graph of variations of AOD with λ for Arctic Aerosol near IR.

Table 4. 8 Regression analysis of OD for Arctic aerosol near Infraredwavelength region

Near Infrared (0.8 to 6.0)							
	Linear			Quadratic			
RH(%)	alpha	Beta	R^2	Alpha1	Alpha2	Beta1	R^2
0	-0.2761	1.0194	0.6796	0.2444	-0.3332	0.9529	0.9610
50	-0.3044	1.1005	0.7248	0.2071	-0.3275	1.0300	0.9632
70	-0.3159	1.1418	0.7403	0.1916	-0.3249	1.0692	0.9628
80	-0.3261	1.1845	0.7526	0.1780	-0.3227	1.1096	0.9620
90	-0.3455	0.7284	0.7736	0.1494	-0.3169	1.2108	0.9585
95	-0.3630	1.4612	0.7922	0.1152	-0.3061	1.3734	0.9523
98	-0.3668	1.8298	0.8101	0.0639	-0.2758	1.7305	0.9403
99	-0.3431	0.8196	2.2388	0.0238	-0.2349	2.1349	0.9288

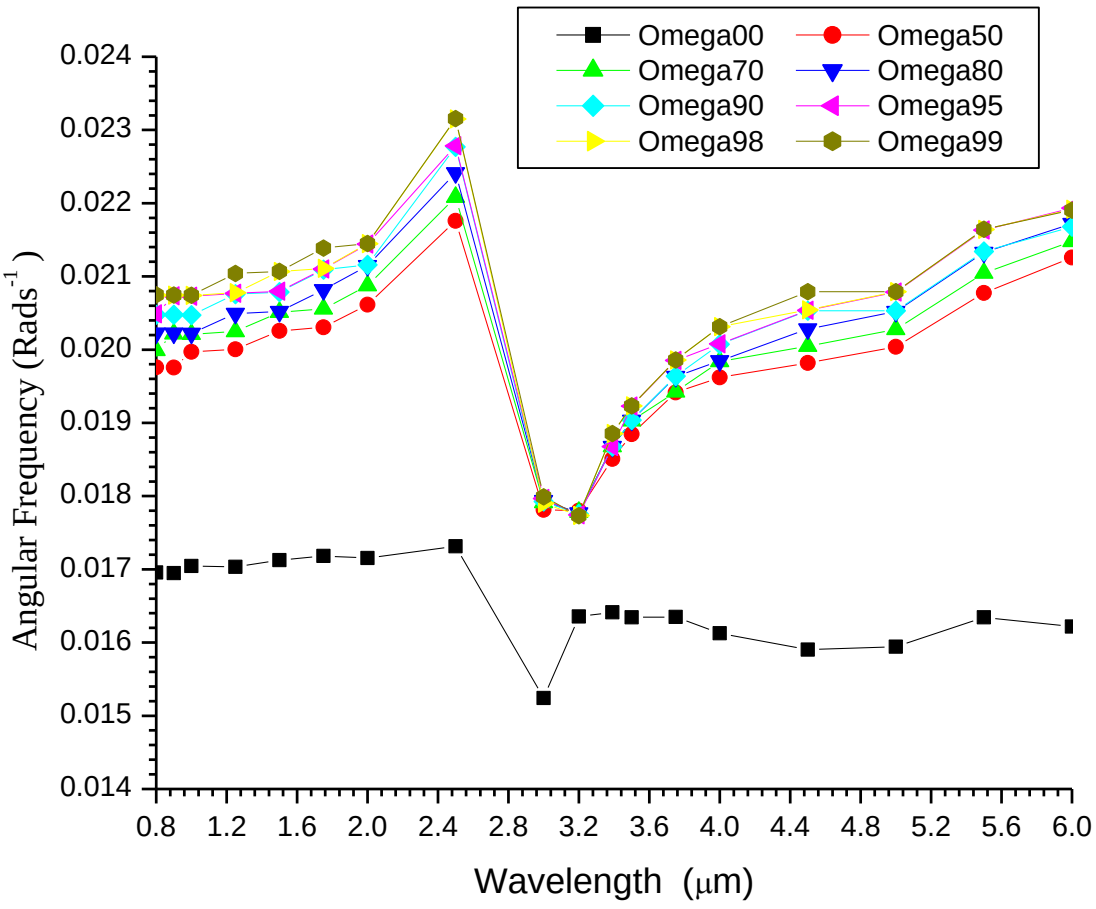

Figure 4. 7A graph of variations of angular frequency (ω) with λ for Artic Aerosol at IR range.

4.3.3 Continental cleanAerosol

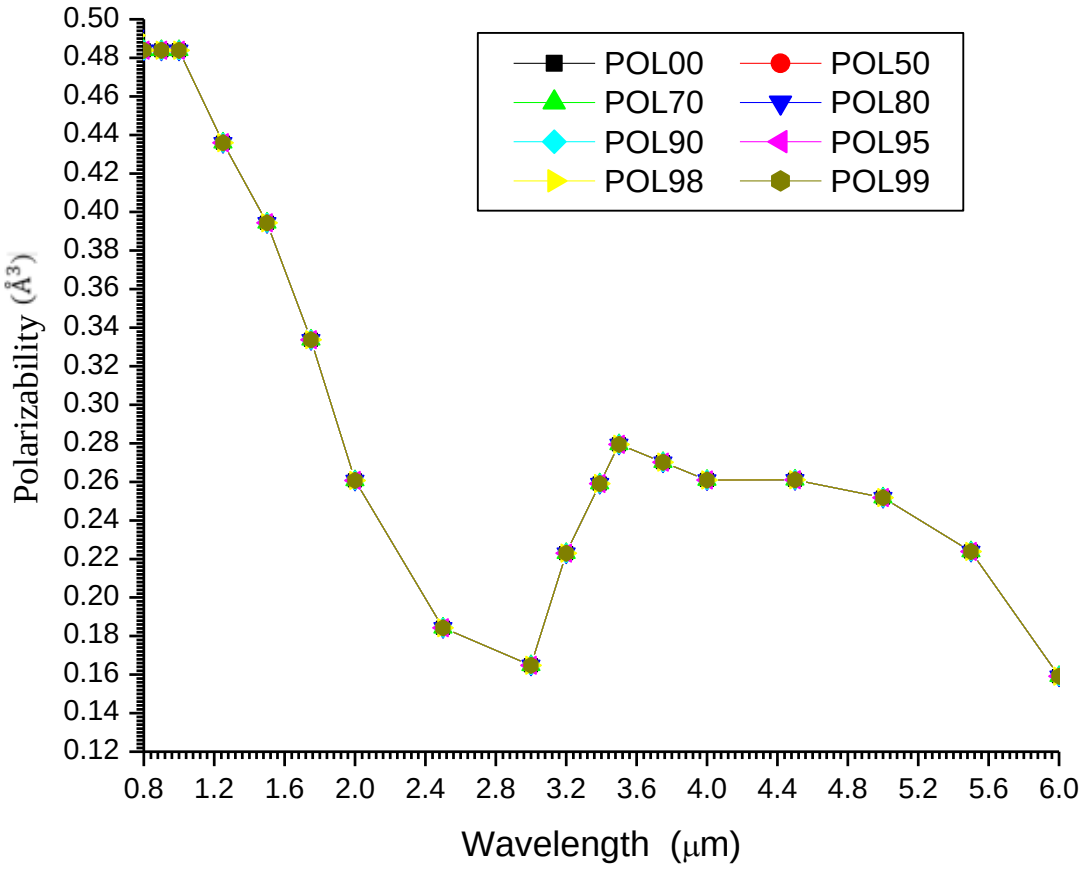

Figure 4. 34.A graph of variations of polarizabilities of continental clean aerosols against λ near infrared to medium spectral range.

From fig. 4.34, the polarizability changes with at least cubic form and decay with respect to λ. The effect of RH is negligible.

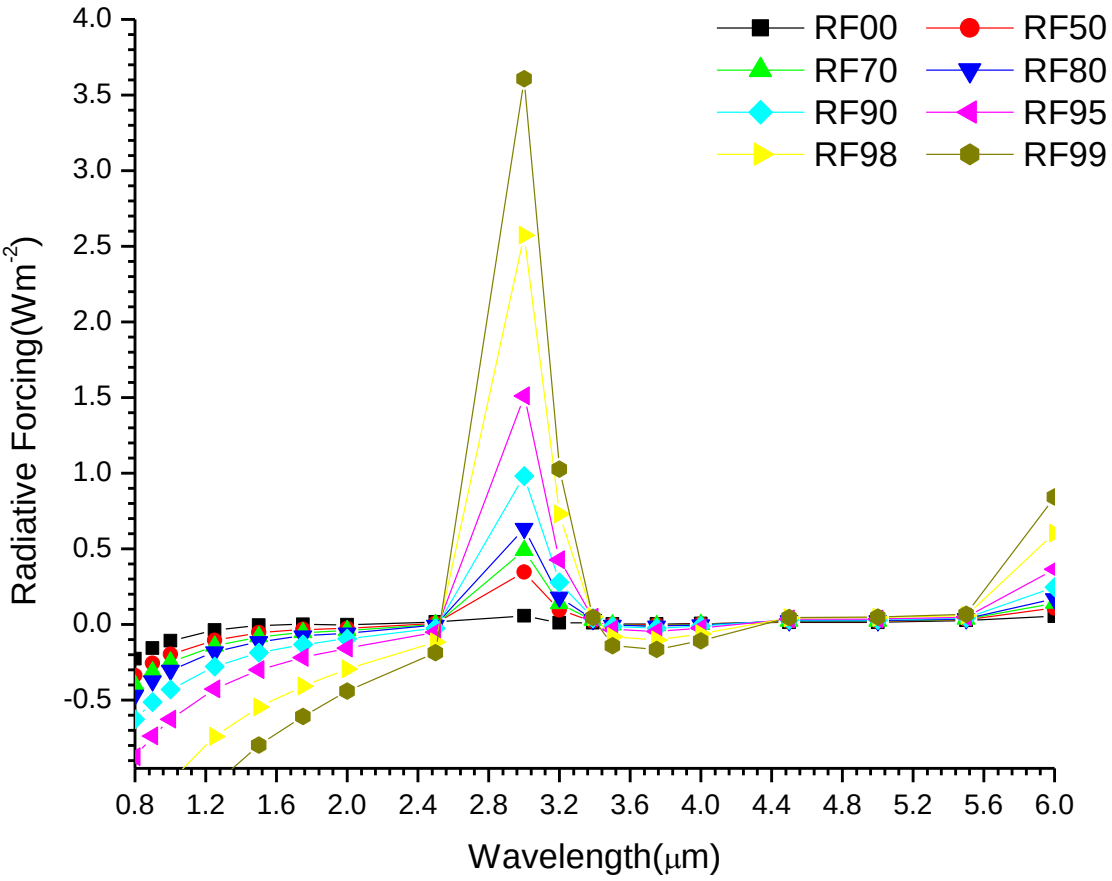

Figure 4. 35.A graph of Radiative forcing of Continental Clean Aerosols against wavelength.

From figure. 4.35, it can be observe that, the behavior of the RF can be describe in to three regions (0.8 to 2.4 μm, 2.4 to 3.4 μm and 3.4 to 6.0 μm).

In region I, the cooling effect occurred which decreases with increase in λ and increases with incresase in RH. In region II, the atmospheric window was occurred where the maximum warming effect was recorded and increases with increase in RH. In region III, neutral point slightly recorded with varnish gradually with increase in RH and λ respectively.

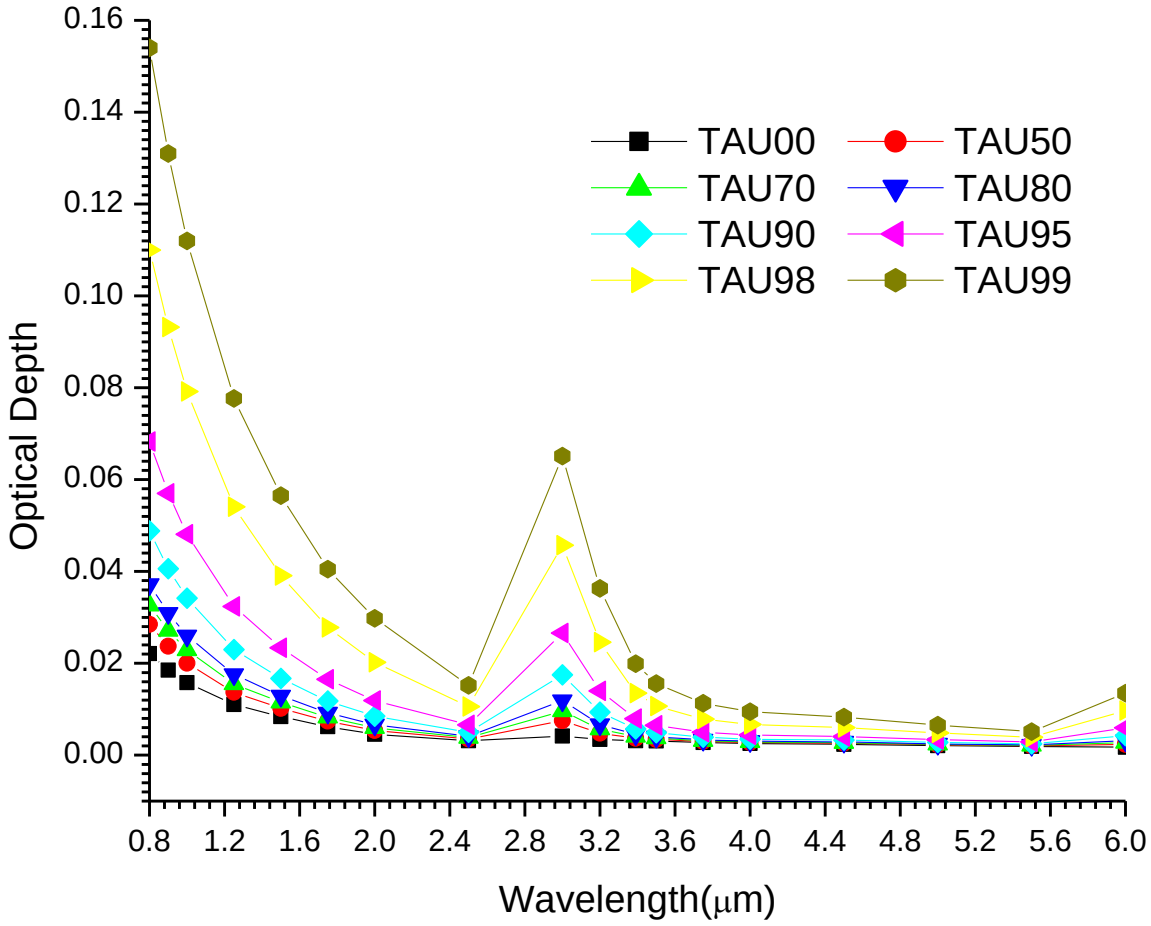

Figure 4. 34. A graph of variations of AOD with λ for Continental Clean near IR.

Table 4. 9Regression analysis of AOD for Continental Clean aerosol near Infraredwavelength region.

Near Infrared (0.8 to 6.0)μm							
	Linear			Quadratic			
RH(%)	α	β	R^2	α_1	α_2	β_1	R^2
0	1.2573	0.0148	0.9752	1.6406	-0.2496	0.0152	0.9871
50	1.2970	0.0187	0.9477	1.7012	-0.2633	0.0192	0.9598
70	1.3195	0.0213	0.9306	1.7301	-0.2674	0.0219	0.9425
80	1.3411	0.0241	0.9153	1.7524	-0.2679	0.0248	0.9266
90	1.3835	0.0317	0.8894	1.7785	-0.2573	0.0326	0.8989
95	1.4260	0.0448	0.8683	1.7708	-0.2245	0.0459	0.8750
98	1.4618	0.0745	0.8540	1.6967	-0.1530	0.0757	0.8569
99	1.4678	0.1063	0.8512	1.6144	-0.0955	0.1074	0.8523

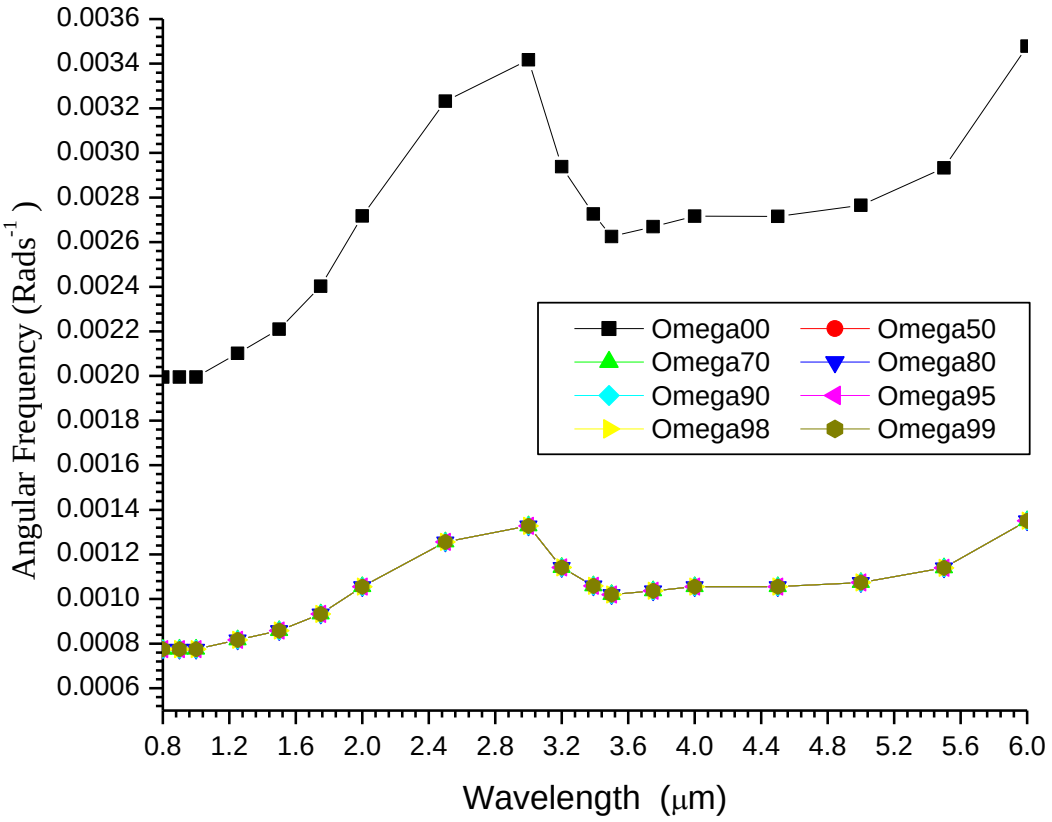

Figure 4. 37.A graph of variations of angular frequency (ω) with λ for continental clean Aerosol at IR range.

4.3.4 Maritime Tropical Aerosol

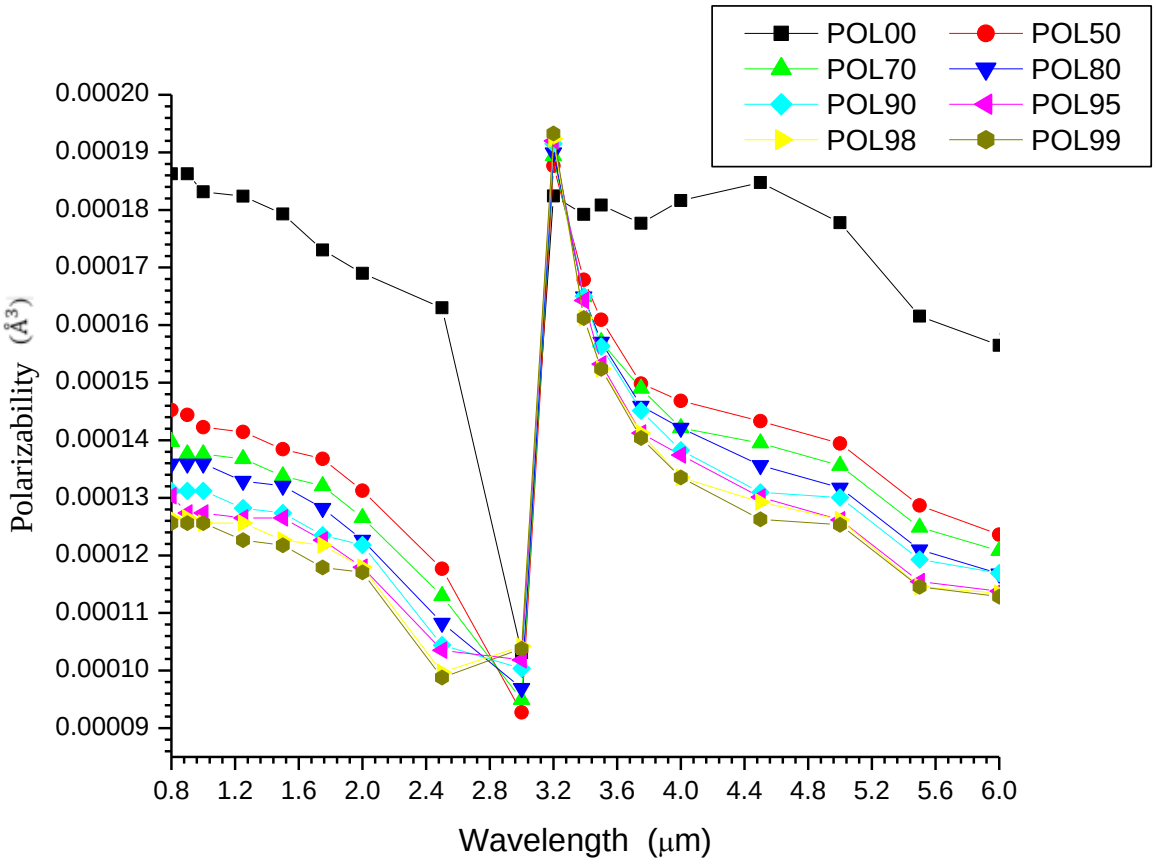

Figure 4. 38.A graph of polarizabilities of Maritime tropical aerosols againstλ near infrared to medium spectral range.

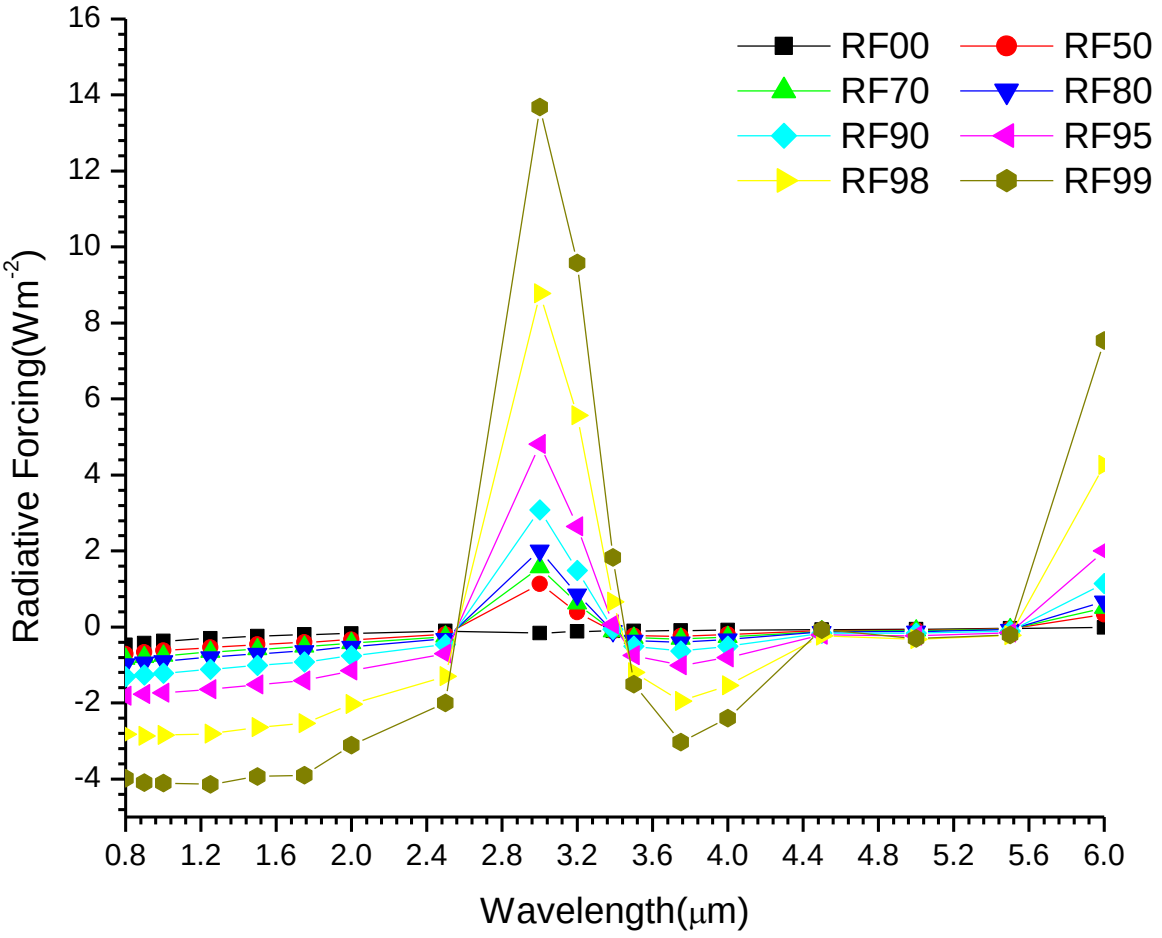

Figure 4. 39.A graph of Radiative forcing of Maritime tropical aerosols against wavelength near infrared to medium spectral range.

From figure 4.39, the cooling effect were recorded and increase with increase in RH up to $\lambda = 2.5$ μm. Atmospheric window occurred at 2.5 to 3.5 μm where the maximum warming effect were recorded which increases with increase in RH. The neutral point slightly recorded from 3.5 to 5.5 μm.

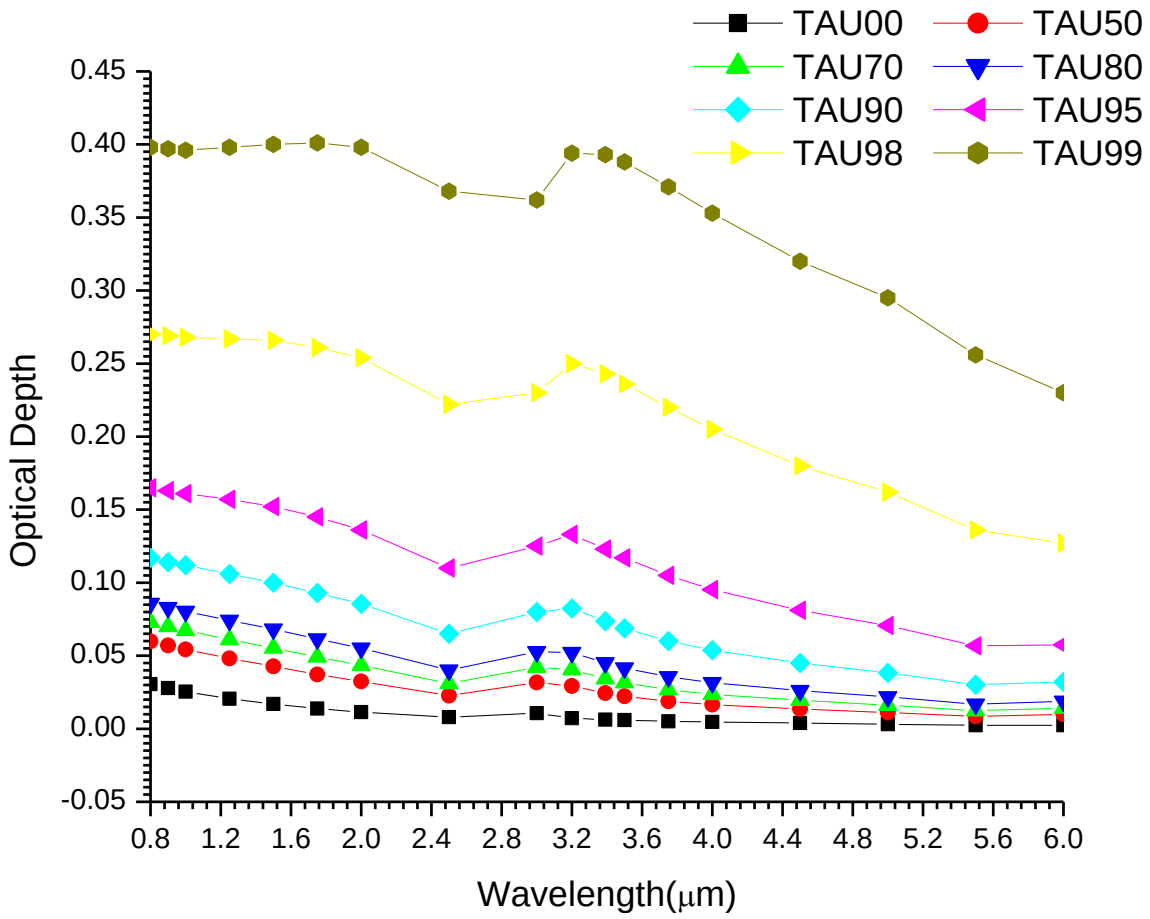

Figure 4. 40.A graph of variations of AOD with λ for Maritime Tropical near IR.

Table 4. 10 Regression analysis of AOD for Maritime Tropical aerosol near Infraredwavelength region.

Near Infrared to Visible (0.8 to 6)							
	Linear			Quadratic			
RH(%)	α	β	R^2	α_1	α_2	β_1	R^2
0	1.2715	0.0270	0.9636	0.7608	0.3269	0.0252	0.9817
50	0.9049	0.0585	0.8967	0.2703	0.4063	0.0539	0.9481
70	0.8137	0.0729	0.8774	0.1637	0.4162	0.0670	0.9426
80	0.7407	0.0873	0.8598	0.0824	0.4215	0.0801	0.9389
90	0.6093	0.1218	0.8219	-0.0460	0.4195	0.1119	0.9327
95	0.4729	0.1754	0.7679	-0.1559	0.4025	0.1617	0.9260
98	0.2963	0.2895	0.6468	-0.2464	0.3475	0.2698	0.8997
99	0.1823	0.4230	0.5004	-0.2616	0.2842	0.3994	0.8461

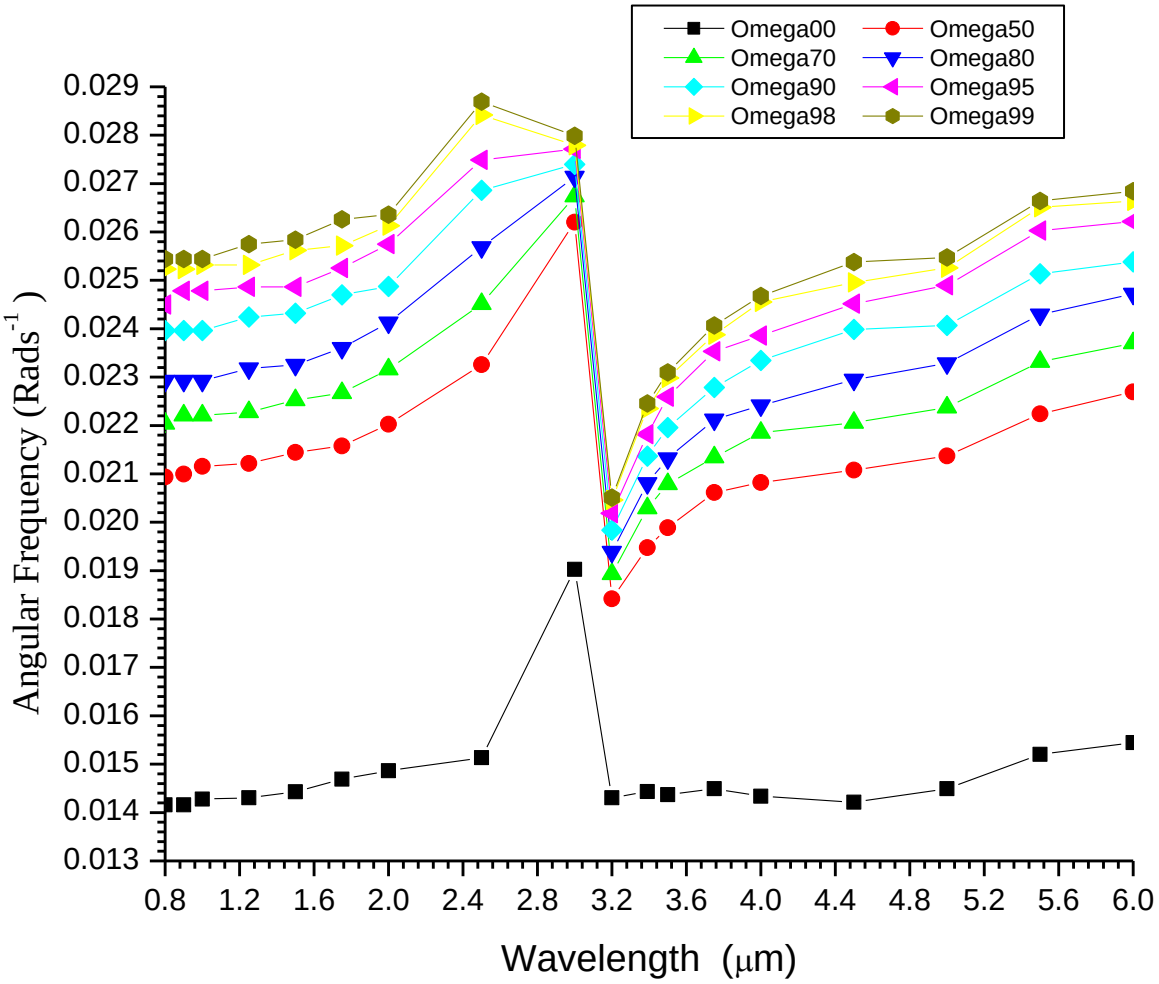

Figure 4. 41.A graph of variations of angular frequency (ω) with λ for maritime tropical Aerosol at IR range.

4.3.5 Sahara / Desert Aerosol

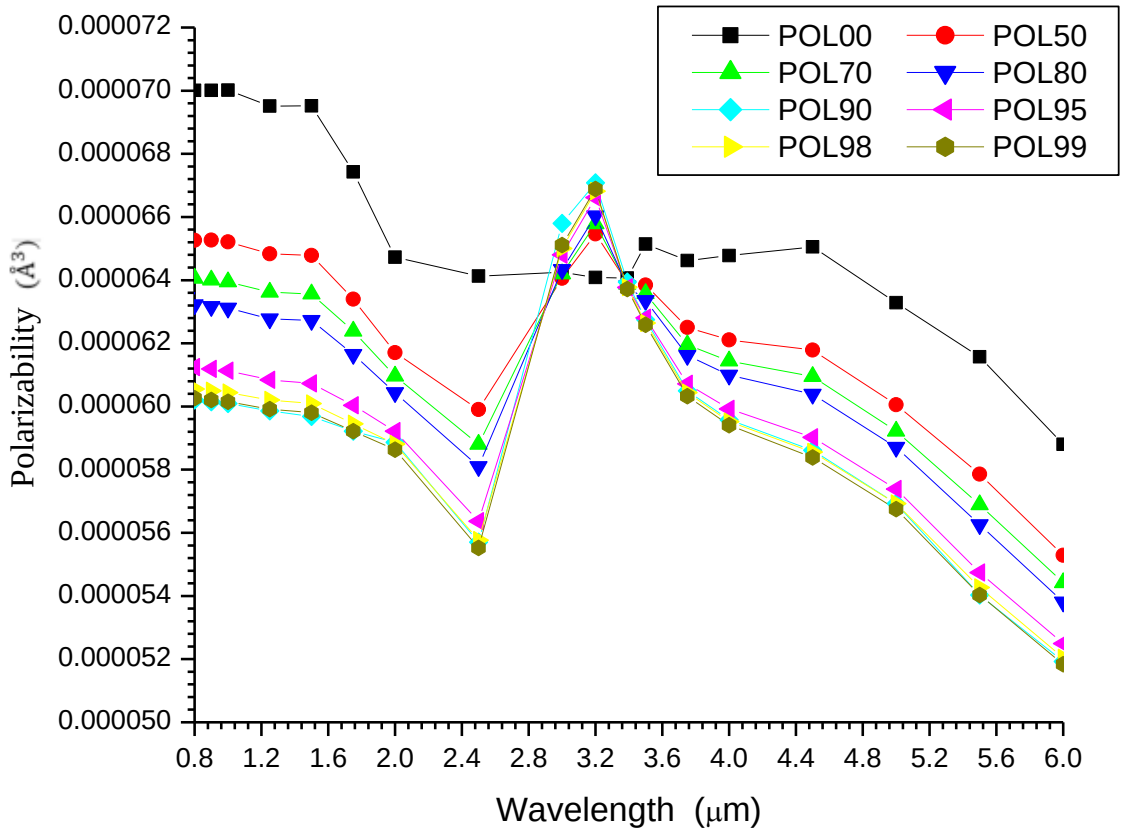

Figure 4. 42.A graph of polarizabilities of Sahara aerosols against λ near infrared to medium spectral range. .

From fig. 4.42, The polarizability decreases with increase in λ.

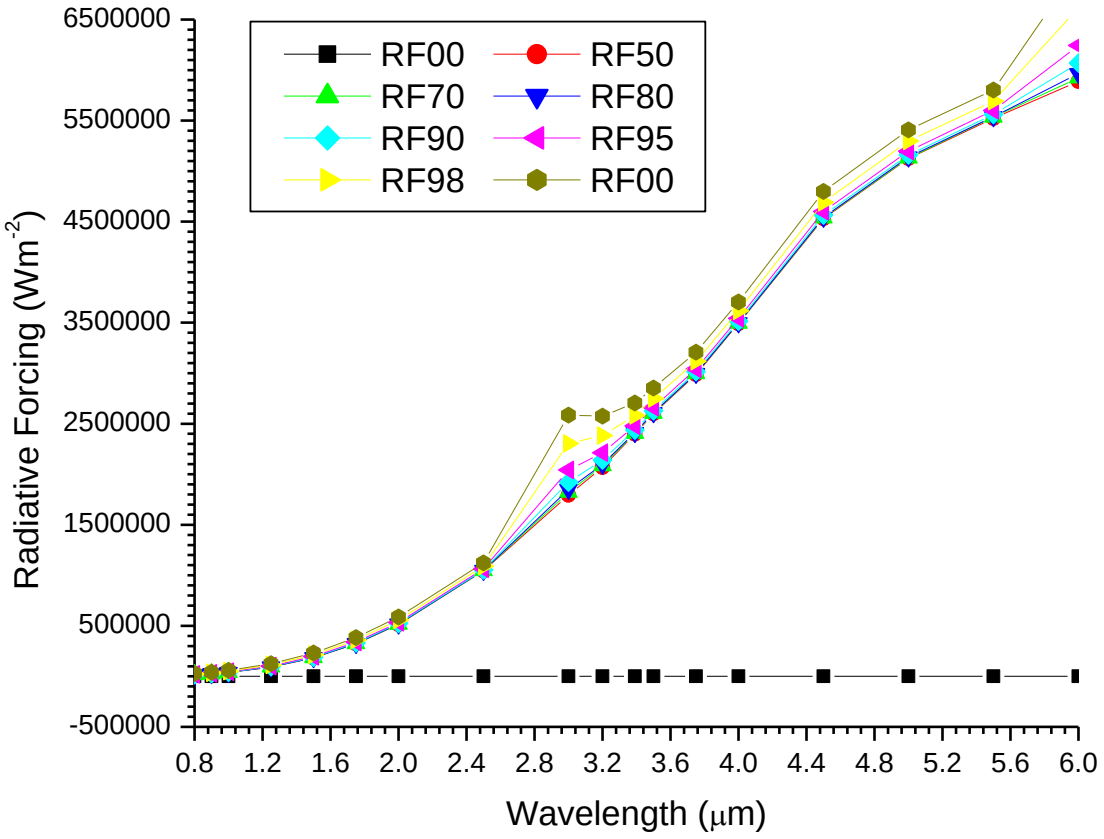

Figure 4. 43. A graph of Radiative forcing of Sahara aerosols against wavelength near infrared to medium spectral range.

From figure 4.43, at dry state, there are neutral point and it is constants with increase in λ. The warming effects occurred with increases in RH and λ.

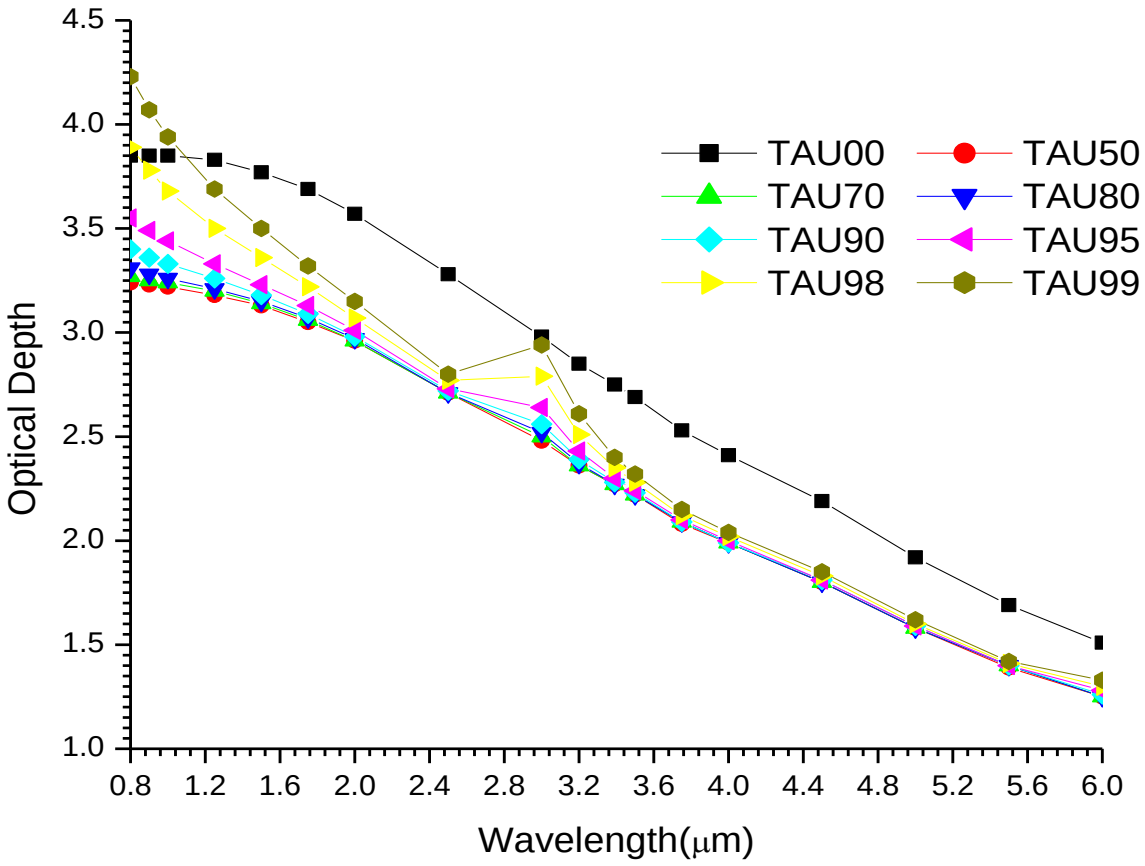

Figure 4. 44.A graph of variations of AOD with λ for Sahara near IR.

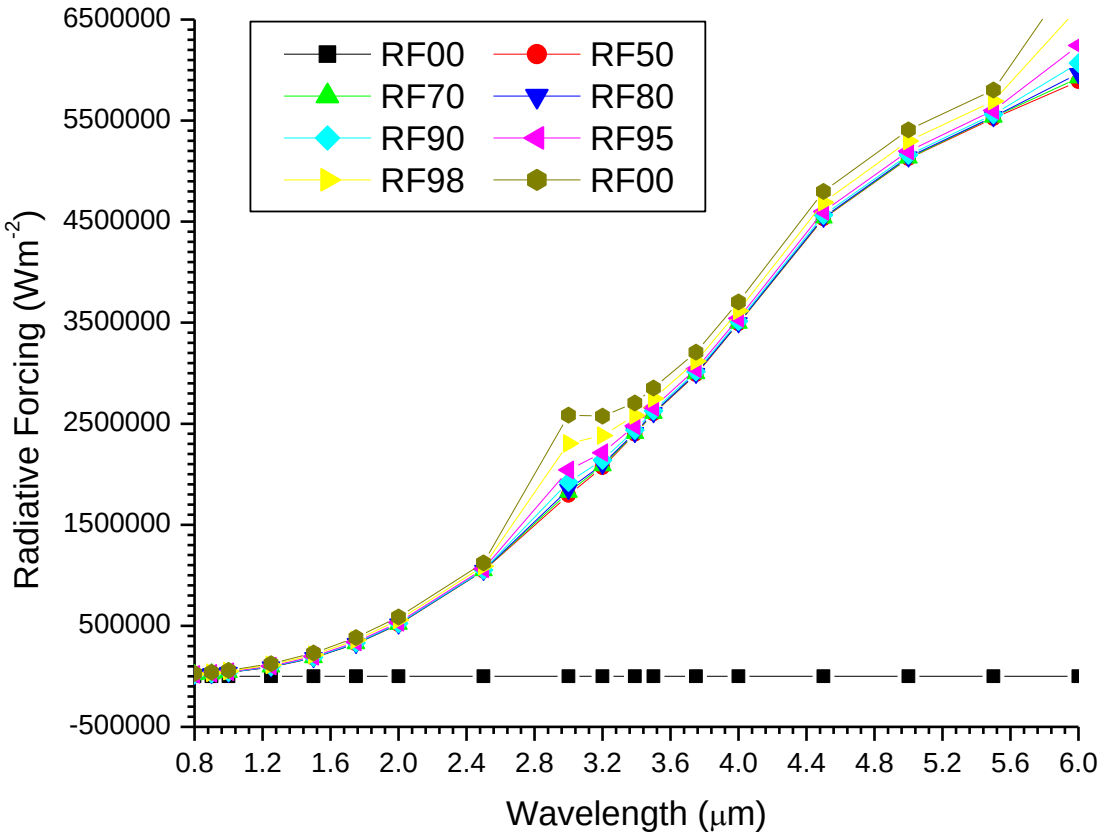

Figure 4. 8 A graph of Radiative forcing of Sahara aerosols against wavelength near infrared to medium spectral range.

From figure 4.45, at dry state, there are neutral point and it is constants with increase in λ. The warming effects occurred with increases in RH and λ.

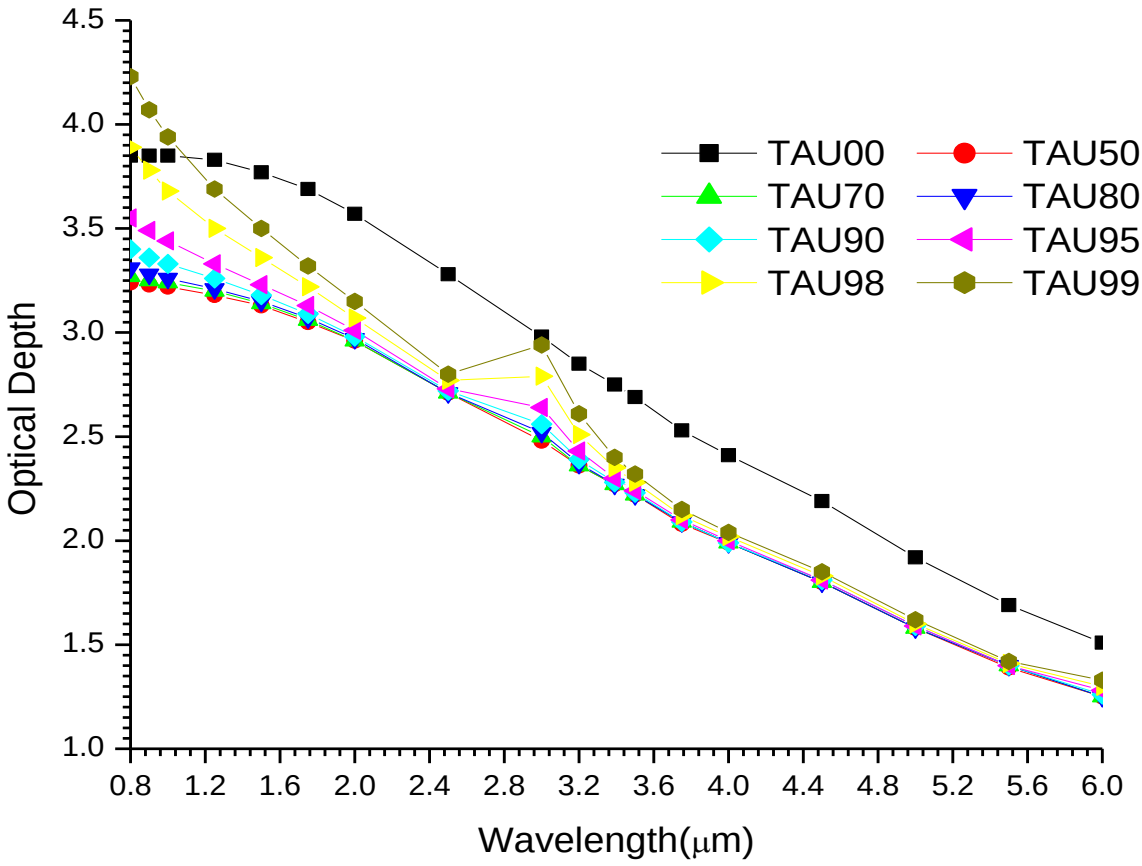

Figure 4. 46. A graph of variations of AOD with λ for Sahara near IR.

Table 4. 11Regression analysis of AOD for Sahara aerosol near Infraredwavelength region.

Near Infrared (0.8 to 6.0)							
	Linear			Quadratic			
RH(%)	α	β	R^2	α_1	α_2	β_1	R^2
0	0.4235	4.1911	0.8212	-0.1462	0.3652	3.8937	0.9942
50	0.4322	3.4994	0.8307	-0.1295	0.3601	3.2544	0.9940
70	0.4358	3.5218	0.8350	-0.1212	0.3571	3.2771	0.9938
80	0.4400	3.5469	0.8397	-0.1120	0.3539	3.3027	0.9934
90	0.4503	3.6119	0.8506	-0.0890	0.3457	3.3687	0.9925
95	0.4671	3.7222	0.8660	-0.0526	0.3332	3.4804	0.9908
98	0.5020	3.9680	0.8900	0.0175	0.3106	3.7271	0.9865
99	0.5352	4.2264	0.9055	0.0793	0.2923	3.9846	0.9820

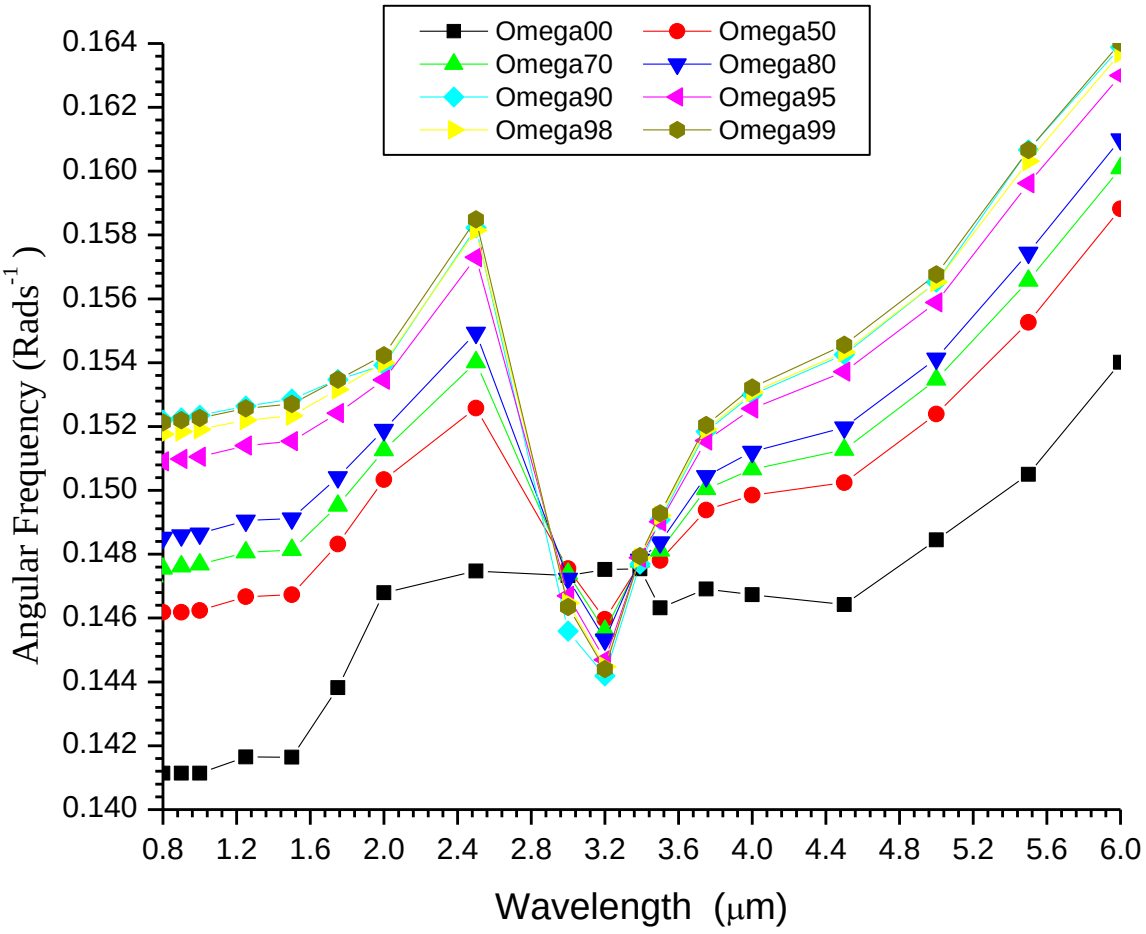

Figure 4. 47.A graph of variations of angular frequency (ω) with λ for Sahara Aerosol at IR range.

4.3.6 UrbanAerosol

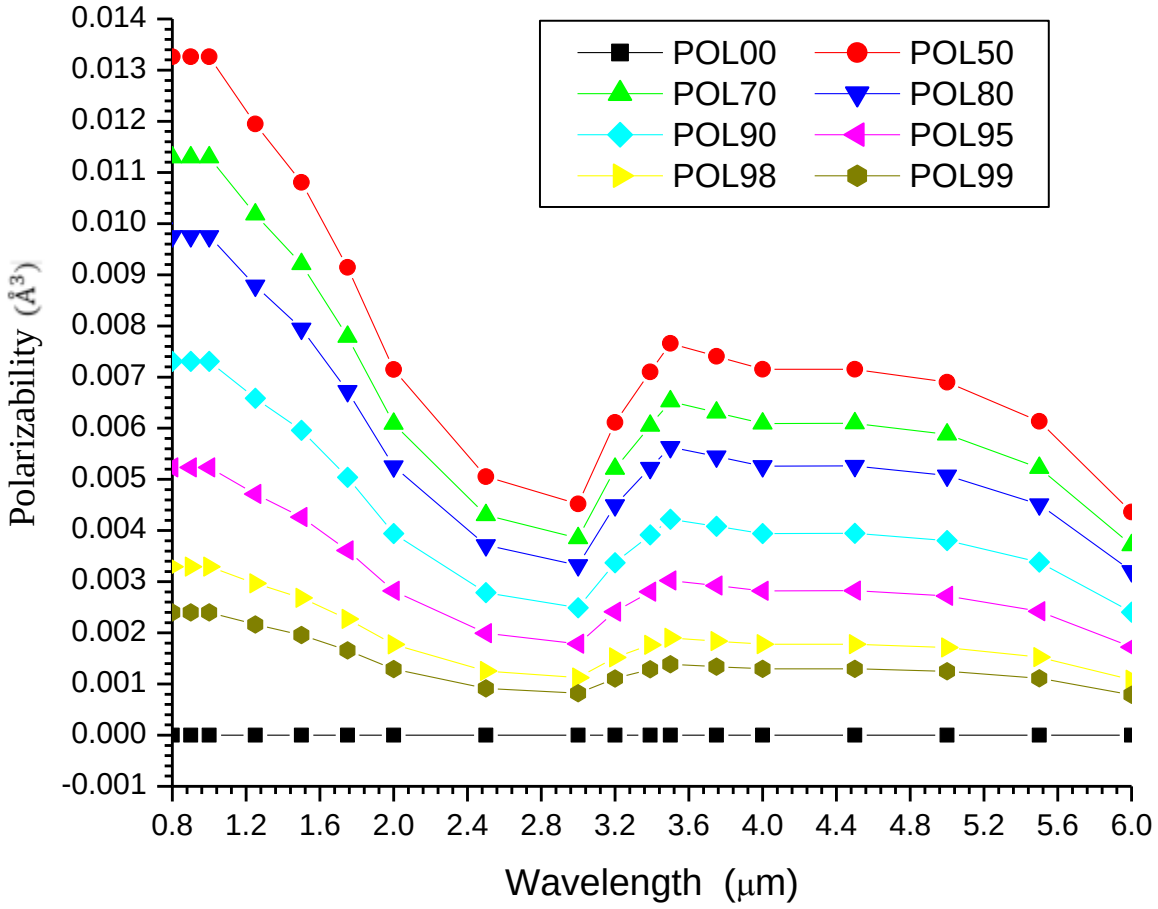

Figure 4. 48.A graph of variations of polarizabilities of Urban aerosols against wavelength near infrared to medium spectral range. .

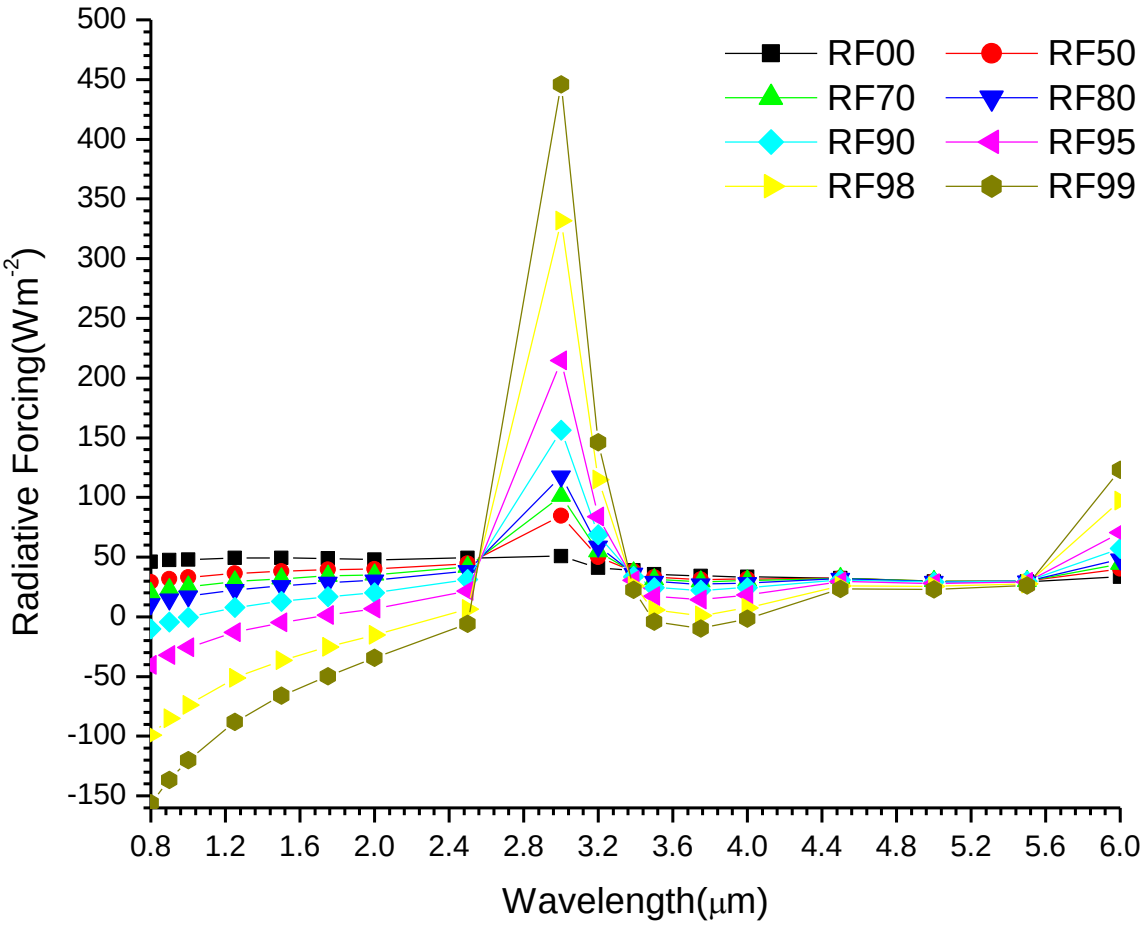

Figure 4. 49.A graph of Radiative forcing of Urban aerosols against wavelength near infrared to medium spectral range.

From figure 4.49, the warming effect occurred at 0 to 90% and decreases with increase in RH. The cooling effects begins to occurred at 95% to 99%. These effects decreased with increase in λ from 0.8 μm to 25 μm. The maximum warming effect occurred between 0.25 to 3.4 μm and increases with RH. The warming condition falls to minimum and does not varies significantly with λ.

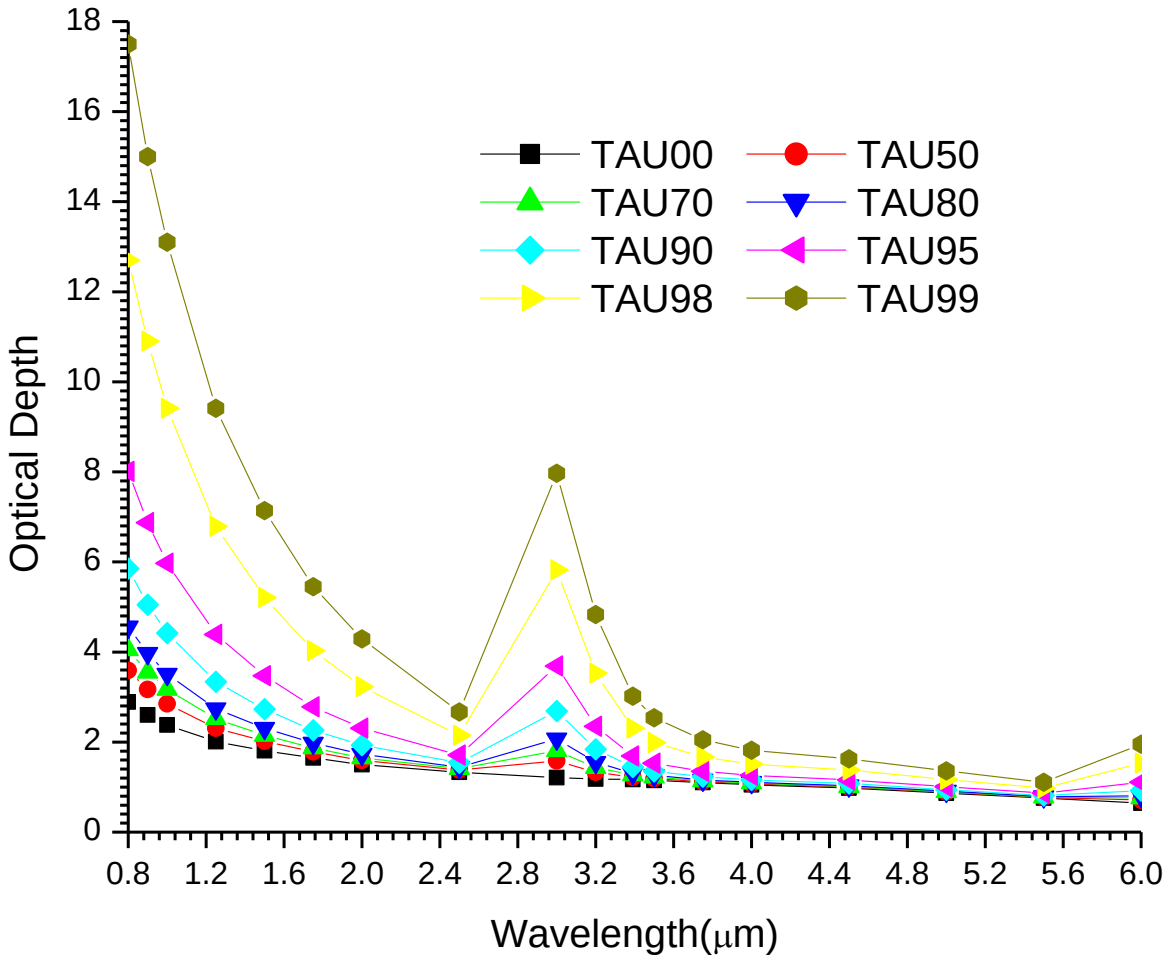

Figure 4. 9A graph of variations of AOD with λ for Urban near IR.

Table 4. 12 Regression analysis of AOD for Urban aerosol near Infraredwavelength region.

Near Infrared (0.8 to 6.0)							
	Linear			Quadratic			
RH(%)	α	β	R^2	α_1	α_2	β_1	R^2
0	0.6464	0.8868	0.9803	0.5555	0.0582	0.8751	0.9826
50	0.7269	1.0543	0.9751	0.7017	0.0162	1.0511	0.9753
70	0.7717	1.1508	0.9641	0.7775	-0.0037	1.1515	0.9641
80	0.8159	1.2481	0.9517	0.8478	-0.0204	1.2522	0.9518
90	0.9095	1.4649	0.9260	0.9819	-0.0464	1.4743	0.9267
95	1.0223	1.7539	0.9000	1.1127	-0.0579	1.7656	0.9009
98	1.1687	2.2071	0.8756	1.2215	-0.0339	2.2140	0.8758
99	1.2500	2.5394	0.8656	1.2390	0.0070	2.5380	0.8656

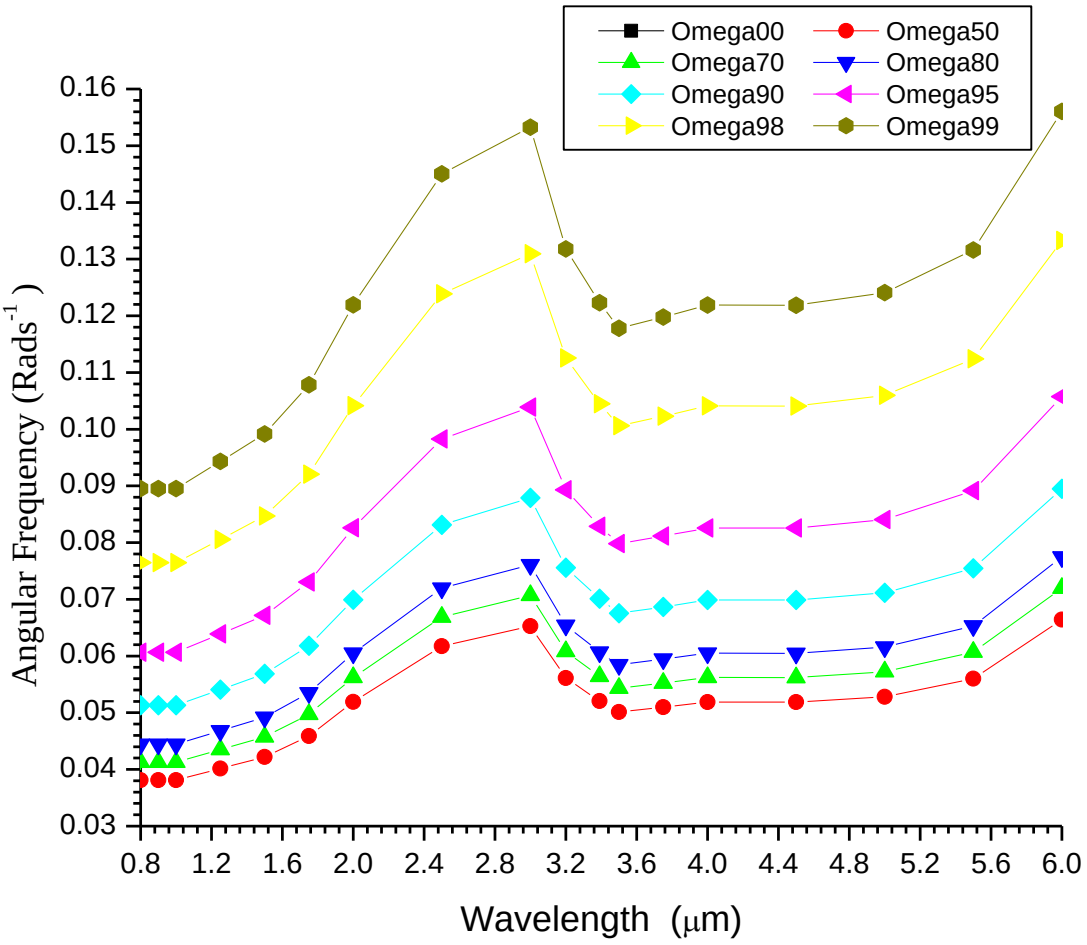

Figure 4. 51.A graph of variations of angular frequency (ω) with λ for Urban Aerosol at IR range.

4.4 PART III Far Infrared (6.0 - 40.0 μm)

4.4.1 AntarcticAerosol

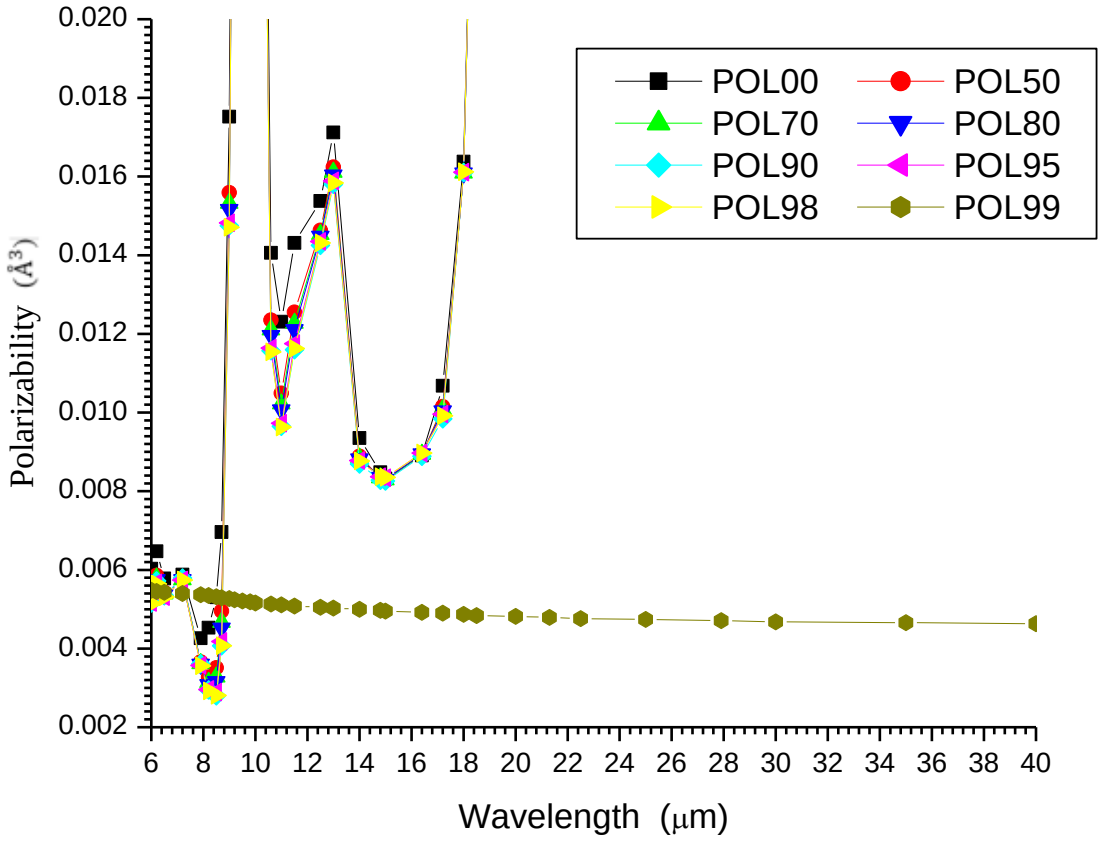

Figure 4. 10 A graph of polarizabilities of Antarctic aerosols against wavelength at far infrared spectral range.

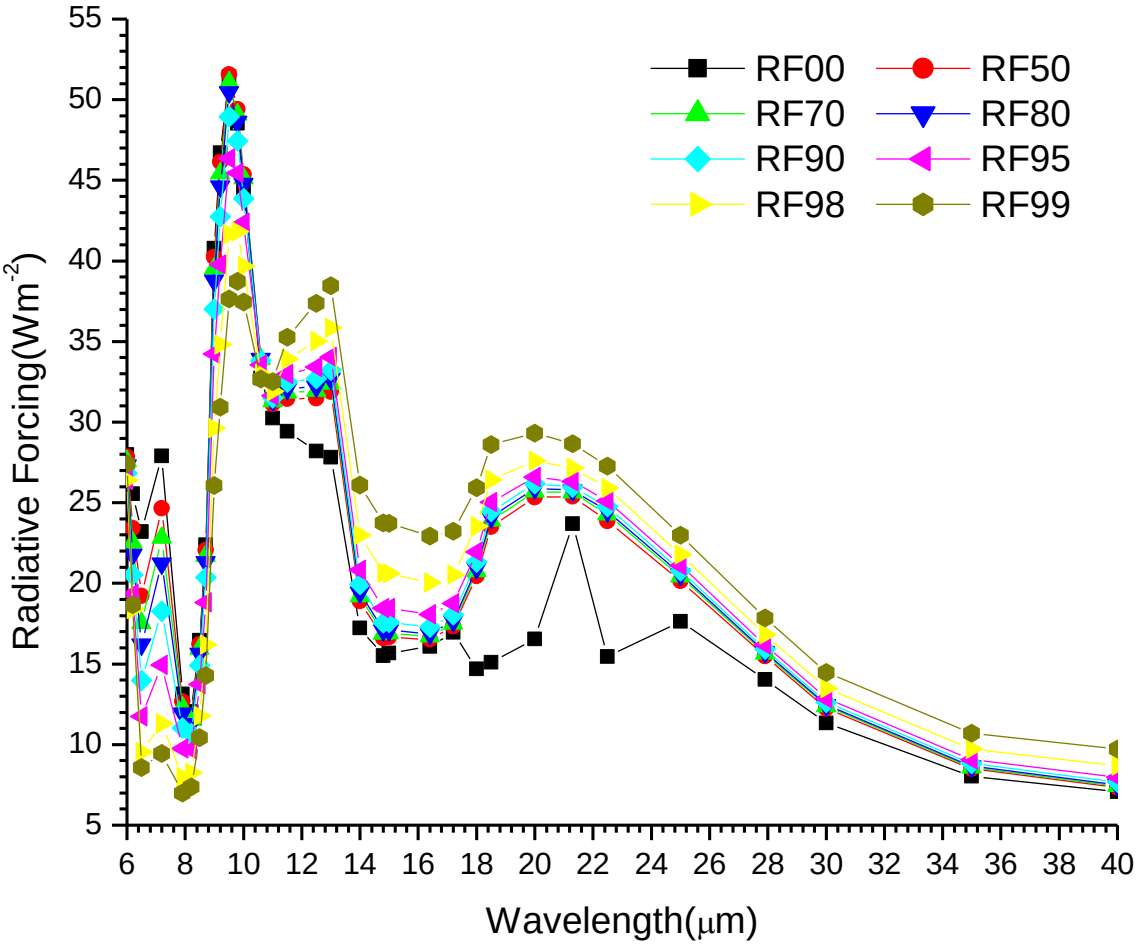

Figure 4.53. A graph of Radiative forcing of Antarctic aerosols against wavelength at far infrared region.

From figure 4.53. The warming effect was observed and decreases with increase in RH. It varies sinusoidally with λ.

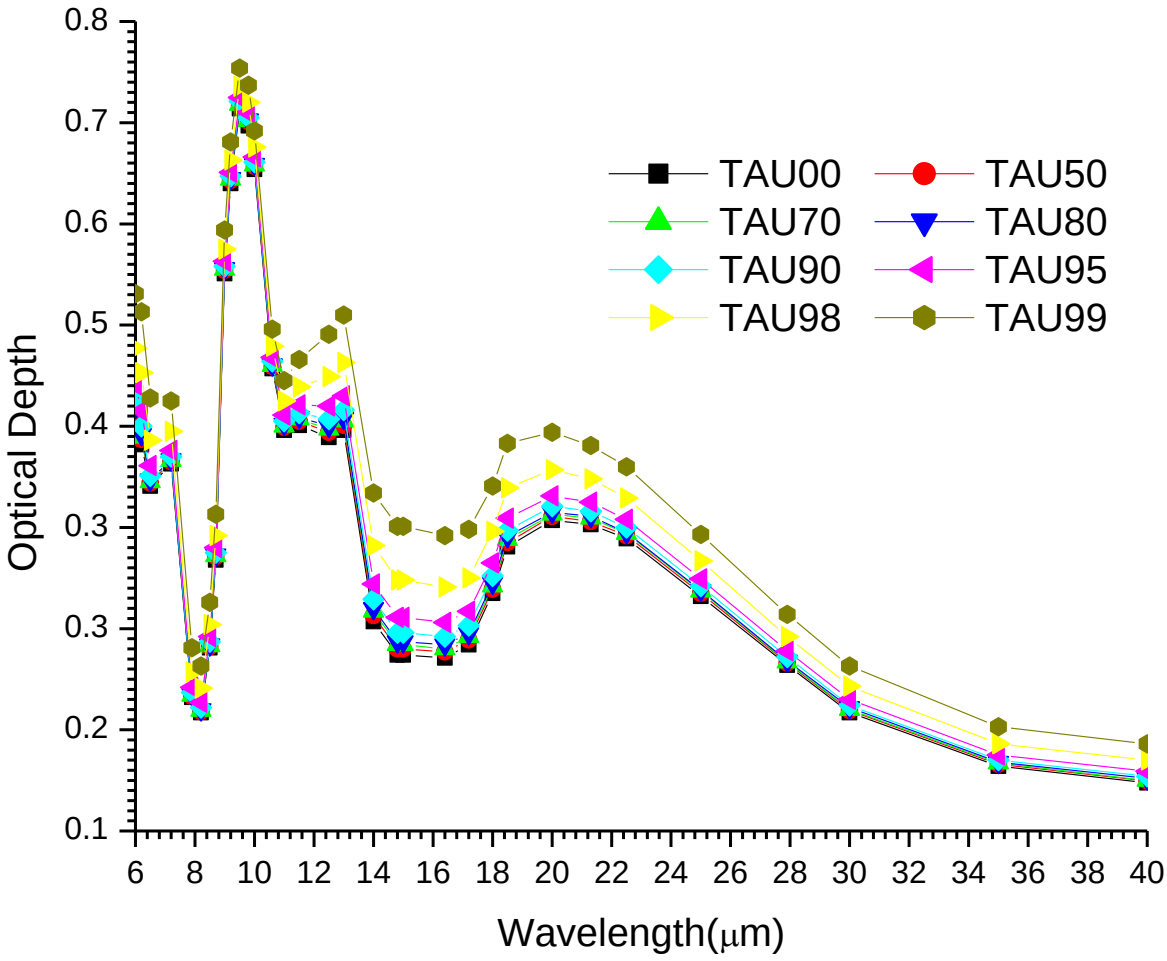

Figure 4. 54.A graph of variations of AOD with λ for Antarctic Aerosol at far IR region.

Table 4. 13 Regression analysis of AOD for Antarctic aerosol at far Infraredwavelength band.

Far Infrared (6.0 to 40.0)							
	Linear			Quadratic			
RH(%)	α	β	R^2	α_1	α_2	β_1	R^2
0	0.58863	1.48501	0.34182	-2.86192	0.64209	0.01709	0.45522
50	0.58293	1.47957	0.34002	-2.89572	0.64732	0.01642	0.45691
70	0.57931	1.47526	0.33907	-2.91447	0.65013	0.01605	0.45813
80	0.57567	1.47096	0.33826	-2.92762	0.65191	0.01581	0.45919
90	0.56772	1.46331	0.33678	-2.95894	0.65625	0.01526	0.46223
95	0.18291	2.36267	0.27713	-0.69016	0.16246	0.76343	0.33808
98	0.52831	1.45025	0.33379	-3.04938	0.66575	0.01415	0.48156
99	0.49913	1.46869	0.33558	-3.04558	0.65961	0.01496	0.49897

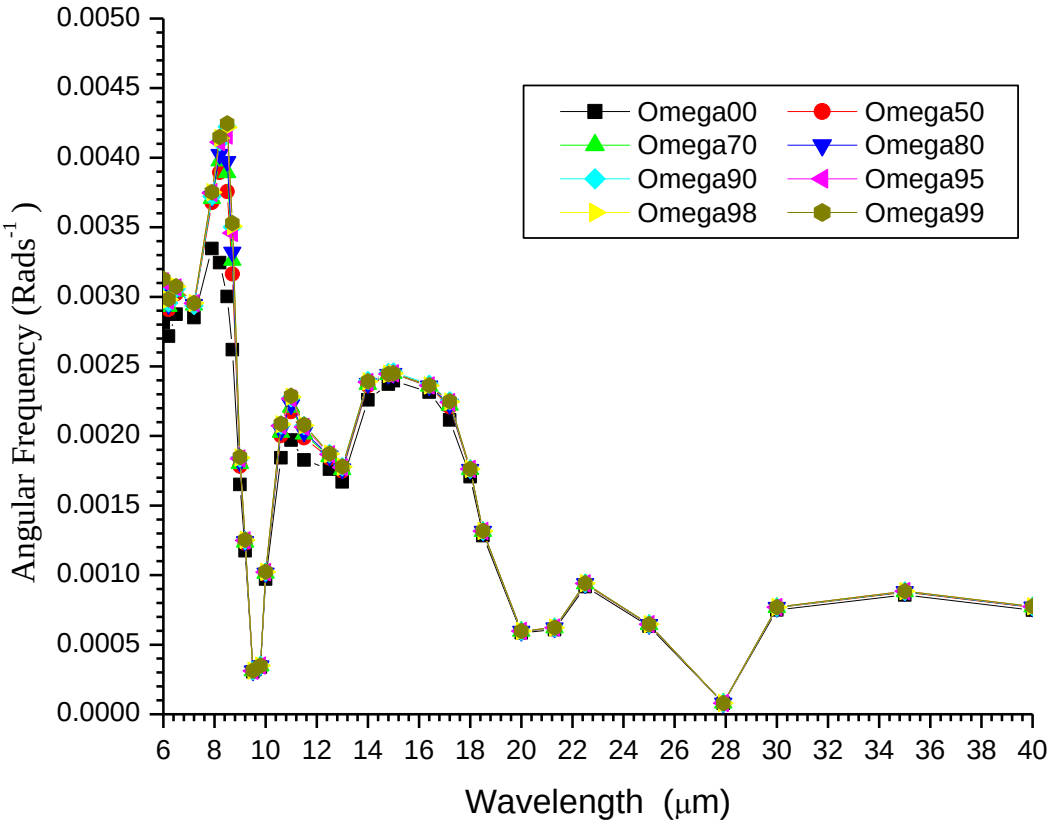

Figure 4. 11A graph of variations of angular frequency (ω) with λ for Antarctic Aerosol at far IR range.

4.4 .2 ArcticAerosols

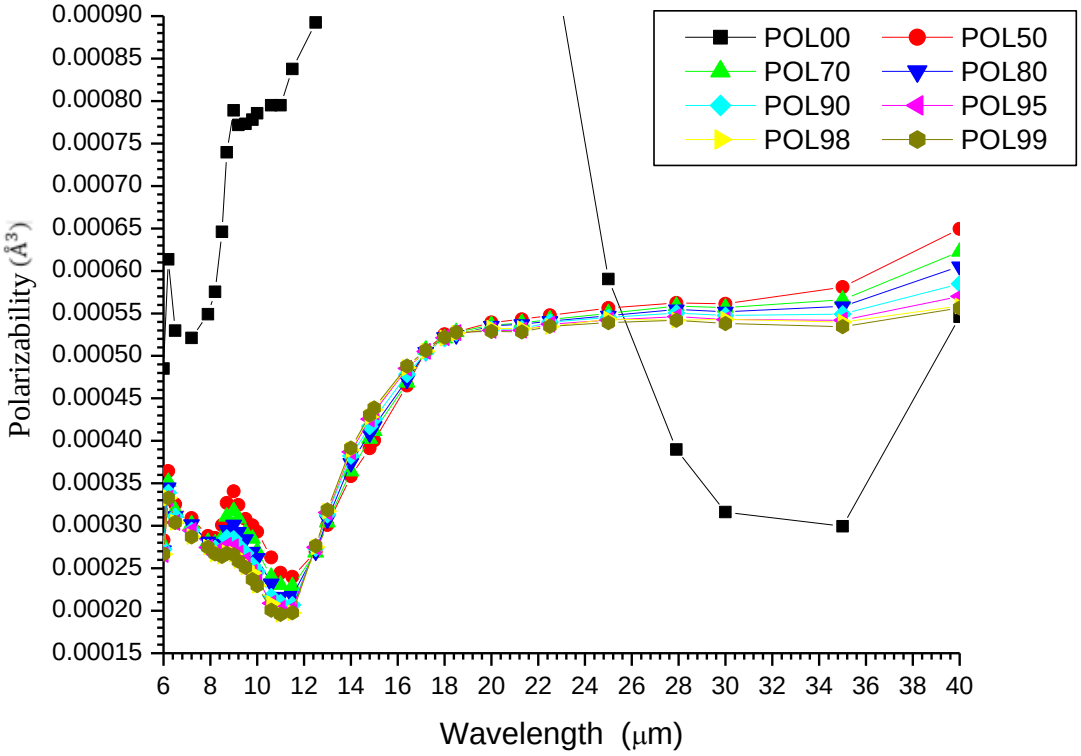

Figure 4. 56. A graph of polarizabilities of Arctic aerosols against wavelength at far infrared spectral region.

From figure 4.56, The polarizability increases with increase in λ. The polarizabilities decreases with increase in RH.

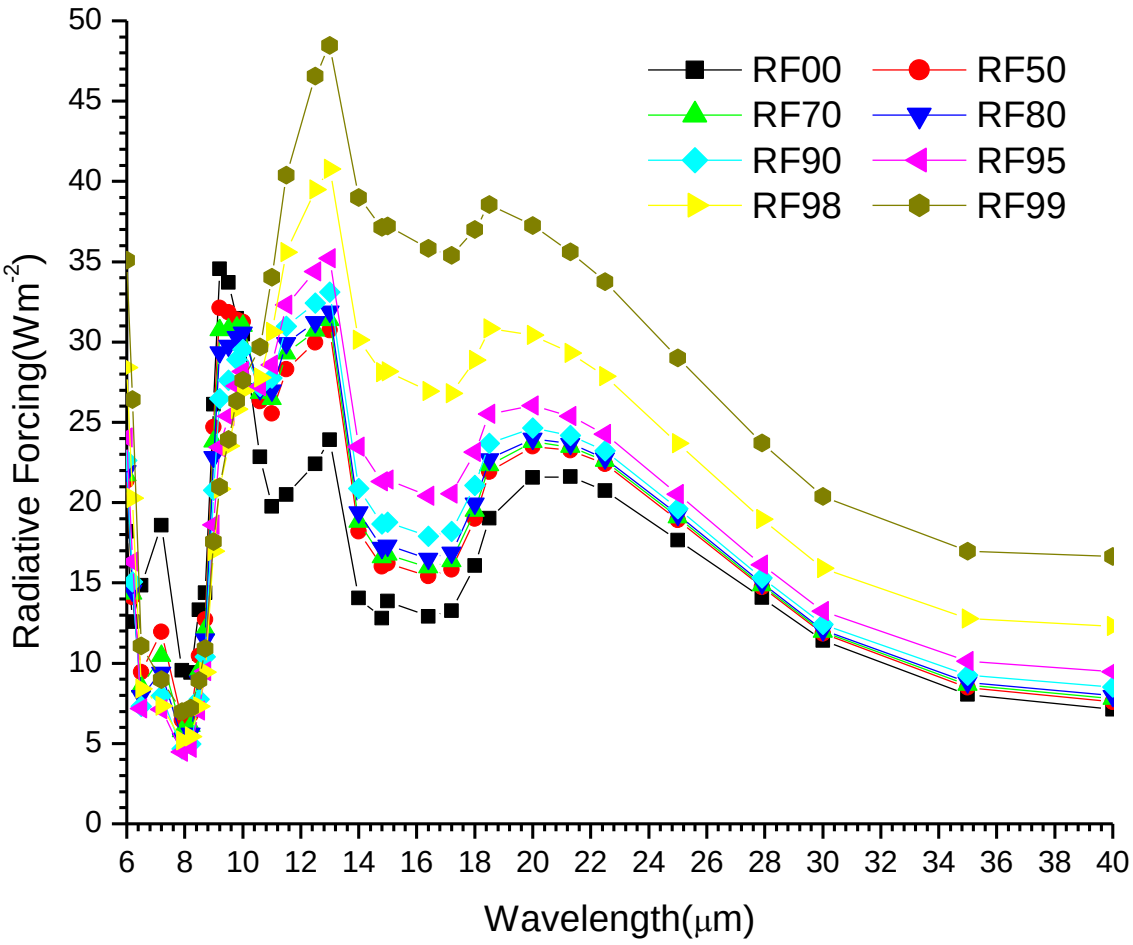

Figure 4. 12 A graph of Radiative forcing of Arctic aerosols against wavelength at far infrared region.

From figure 4.57, the warmingeffect increases with decrease in RH and varies sinusoidally with while the increase in λ.

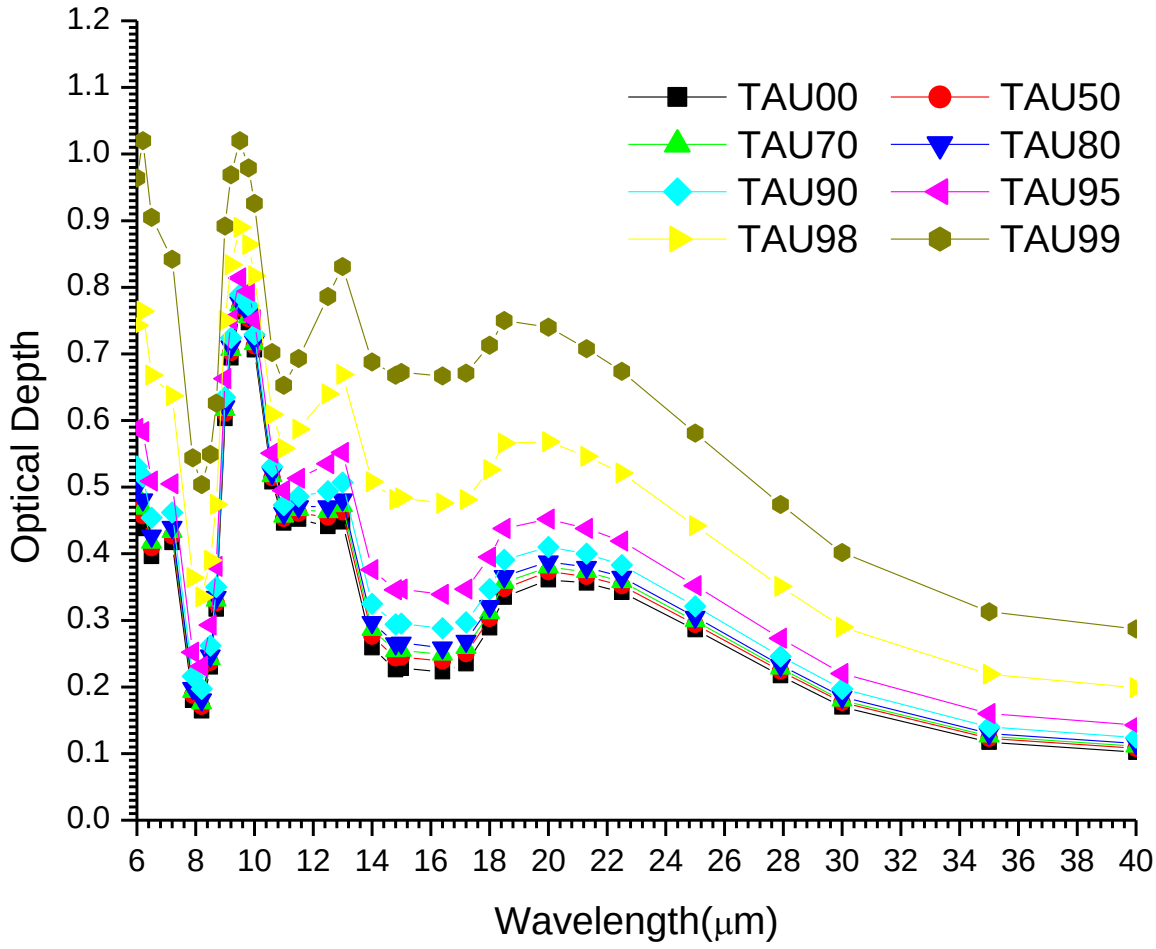

Figure 4. 13A graph of variations of AOD with λ for Arctic Aerosol at far IR region.

Table 4. 14Regression analysis of AOD for Arctic aerosol at far Infrared wavelength band.

Far Infrared (6.0 to 40.0)							
Linear				Quadratic			
RH(%)	α	β	R^2	α_1	α_2	β_1	R^2
0	-0.5752	1.4452	0.3321	2.7772	-0.6238	0.0189	0.4410
50	-0.5625	1.4484	0.3350	2.7945	-0.6247	0.0188	0.4502
70	-0.5560	1.4528	0.3372	2.7995	-0.6244	0.0189	0.4558
80	-0.5495	1.4599	0.3401	2.8016	-0.6236	0.0191	0.4622
90	-0.5335	1.4844	0.3492	2.7766	-0.6160	0.0205	0.4790
95	-0.5100	1.5438	0.3691	2.6731	-0.5923	0.0251	0.5079
98	-0.4639	1.7302	0.4231	2.2887	-0.5122	0.0491	0.5669
99	-0.4182	2.0060	0.4821	1.7783	-0.4087	0.1169	0.6105

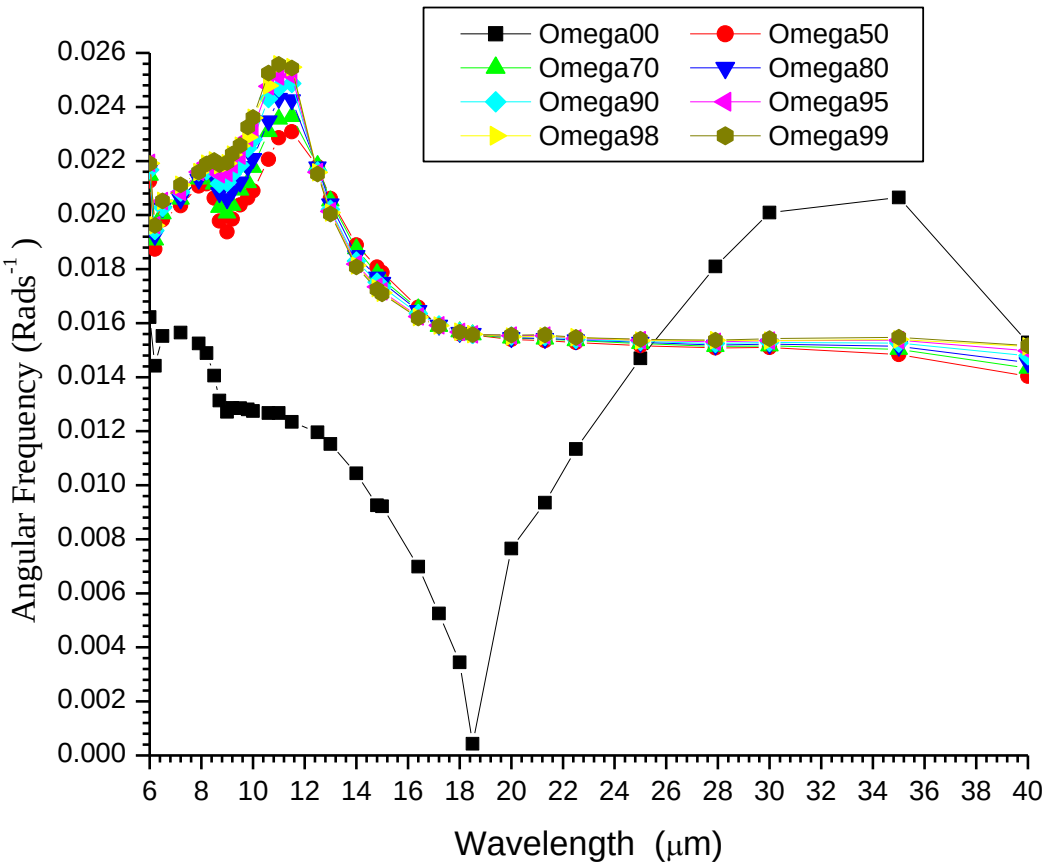

Figure 4. 14A graph of variations of angular frequency (ω) with λ for Artic Aerosol at far IR spectral range.

4.4.3 Continental clean aerosol

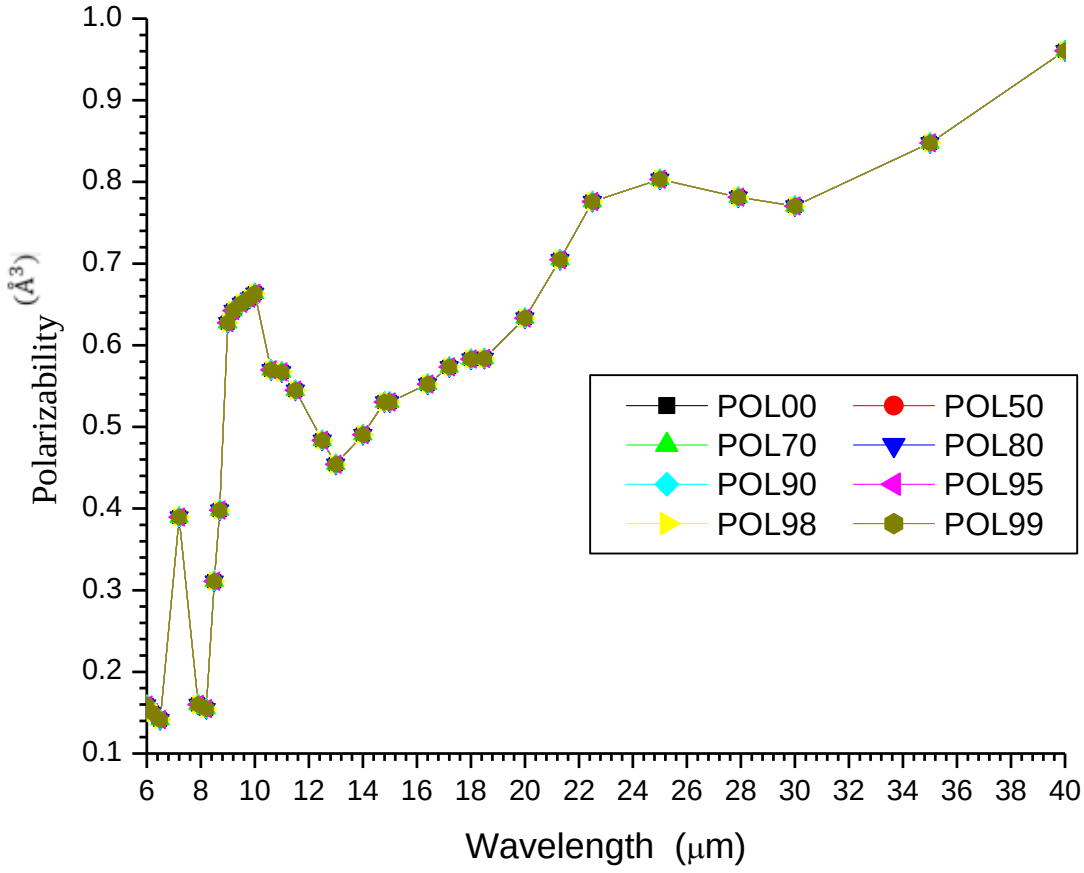

Figure 4. 60. A graph of polarizabilities of Continental cleanaerosols against wavelength at far infrared region.

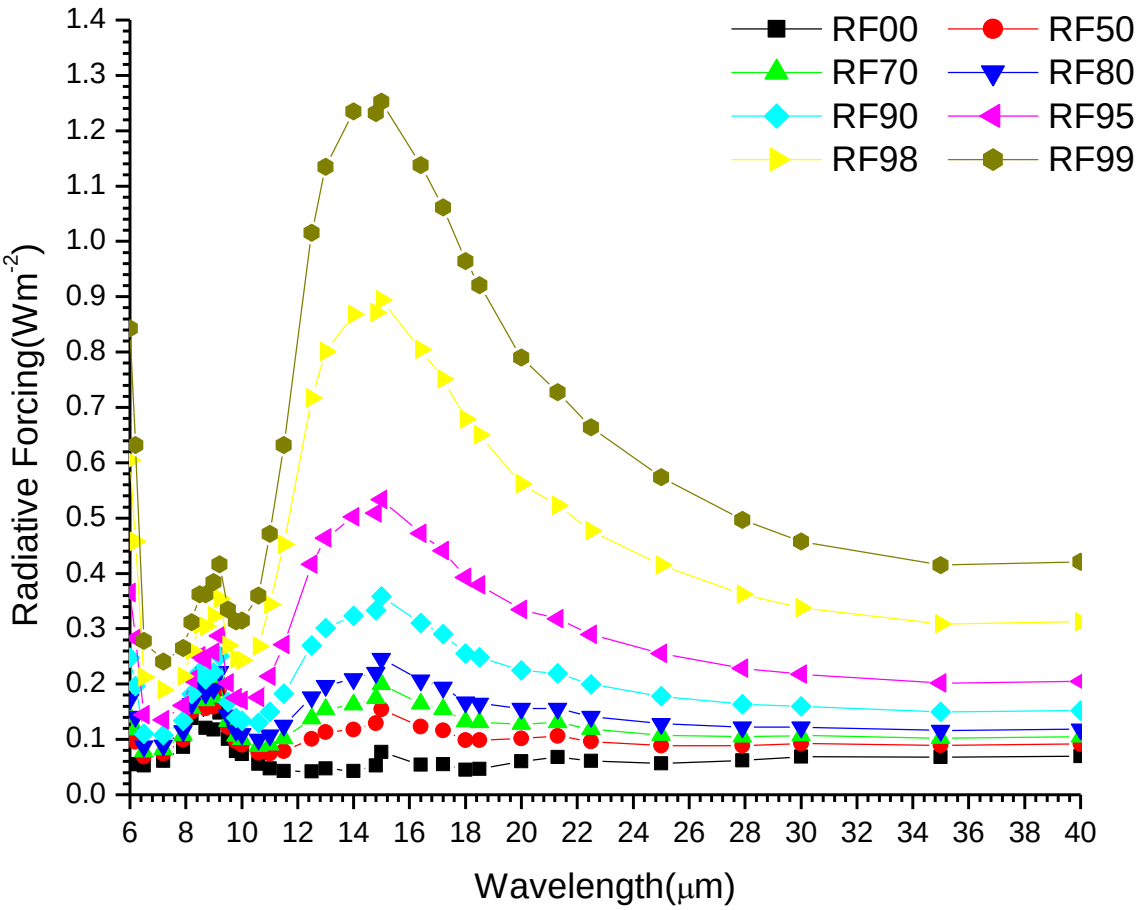

Figure 4. 151.A graph of Radiative forcing of Continental clean aerosols against wavelength at far infrared region.

From figure 4.61, The warming effect occurred as RH increases.

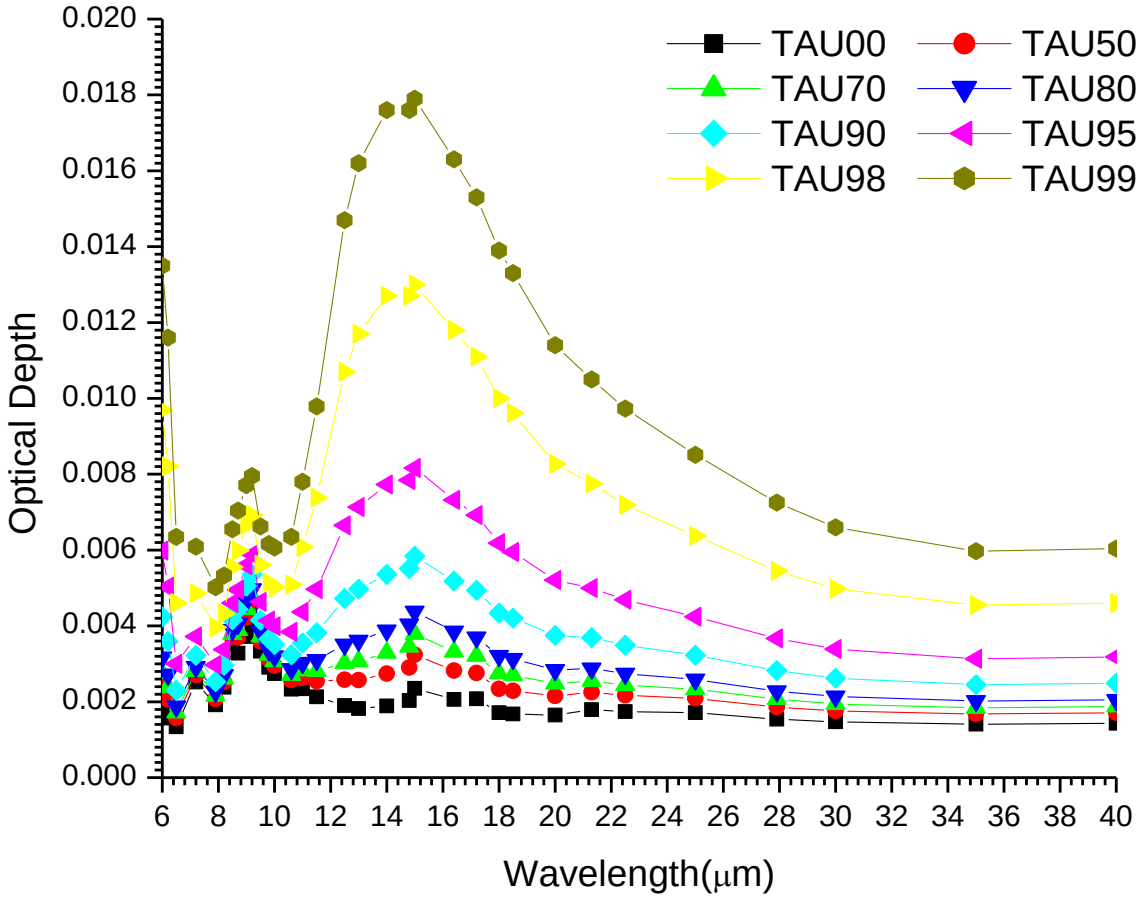

Figure 4. 62.A graph of variations of AOD with λ for Continental Clean Aerosol at far IR region.

Table 4. 15 Regression analysis of AOD for Continental Clean aerosol at far Infraredwavelength band.

Far Infrared (6.0 to 40.0)							
	Linear			Quadratic			
RH(%)	α	β	R^2	α_1	α_2	β_1	R^2
0	-0.3027	1.0049	1.0376	-0.0343	-1.9074	1.0001	1.6247
50	-0.2369	0.0047	0.2172	2.3892	-0.4887	0.0002	0.4750
70	-0.2003	0.0047	0.1687	2.6867	-0.5372	0.0001	0.5068
80	-0.1657	0.0048	0.1180	2.9405	-0.5780	0.0001	0.5180
90	-0.0978	0.0049	0.0369	3.3723	-0.6457	0.0001	0.4853
95	-0.0238	0.0052	0.0017	3.7469	-0.7017	0.0000	0.4046
98	0.0624	0.0060	0.0077	4.0525	-0.7425	0.0000	0.3100
99	-0.1066	0.0070	0.0179	4.1359	-0.7498	0.0000	0.2651

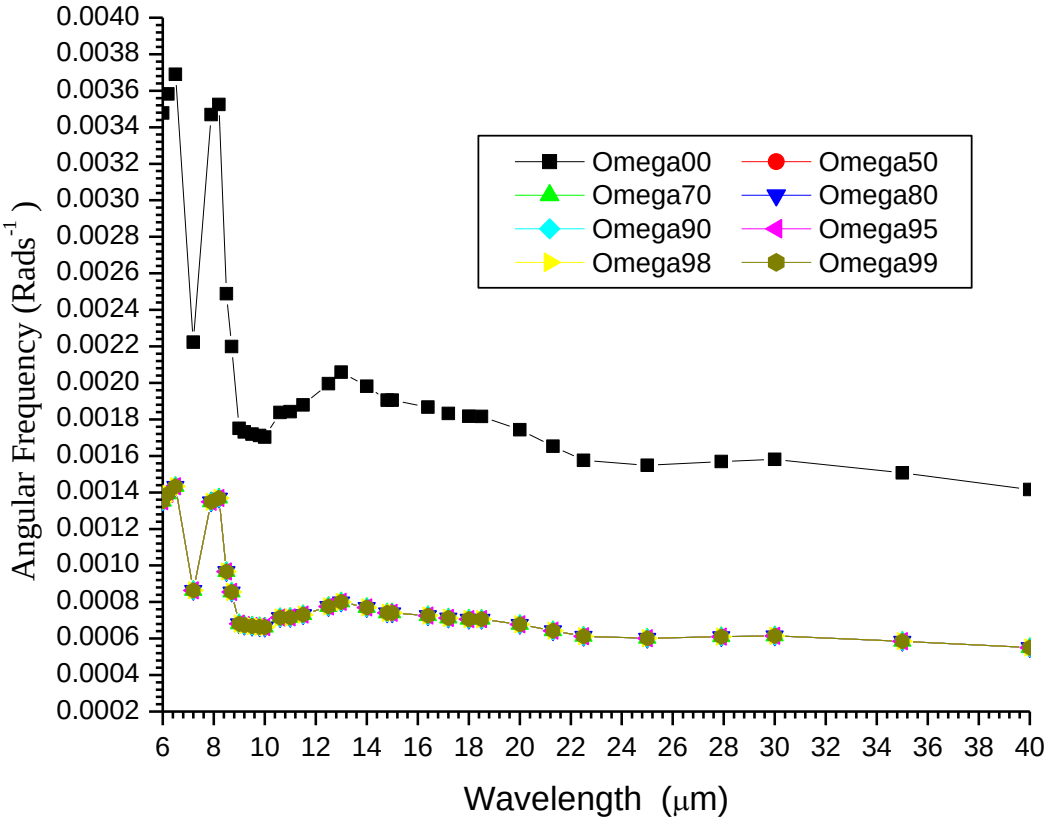

Figure 4. 63.A graph of variations of angular frequency (ω) with λ for continental clean Aerosol at far IR range.

4.4.4 Maritime Tropical Aerosol

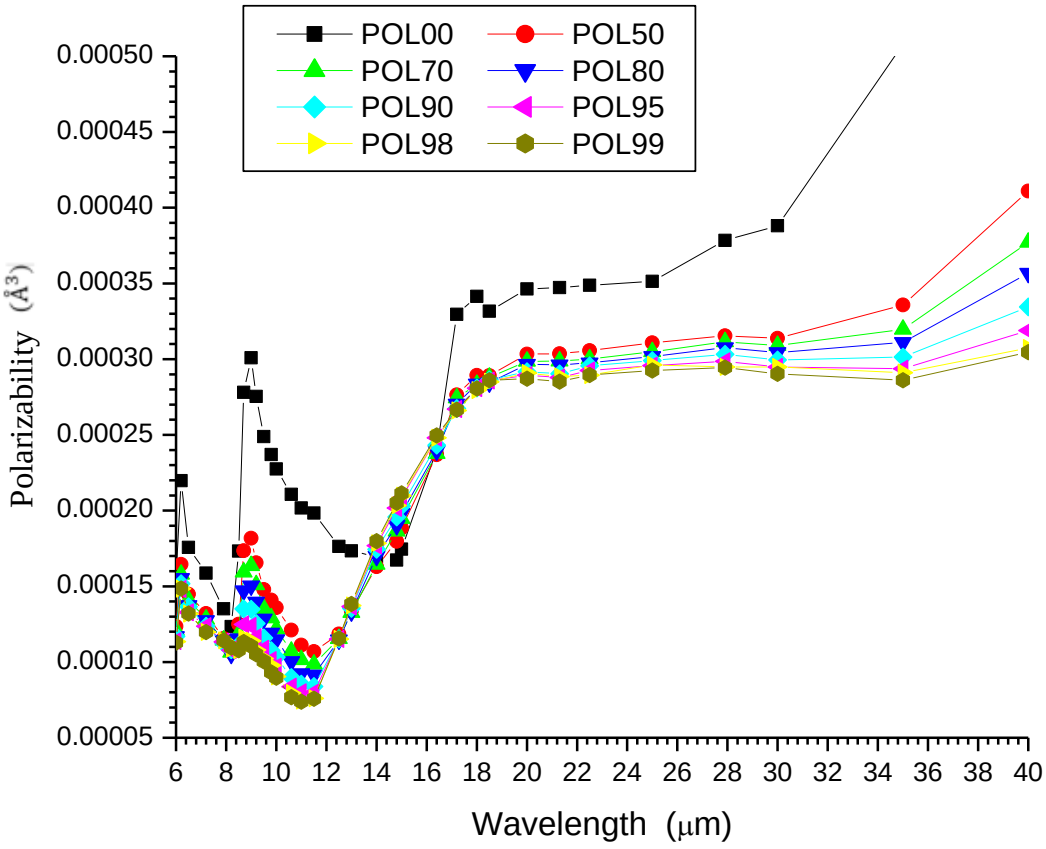

Figure 4. 64.16 A graph of polarizabilities Maritime Tropical Aerosols against λ at far infra red region.

From figure 4.64, the polarizability decreases with increase in RH.

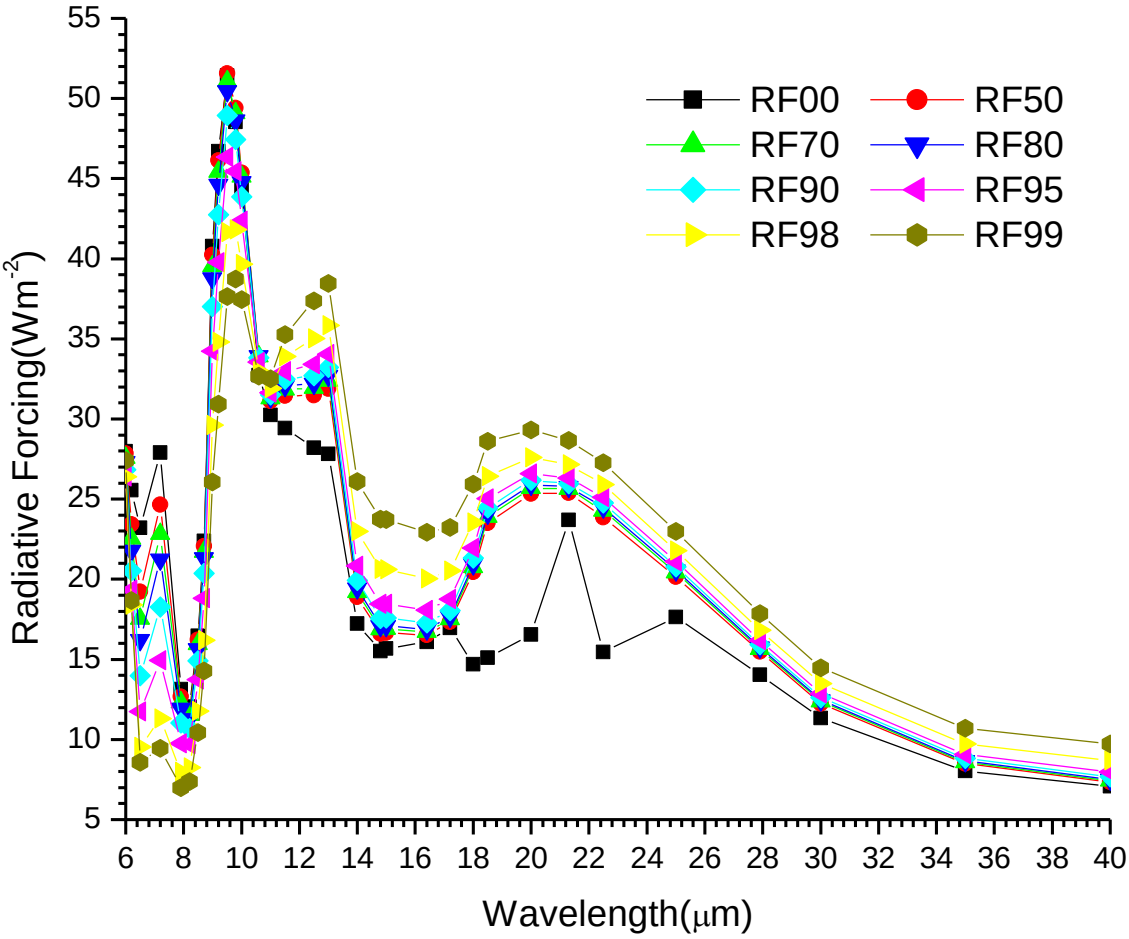

Figure 4. 175 A graph of Radiative forcing Maritime tropical aerosols against wavelength at far infrared region.

From figure 4.65, the warming effect was observed and increase with increase in RH but decreases with increase in λ.

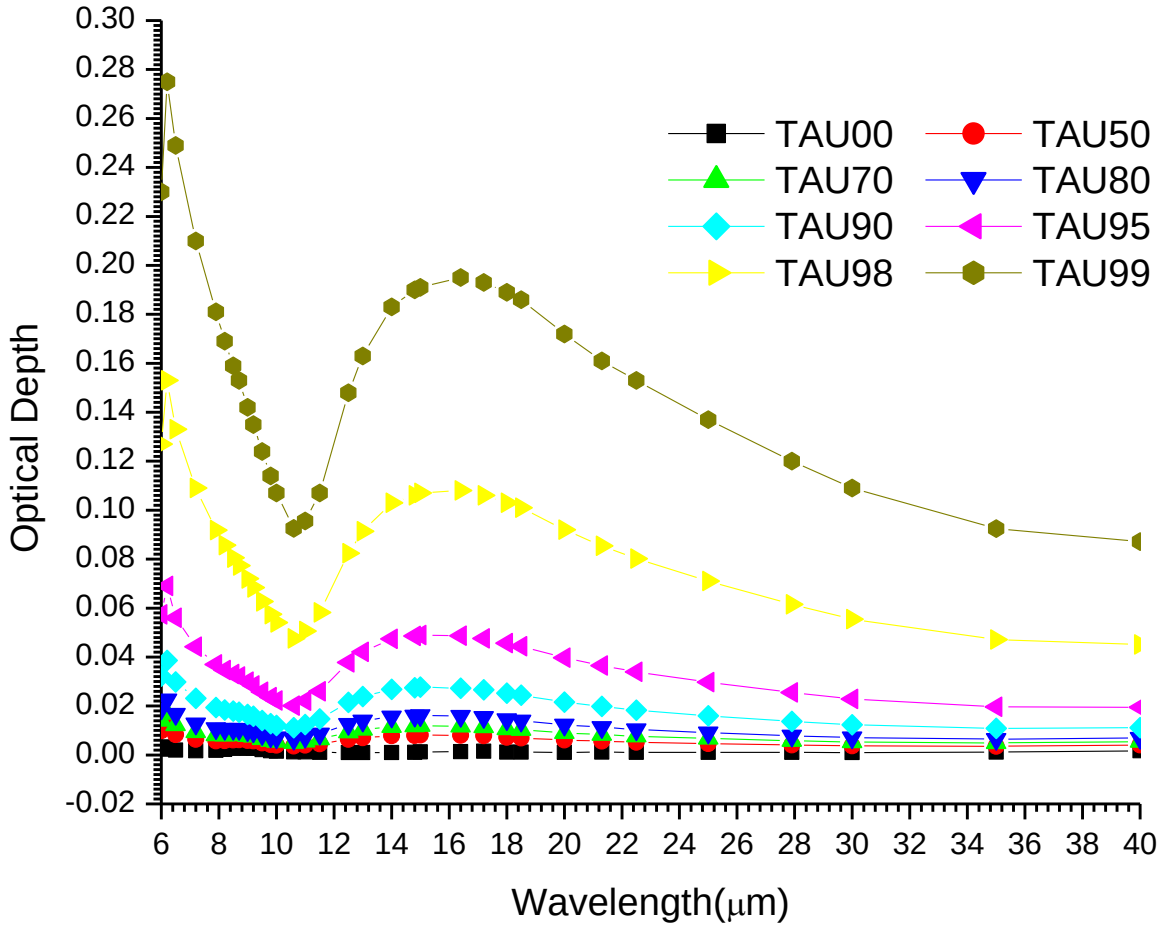

Figure 4. 66. A graph of variations of AOD with λ for Maritime tropical at far IR region.

Table 4. 16 Regression analysis of AOD for Maritime tropical aerosol at far Infraredwavelength band.

Far Infrared (6.0 to 40.0)							
	Linear			Quadratic			
RH(%)	α	β	R^2	α_1	α_2	β_1	R^2
0	0.4890	0.0053	0.4451	3.7241	-0.6020	0.3470	0.6332
50	0.2584	0.0114	0.1874	-0.0464	0.0567	0.0077	0.1899
70	0.2417	0.0154	0.1450	-0.3319	0.1067	0.0074	0.1529
80	0.2352	0.0203	0.1279	-0.4546	0.1284	0.0083	0.1385
90	0.2353	0.0347	0.1210	-0.5025	0.1373	0.0134	0.1325
95	0.2422	0.0643	0.1304	-0.3913	0.1179	0.0283	0.1390
98	0.2520	0.1535	0.1607	-0.1048	0.0664	0.0967	0.1638
99	0.2531	0.2913	0.1888	0.1353	0.0219	0.2501	0.1892

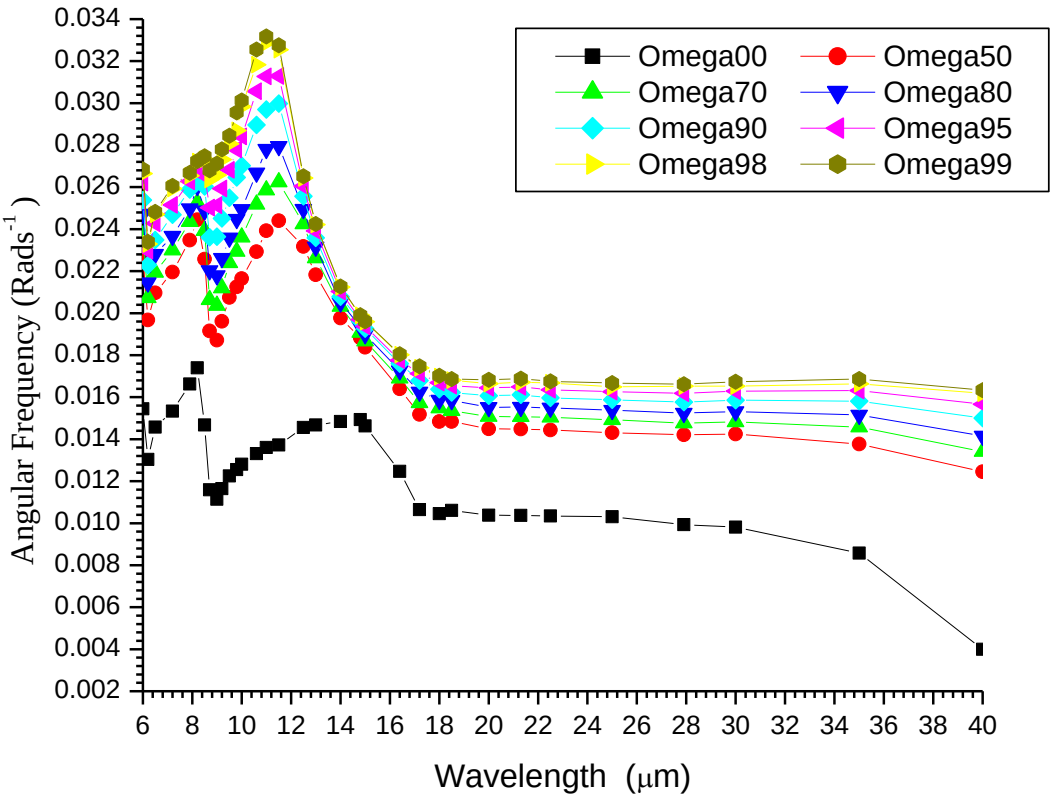

Figure 4. 18A graph of variations of angular frequency (ω) with λ for maritime tropical Aerosol at far IR range.

4.4.5 Sahara/ Desert Aerosols

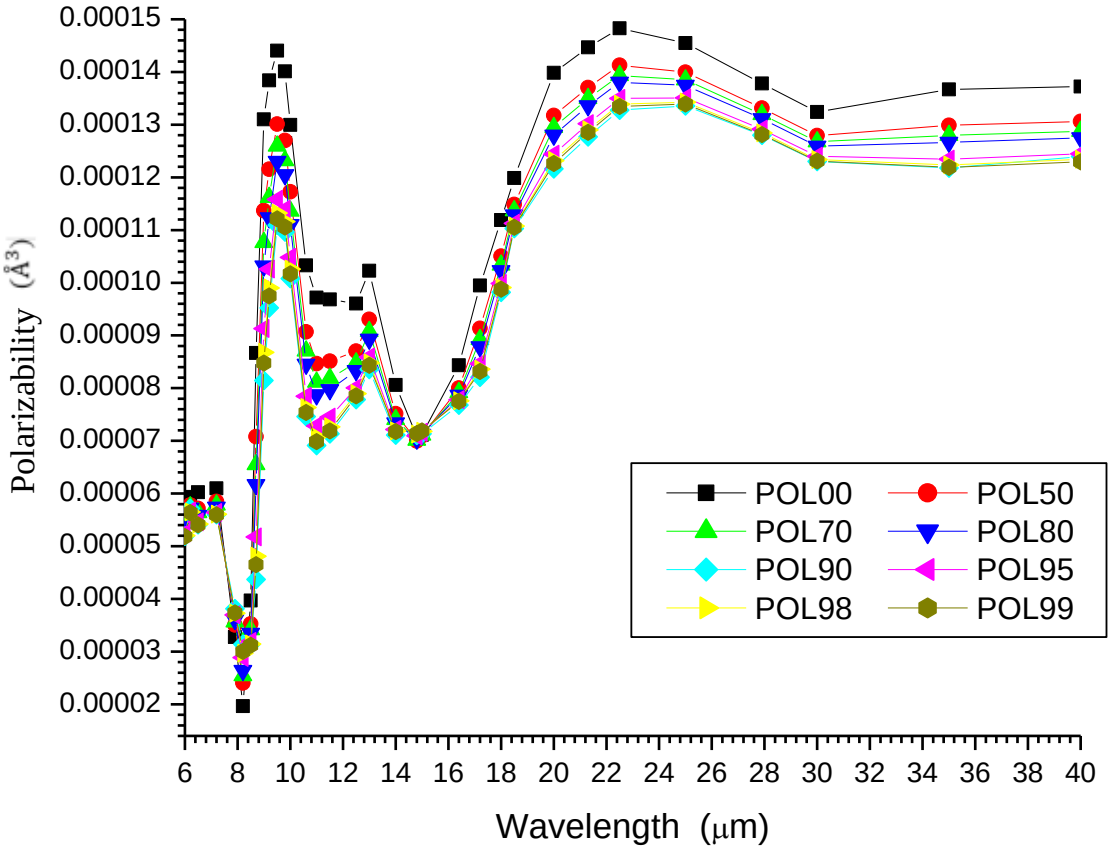

Figure 4. 198. A graph of polarizabilities Sahara aerosols against λ at far IR spectral region.

The effect of RH was negligible.

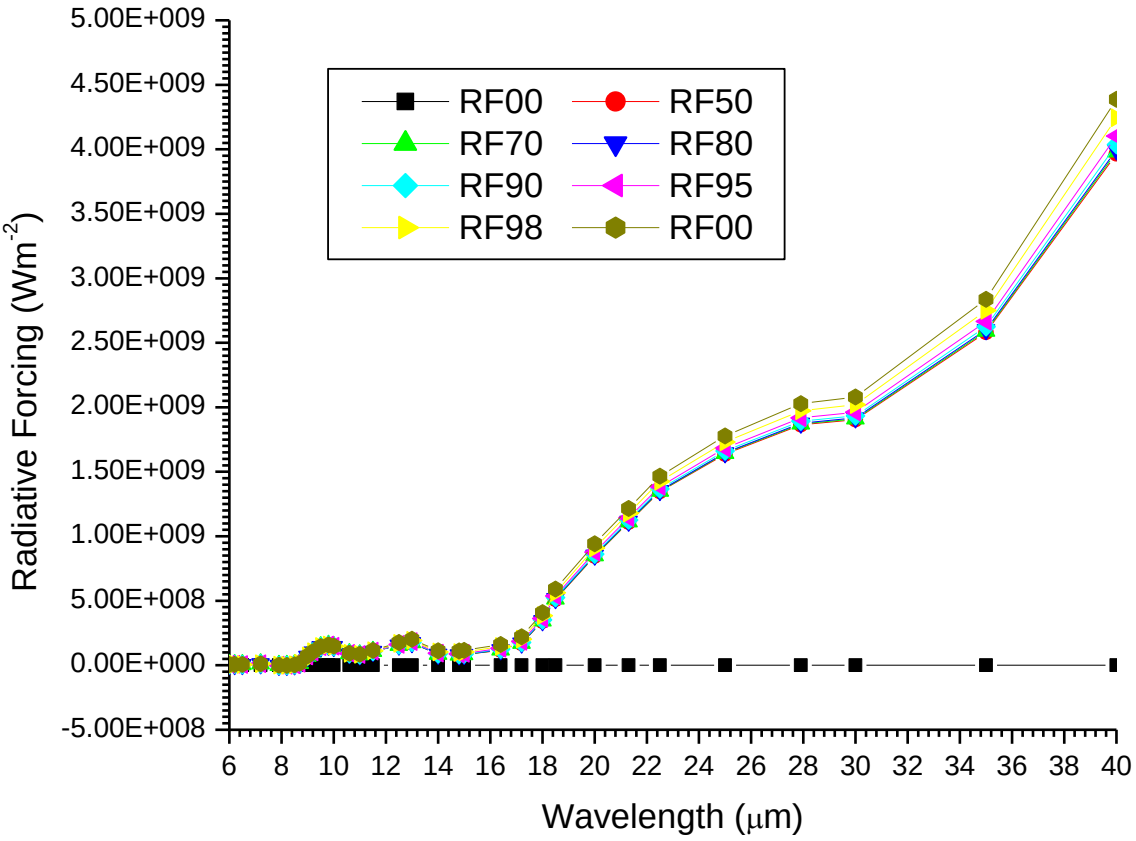

Figure 4. 209. A graph of Radiative forcing for Sahara aerosols against wavelength at far infrared region.

From figure 4.69, at 0% RH neither its warming nor cooling effect, it is a neutral point. The warming effect increase with increase in RH and steadily increases with increases i

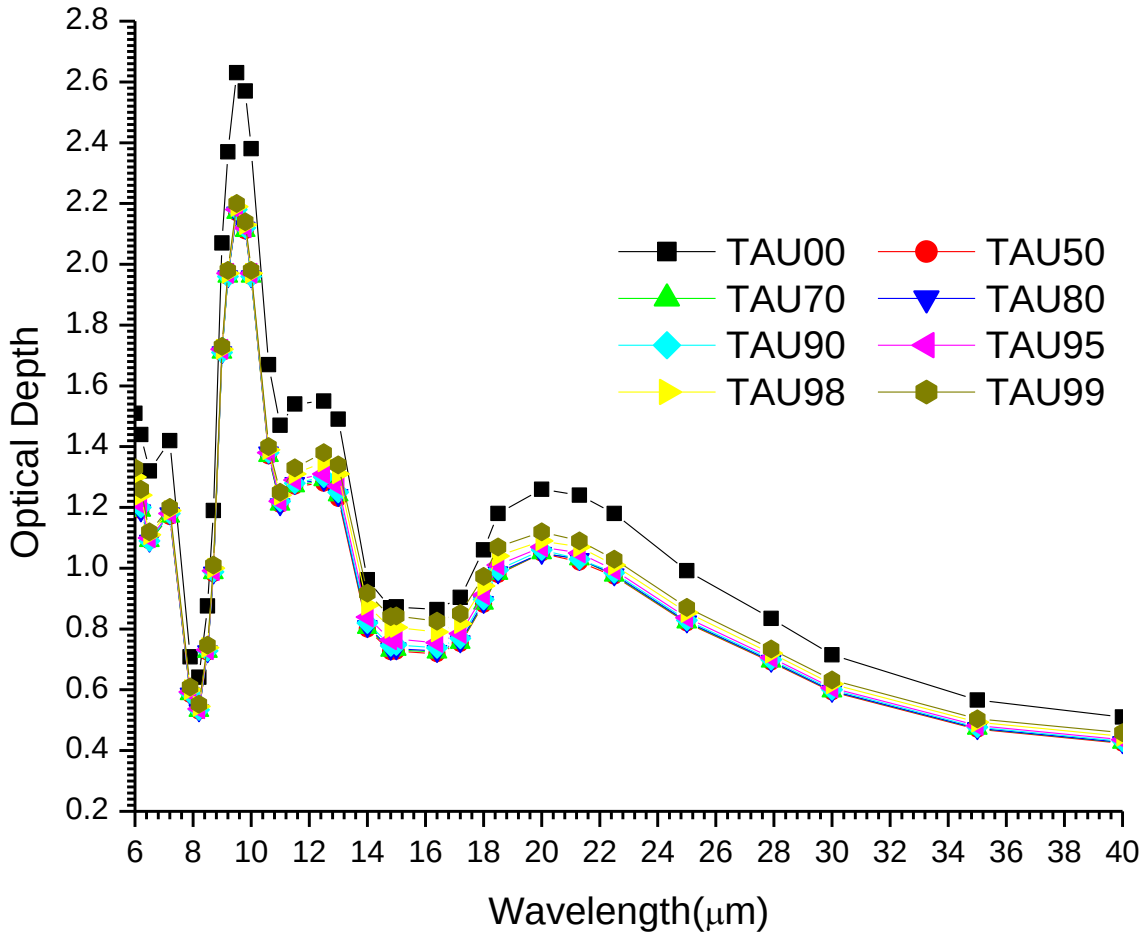

Figure 4. 21A graph of variations of AOD with λ for Sahara Aerosol at far IR region.

Table 4. 17 Regression analysis of AOD for Sahara aerosol at far Infraredwavelength band.

	Far Infrared (6.0 to 40.0)						
	Linear			Quadratic			
RH(%)	α	β	R^2	α_1	α_2	β_1	R^2
0	0.4506	3.8095	0.2955	-2.1256	0.4795	0.1360	0.3893
50	0.4469	3.1216	0.2940	-2.1316	0.4799	0.1111	0.3891
70	0.4455	3.1176	0.2933	-2.1422	0.4816	0.1097	0.3895
80	0.4439	3.1133	0.2925	-2.1541	0.4835	0.1081	0.3899
90	0.4403	3.1037	0.2907	-2.1820	0.4880	0.1044	0.3910
95	0.4345	3.0885	0.2878	-2.2252	0.4950	0.0990	0.3926
98	0.4235	3.0633	0.2822	-2.3080	0.5084	0.0895	0.3963
99	0.4129	3.0419	0.2766	-2.3843	0.5206	0.0816	0.3999

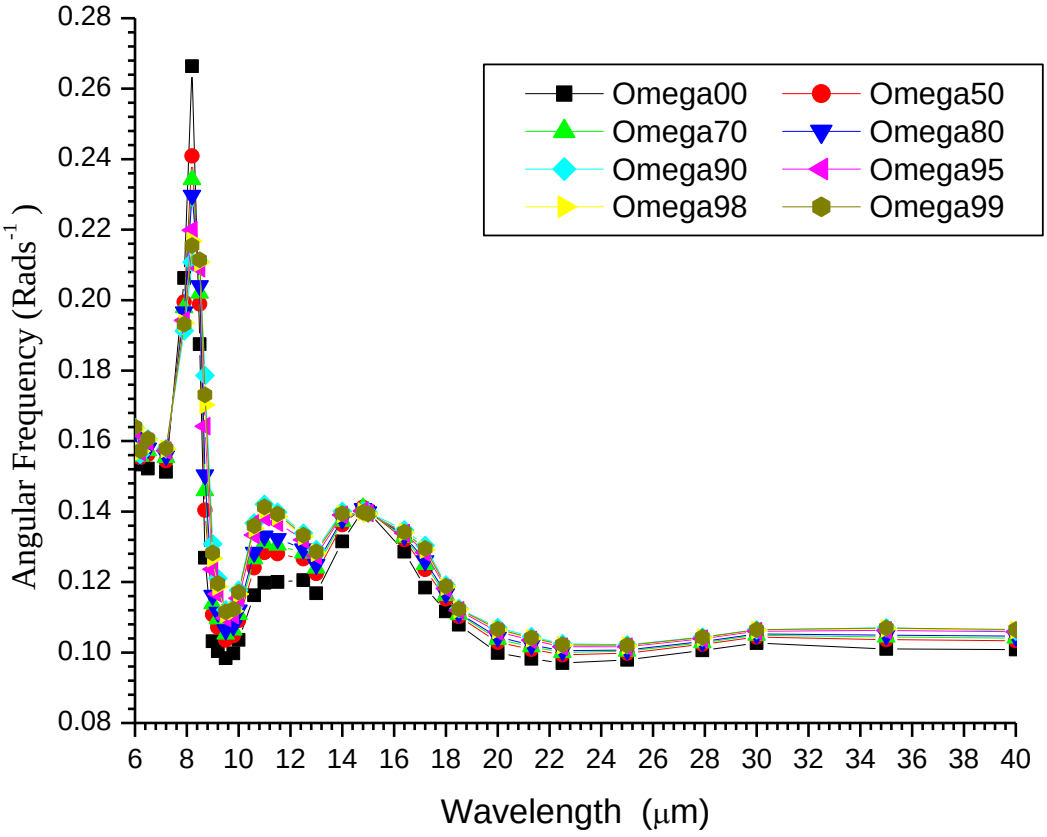

Figure 4. 71.A graph of variations of angular frequency (ω) with λ for Sahara Aerosol at far IR range.

4.4.6 UrbanAerosol

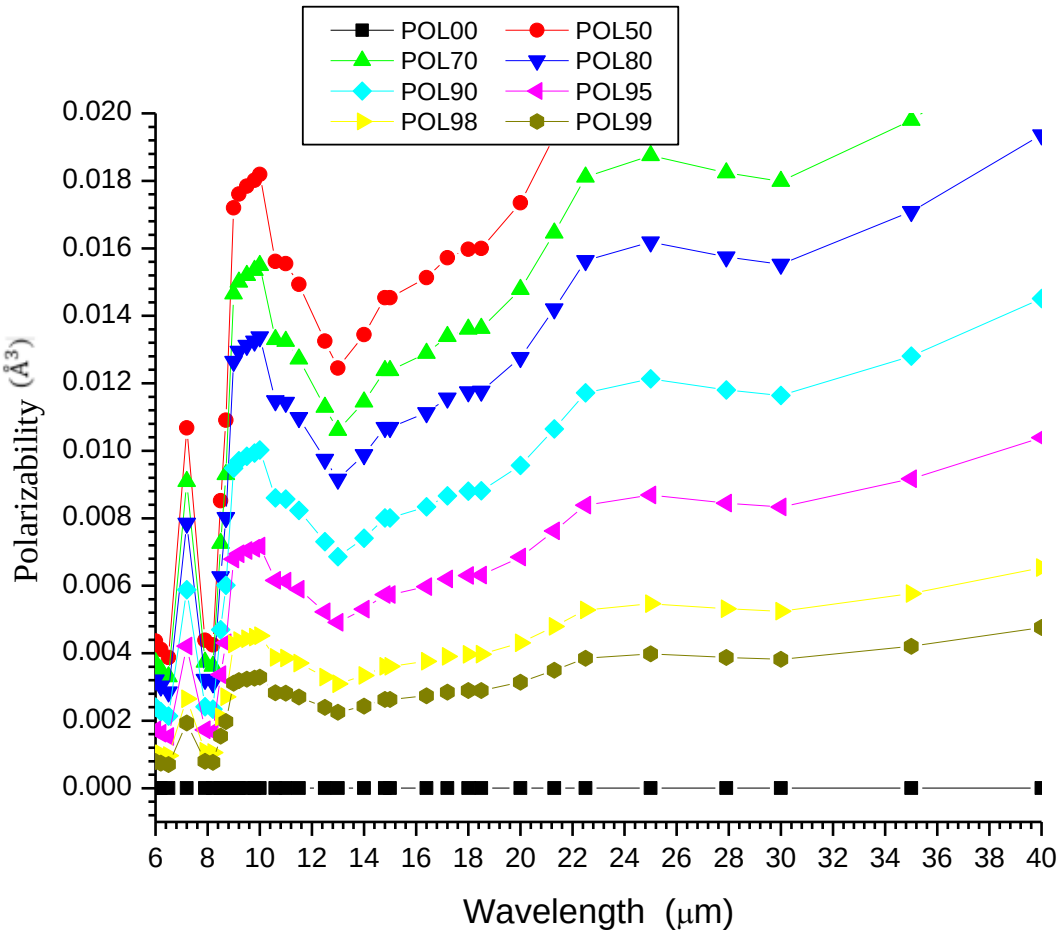

Figure 4. 72. A graph of PolarizabilitiesUrban aerosols against wavelength at far infrared region.

From figure 4.72, the Polarizability increases with increase in RH and increases in λ.

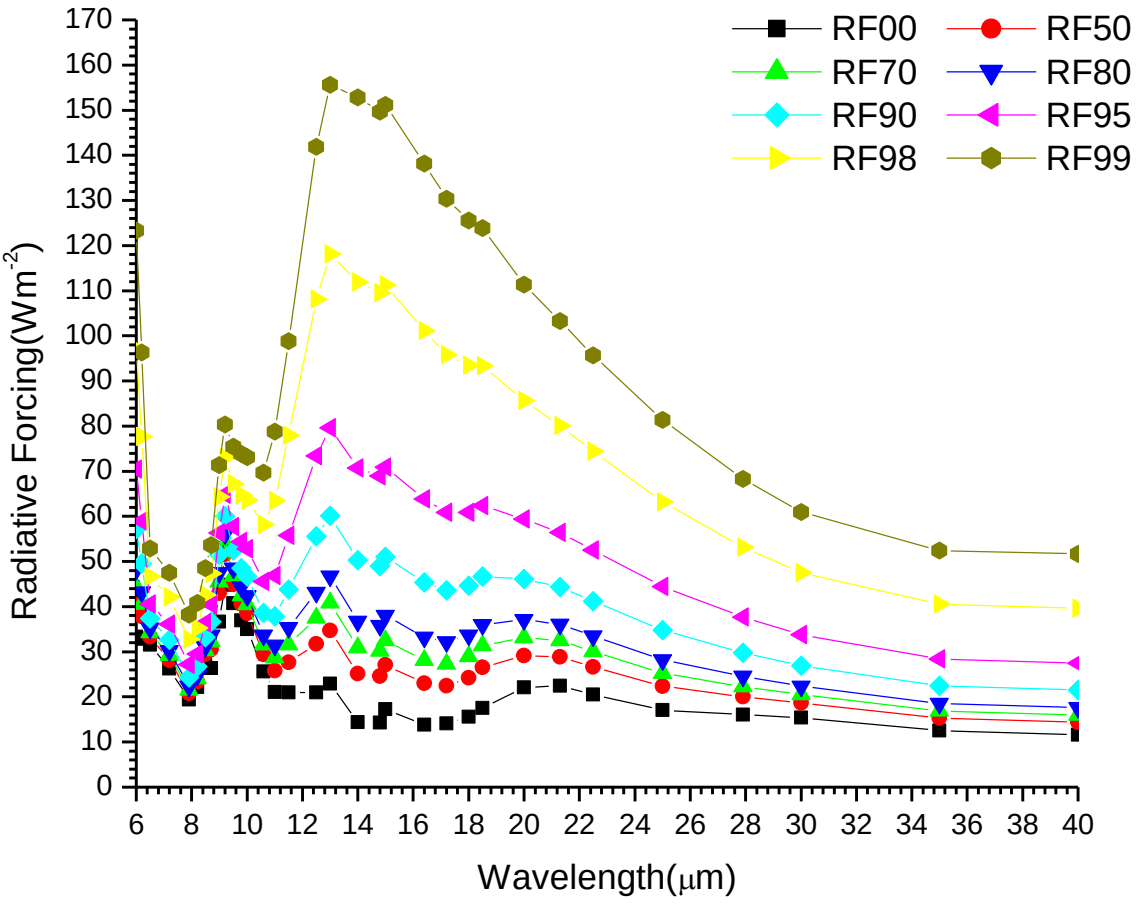

Figure 4. 73. A graph of Radiative forcing Urban Aerosols against wavelength at far infrared region.

From figure 4.73, the maximum warming effect was observed at highest RH and decreases as λincreases.

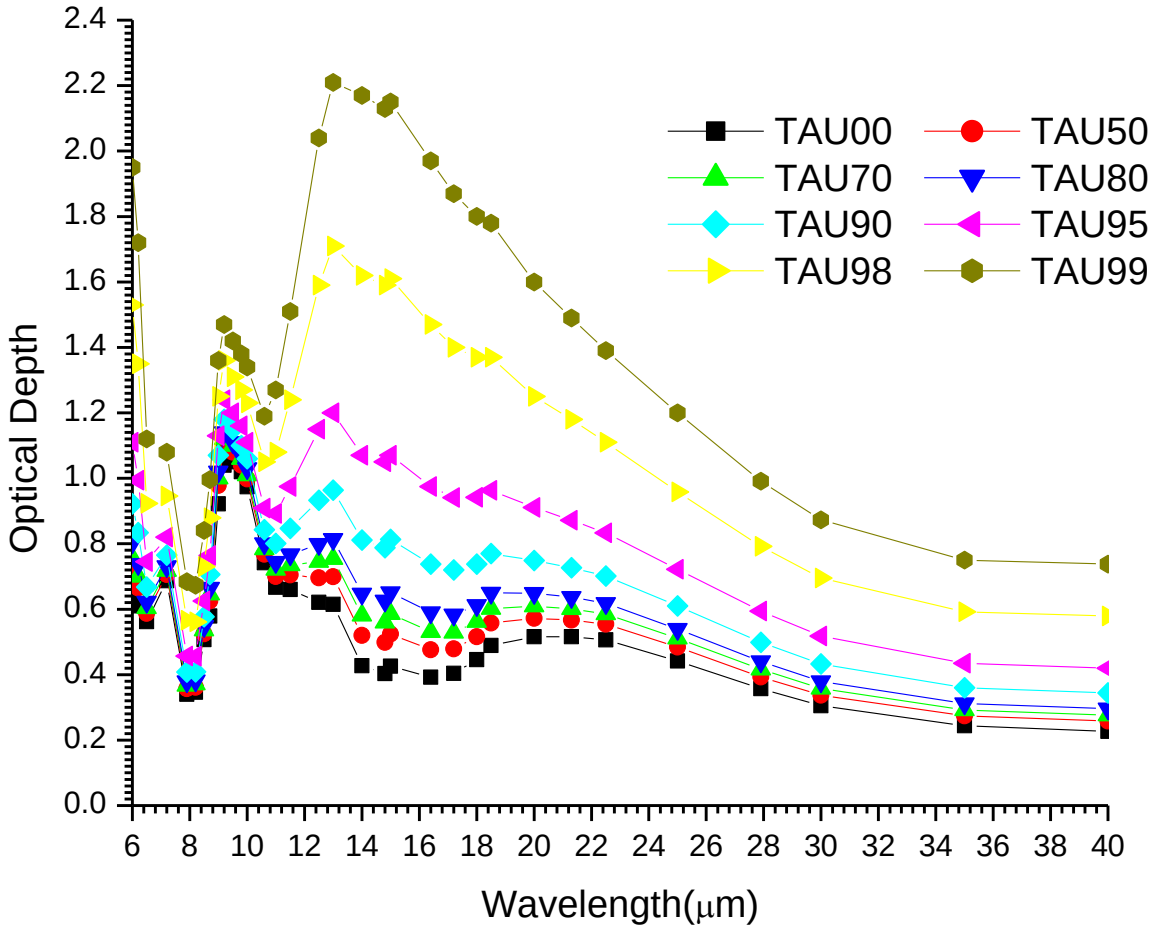

Figure 4. 74. A graph of variations of AOD with λ for Urban Aerosol at far IR region.

Table 4. 18 Regression analysis of AOD for Urban aerosol at far Infraredwavelength band.

Far Infrared (6.0 to 40.0)							
	Linear			Quadratic			
RH(%)	α	β	R^2	α_1	α_2	β_1	R^2
0	0.49086	0.62552	0.40717	-1.98298	0.46034	-2.57558	0.50701
50	0.43857	0.58484	0.37432	-2.33137	0.51544	-2.99942	0.51847
70	0.40823	0.55990	0.34861	-2.52930	0.54663	-3.24121	0.52287
80	0.37823	0.53591	0.31851	-2.71509	0.57562	-3.46678	0.52417
90	0.31459	0.48942	0.24290	-3.07607	0.63095	-3.89801	0.51531
95	0.23658	0.44644	0.14334	-3.45436	0.68683	-4.32957	0.48013
98	0.12995	0.43050	0.03954	-3.85064	0.74072	-4.72030	0.39765
99	0.06410	0.46409	0.00845	-4.01707	0.75944	-4.81685	0.33899

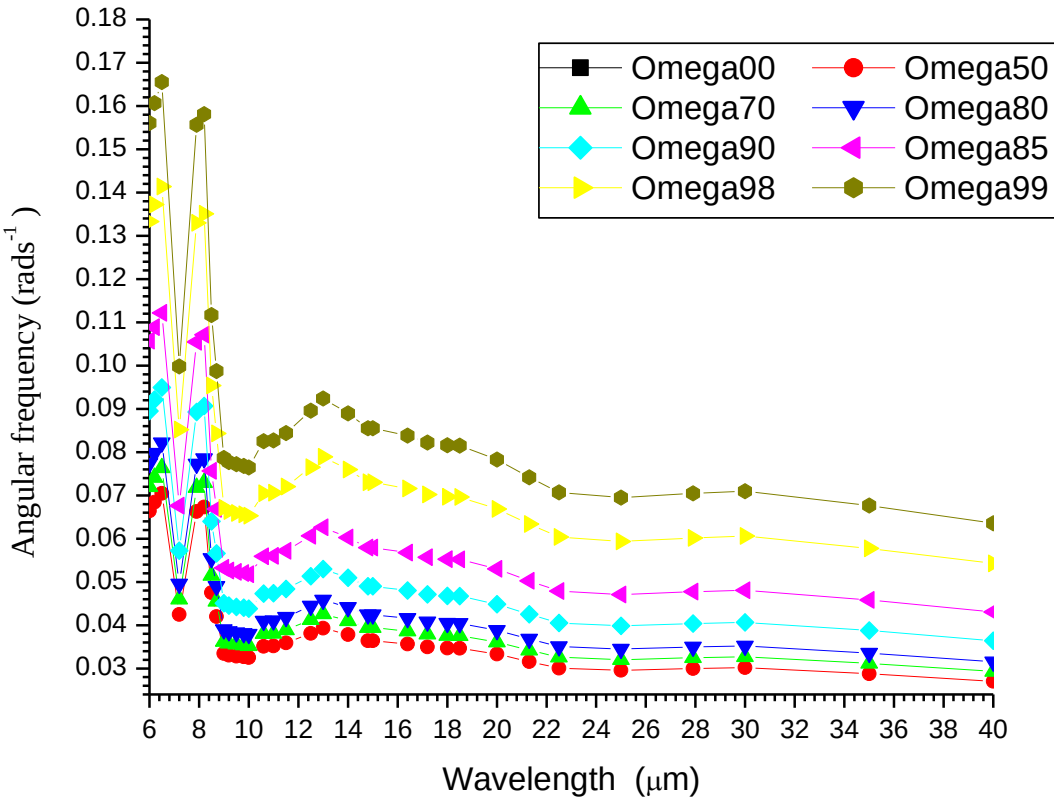

Figure 4. 22A graph of variations of angular frequency (ω) with λ for Urban Aerosol at far IR range.

4.5 Discussions

From the results above, I determined the mean effective polarizabilities and radiative forcing at each spectrumwavelength and correlate the results with the net effect of the radiative forcing. The results is presented in the table 5.1.

Table 5.1the mean polarizabilities and effect of radiative forcing for various wavelengths Range.

AEROSOL MODELS	Part I :Near UV to Visible		Part II : Near IR		Part III : Far IR	
	Mean pol. ($Å^3$)	effect of RF	Mean pol. ($Å^3$)	effect of RF	Mean pol. ($Å^3$)	effect of RF
CC	0.49105143	Cooling	0.3007767	Warming	0.54080264	Warming
Urban	0.006666	warming	0.003937	Warming	0.007341	Warming
Antarctic	0.00625	Cooling	0.00604	Warming	0.25594	Warming
Artic	0.00033288	Cooling	0.0003351	Warming	0.00311177	Warming
Maritime	0.0001437	Cooling	0.0001386	Warming	0.0002046	Warming
Desert/ Saharan	0.00006627	warming	0.00006134	Warming	0.00009091	Warming

From table 5.1, the mean Polarizabilities for each aerosol model were obtained by taking the mean of all the effective polarizabilities of each aerosol model within each of the wavelength ranges and eight Relative humidities.

It was observed that,polarizability is maximum at far IR, moderate near UV to visible and minimum near IR spectral wavelength ranges. Continental clean, Urban, Antarctic, Artic, Maritime Tropical and Desert/ Saharan aerosols models are in order of decreasing magnitude in polarizabilities.

The dependency of the polarizability on the frequency of the driving field is physically reasonable. However, as the frequency increases to extremely high values, eventually the charges are unable to follow the changing field, and the polarizability then approximately equal to zero.

The plots for these results have shown that, the polarizabilities of the aerosol generally decrease with increase in RH.This is due to the fact that, With a change of relative humidity in the atmosphere, condensation or evaporation of water take place on the aerosol particles and these, at the same time, change the particle optical parameters . It is evident that, when the relative humidity increases, the size of an aerosol particle increases through the accretion of water. At the RH above 95% together with the growth in size, the complex refractive index of the aerosols also varies.

For the RF, the cooling effects of the atmosphere occurred near UV to IR spectral regions for Artic, Antarctic, Maritime Tropical and Urban aerosol models and warming effect for Urban and desert aerosols. At near IR region the warming effect were observed for all the models, but very high for Saharan. At far IR region, the warming effects also persisted for Saharan aerosol models.

The regression analysis have shown that, as the RH increases, the aerosol increases in size and the dipole decreases hence the polarizabilities decreases with increase in RH.

Finally, I observed that computations remain the only reasonable approach to a complete data set of aerosol optical properties needed for a global modelling of climate.

CHAPTER FIVE

SUMMARY, CONCLUSION ANDRECOMMENDATION

5.1 SUMMARY

The atmosphere is a mixture of various gases, achieved by complex mixture with constant Chemical reactions held in an envelope around the earth by gravitational attraction. It contains amounts of water vapour, dust, and other liquid or solid particles which vary with time ,location and altitude collectively known as aerosols. The world's climate have changed in the past and are changing now and there is every reason to researchers to expect that they will change in the future (Hobbs, 1980). Aerosols can both scatter and absorb sunlight and they also absorb and re-emit infrared radiation. These heat imbalance is accounted for by radiative forcing and resulted in global weather conditions.

Aerosols in the atmosphere have several important environmental and climate effects. They are a respiratory health hazard at the high concentrations found in urban environments. They scatter and absorb visible radiation, limiting visibility. They affect the Earth's climate both directly (by scattering and absorbing radiation) and indirectly (by serving as nuclei for cloud formation).

in this research, I presented a general quantitative descriptions of the aerosols sources, classification, abundancesand aerosols – matter interaction. The main aerosols models under study are;

i. The continental clean; aerosol which is assumed to occur in regions remaining essentially unaffected by humans or anthropogenic sources.
ii. Desert aerosols are greatly influenced by dust storms, which raise number and mass concentrations of particles >1 mm.
iii. The urban aerosol; is associated with the high population density that creates a unique urban environment. A large fraction of the urban aerosol is due to emissions from automobiles traffic (exhaust emissions, road dust, etc.), home heating and industrial activities.
iv. The maritime aerosol, characteristic of the marine boundary layer, is composed of sea salt particles modified in the accumulation range by nitrate resulting from the interaction with nitric acid, ammonium sulfate from the oxidation of sulfur compounds, and a possible admixture of the tropospheric background aerosol.
v. The Antarctic and the Arctic are regions of low particle concentrations but with a significant marine components. At least the Arctic, however, receives an input of aged aerosol particles from the adjacent continents, which in the winter can accumulate to form an Arctic haze.

The attenuation of an electromagnetic wave propagating in the atmosphere arises from aerosol Molecular polarizabilities. The concentration, composition and size distribution of atmospheric aerosol particles are temporally and spatially highly variables. Particles from specific sources can fall into characteristic size ranges and, therefore, particle composition can vary with particle size, reflecting this effect. For example, Sulphate arising from the oxidation of SO_2 is typically present in fine particles, whereas silicon from the resuspension of soils and surface dusts is normally found in coarse particles. The

composition of the individual particles can be fairly uniform or very different from the ensemble composition depending on the particle sources and atmospheric aging processes involved.

In general, the predominant chemical components are sulphate, nitrate, ammonium, sea salt, mineral dust, organic compounds and black or elemental carbon, each of which typically contributes of the overall mass load. Furthermore, during their rise through the water, bubbles scavenge many surface-active organic materials, which are partly injected into the air when the bubbles burst. Volcanic gases, particles are directly emitted into the atmosphere, and the gases may eventually transform into secondary aerosol. Dust is also lift from the soil by wind and, if small enough, may become airborne and transported over long distances. Biological processes emit primary aerosols in the form of plant debris, humic matter and microbial particles (pollen, fungi, spores, bacteria etc.), as well as substances in the gas phase that contribute to secondary aerosol formation.

5.2 CONCLUSION

The research reveals that:

1. The magnitude of Polarizabilities have shown clear decrease with increase in RH for all the aerosols models.
2. The magnitude of polarizabilities is minimum near IR region, moderate atnear Ultra Violet to Visible and maximum at far IR spectral range.
3. Similarly, for the Radiative Forcing, the cooling effects occurred as Relative Humidities and wavelengths decrease.

4. As the polarizability increases, the radiative forcing tends to decrease.
5. The vibrational polarizability increases with increase in Relative Humidities.
6. Why polarizabilities varies or absorb in particular region of the spectrum can only be determined through quantum chemical calculations.
7. It is therefore, observed that polarizability is one of the major useful information for the analysis of EM interactions of atmospheric aerosols.
8. I hope the results provide a useful viewpoint of the polarizabilities of atmospheric aerosols.
9. Finally, my results show that, there is a great computational complication in the determinations of polarizabilities at various Relative Humidities and wavelength which required quantum treatments for detail analysis.

5.3Findings / Contributions to knowledge

1. I determined and analyzed one of the most hidden and silent aspects (polarizabilities) of atmospheric aerosols within wide spectral wavelength range.
2. I determinedthe polarizabilities for atmospheric aerosols recommended by many researchers ((Yangang and Peter, 2008,Sihvola, A. et al 2004).
3. I determined polarizabilities at various relative humidities, whichhave not been done.(i.e. effect of RH on polarizability) for real atmospheric aerosols.
4. I determined the polarizability at various wavelengths (i.e. effect of wavelengths on polarizability) for real atmospheric aerosols.

5. Most of polarizabilities are determined in laboratories, here I developed a new and relatively simple computational technique applicable for wide range of substances within a very wide range of wavelengthsby changing few input parameters, which is difficult in the laboratory.

6. I justifiedthat; OPAC can be a very good data for the determination of polarizability.

5.4 Recommendations

1. There is need from both experiment and theory to improve on these resultsand produce more precise data for the polarizabilitiesof atmospheric aerosols.

2. I strongly recommend for future work that, VERSON 4.0 of the OPAC, which have been recently released, should be used. This version has taken care of the effect of non-sphericity of the aerosols.

3. Higher order polarizabilities (hyperpolarizability) should be computed to analyze aerosols electromagnetic wave interactions.

4. Quantum and relativistic effects should be taken into account.

References

Agranovski I. (2010), Aerosols Science and Technology; WILEY-VCH Verlag GmbH & Co. KGaA, Weinheim.

Akhter, M. S., Chughtai, A. R., & Smith, D. M. (1985). The structure of hexane soot I: Extraction studies. Appl. Spectrosc. 39,154–167.

Bohren, C.F. and D.R. Huffman (1983), Absorption and scattering of light by small particles, Wiley, New York.

Born. M.Wolf E. (2005):Principles of Optics, 7 edn. Cam-bridge Univ. Press, Cambridge

Cloude, S. R. (2009) Depolarization by aerosols: Entropy of the Amsterdam light scattering database," J.Quant. Spectrosc. Radiat. Transfer, Vol. 110, 1665–1676,

David, R. Lide . (2003), RC Handbook of Chemistry and Physics, CRC Press.

Deepak, A. (1982). Atmospheric Aerosols, Spectrum Press, Hampton, Virginia.

Deirmendjian, D. (1969). Electromagnetic scattering on spherical Polydispersions, Elsevier, New York.

Doyle, W.T. (1978), The Clausius -Mossotti problem for cubic array of spheres," J. Applied Physics, Vol.49(2), , pp. 795-797.

Grieken, R. (eds.), (1995), Atmospheric particles. John Wiley, New York. Cox, C. S.,
& Wathes, C. M.Bioaerosols handbook. NY: Lewis Publishers.

Hansen, J. E. and Lacis, A. A. (1990), Sun and dust versus greenhouse gases: An assessment of their relative roles in global climate change, Nature, Vol. 346, 713–719,

Hansen, J. E. and Travis, L. D., (1974), Light scattering in planetary atmospheres. Space Science Reviews, Vol. 16, 527–610,

Hinds, W. C. (1999). Aerosol technology. NY: Wiley-Inter science.

Hobbs, J.E. (1980). A study of atmospheric resources. Wm Dawson and Sons Ltd.

http://physics.tutorvista.com/waves/wavelength-spectrum.html

IPCC (2007). Climate Change :The Scientific Basis. Contribution of Working Group I to the Fourth Assessment Report of the Intergovernmental Panel on Climate Change.

Meszaros. E (1981), Atmospheric Chemistry. Fundamental Aspects. Elsevier Scientific Publishing Company, New York.

Mian, C. (2009) “Atmospheric Aerosol Properties and Climate Impacts; Synthesis and

Assessment Product 2.3 Report by the U.S. Climate Change Science

Program and the Subcommittee on Global Change Research..

Ottcher, B. C.J. F. (1952), Theory of electric polarization, Elsevier, Amsterdam.

Sihvola, A. et al (2004), Polarizabilities of Platonic solids. IEEE Transactions on

Antennas and Propagation.

Stokes, R.A. and Robinson, R.H. (1966) J. Phys. Chem., 70, 2126, 1966.

van De Hulst, H. C. (1969), Light Scattering by Little Particles,John Wiley, New York,

Wang, X. and L.-W. Li, (2009), Numerical characterization of bistatic scattering from

pec cylinder partially embedded in a dielectric rough surface interface:

Horizontal polarization,” Progress In Electromagnetics Research,

Vol. 91, 35–51.

Winiwarter, W., Bauer, H., Caseiro, A., & Puxbaum, H. (2009). Quantifying emissions

of primary biological aerosol particle mass in Europe.Atmospheric

Environment, 43, 1403–1409.

Yalcin, U. (2009), Scattering from perfectly magnetic conducting surfaces: The

extended theory of boundary diffraction wave approach, ”Progress In

Yangang L. and Peter H. D (2008), Relationship of refractive index to mass density and self consistency ”Progress In Electromagnetic Research C, Vol. 12, 66–73.

Zheng, J. P. and K. Kobayashi, (2008), Plane wave diffraction by a finite parallel-plate

waveguide with four-layer material loading: Part I —The case of

polarization, ”Progress In Electromagnetic Research B, Vol. 6, 1–36.

APPENDIX A

Magnitude of Effective polarizabilities of Antarctic Aerosols at 61 wavelengths and 8 RH.

wavelength $\lambda(\mu m)$	Effective Polarizabilities at 8 RH							
	RH00	RH50	RH70	RH80	RH90	RH95	RH98	RH99
0.25	1.6455	0.6297	0.4775	0.3892	0.2822	0.2020	0.1438	0.1169
0.30	1.6384	0.6260	0.4743	0.3863	0.2796	0.1995	0.1413	0.1144
0.35	1.6275	0.6216	0.4709	0.3834	0.2773	0.1977	0.1398	0.1132
0.40	1.6216	0.6191	0.4689	0.3817	0.2760	0.1966	0.1388	0.1121
0.45	1.6158	0.6168	0.4673	0.3804	0.2749	0.1958	0.1382	0.1118
0.50	1.6149	0.6164	0.4668	0.3799	0.2745	0.1955	0.1378	0.1114
0.55	1.6121	0.6151	0.4658	0.3791	0.2738	0.1949	0.1374	0.1110
0.60	1.6101	0.6143	0.4652	0.3786	0.2735	0.1946	0.1371	0.1106
0.65	1.6101	0.6142	0.4651	0.3784	0.2734	0.1945	0.1370	0.1104
0.70	1.6095	0.6140	0.4649	0.3783	0.2733	0.1944	0.1369	0.1104
0.75	1.6095	0.6140	0.4648	0.3782	0.2731	0.1943	0.1368	0.1102
0.80	1.6088	0.6135	0.4646	0.3779	0.2729	0.1940	0.1366	0.1100
0.90	1.6088	0.6135	0.4644	0.3778	0.2727	0.1938	0.1364	0.1098
1.00	1.6081	0.6131	0.4641	0.3775	0.2726	0.1937	0.1362	0.1097
1.25	1.6093	0.6131	0.4640	0.3774	0.2722	0.1931	0.1356	0.1089
1.50	1.6094	0.6130	0.4638	0.3772	0.2719	0.1929	0.1351	0.1086
1.75	1.6096	0.6124	0.4630	0.3762	0.2708	0.1917	0.1337	0.1071
2.00	1.6110	0.6123	0.4627	0.3758	0.2702	0.1908	0.1327	0.1059
2.50	1.5816	0.5976	0.4502	0.3644	0.2599	0.1813	0.1233	0.0968
3.00	1.6279	0.6284	0.4788	0.3924	0.2887	0.2114	0.1574	0.1330
3.20	1.5627	0.6101	0.4674	0.3850	0.2862	0.2122	0.1603	0.1361
3.39	1.5560	0.6026	0.4598	0.3771	0.2777	0.2030	0.1499	0.1252
3.50	1.5545	0.6000	0.4572	0.3743	0.2745	0.1996	0.1459	0.1212
3.75	1.5109	0.5816	0.4425	0.3618	0.2645	0.1913	0.1389	0.1145
4.00	1.5054	0.5781	0.4393	0.3587	0.2614	0.1882	0.1355	0.1112

4.50	1.5084	0.5776	0.4382	0.3573	0.2593	0.1858	0.1325	0.1078
5.00	1.4474	0.5549	0.4213	0.3436	0.2499	0.1794	0.1285	0.1049
5.50	1.3953	0.5335	0.4046	0.3295	0.2388	0.1707	0.1213	0.0985
6.00	1.3492	0.5154	0.3906	0.3180	0.2303	0.1644	0.1168	0.0948
6.20	1.3381	0.5200	0.3973	0.3263	0.2411	0.1772	0.1318	0.1107
6.50	1.2789	0.4955	0.3780	0.3101	0.2284	0.1671	0.1234	0.1032
7.20	1.5510	0.5905	0.4467	0.3632	0.2618	0.1857	0.1304	0.1051
7.90	0.6825	0.2748	0.2136	0.1786	0.1376	0.1071	0.0872	0.0777
8.20	0.4778	0.1957	0.1539	0.1301	0.1033	0.0843	0.0736	0.0688
8.50	0.6057	0.2303	0.1749	0.1433	0.1065	0.0818	0.0690	0.0645
8.70	1.1049	0.4159	0.3130	0.2533	0.1809	0.1283	0.0922	0.0773
9.00	5.4707	1.9998	1.4809	1.1768	0.7999	0.5161	0.2985	0.2009
9.20	12.7196	4.6172	3.4064	2.6963	1.8132	1.1473	0.6323	0.4011
9.50	214.0730	77.3239	56.8958	44.9043	29.9622	18.6840	9.9178	5.9869
9.80	171.8837	62.0888	45.6871	36.0593	24.0626	15.0079	7.9703	4.8143
10.00	19.4105	7.0317	5.1821	4.0970	2.7463	1.7274	0.9378	0.5832
10.60	4.2619	1.5591	1.1550	0.9183	0.6248	0.4038	0.2343	0.1578
11.00	3.4964	1.2813	0.9500	0.7560	0.5156	0.3348	0.1963	0.1339
11.50	4.3002	1.5722	1.1644	0.9255	0.6291	0.4062	0.2349	0.1579
12.50	5.1601	1.8917	1.4033	1.1175	0.7637	0.4973	0.2937	0.2021
13.00	5.7726	2.1134	1.5667	1.2466	0.8504	0.5522	0.3247	0.2228
14.00	2.5357	0.9528	0.7165	0.5789	0.4112	0.2858	0.1945	0.1537
14.80	2.1902	0.8349	0.6326	0.5152	0.3731	0.2669	0.1906	0.1559
15.00	2.1299	0.8153	0.6190	0.5052	0.3676	0.2648	0.1910	0.1573
16.40	2.1984	0.8477	0.6457	0.5288	0.3879	0.2823	0.2068	0.1718
17.20	2.5347	0.9710	0.7373	0.6017	0.4376	0.3149	0.2260	0.1850
18.00	5.1099	1.9026	1.4233	1.1436	0.8002	0.5418	0.3477	0.2596
18.50	10.4462	3.8302	2.8417	2.2630	1.5472	1.0076	0.5951	0.4089
20.00	57.1574	20.6950	15.2480	12.0520	8.0742	5.0722	2.7451	1.7006
21.30	55.7639	20.0805	14.7505	11.6199	7.7136	4.7643	2.4648	1.4351
22.50	25.3177	9.0856	6.6612	5.2364	3.4557	2.1110	1.0589	0.5888
25.00	51.8537	18.6644	13.7071	10.7952	7.1613	4.4174	2.2770	1.3185
27.90	3246.8406	1172.3420	862.4538	680.5339	453.8190	282.6843	149.6213	89.9606
30.00	33.7571	12.2480	9.0343	7.1494	4.8055	3.0371	1.6691	1.0546
35.00	25.2023	9.1592	6.7619	5.3563	3.6096	2.2919	1.2744	0.8170
40.00	33.3242	12.0937	8.9214	7.0608	4.7474	3.0018	1.6519	1.0454

APPENDIX B

Magnitude of Effective polarizabilities of Arctic Aerosols at 61 wavelengths and 8 RH.

wavelength $\lambda(\mu m)$	Effective Polarizabilities at 8 RH							
	RH00	RH50	RH70	RH80	RH90	RH95	RH98	RH99
0.25	8.7245	8.4709	8.4469	8.4227	8.3983	8.3983	8.3983	8.3737
0.30	8.7144	8.4365	8.4123	8.3879	8.3633	8.3633	8.3386	8.3386
0.35	8.7139	8.4123	8.3879	8.3633	8.3633	8.3386	8.3386	8.3386
0.40	8.6917	8.4123	8.3879	8.3633	8.3386	8.3386	8.3137	8.3137
0.45	8.6917	8.4123	8.3879	8.3633	8.3386	8.3137	8.3137	8.3137
0.50	8.6917	8.4123	8.3633	8.3633	8.3386	8.3137	8.3137	8.3137
0.55	8.6919	8.3879	8.3633	8.3386	8.3386	8.3137	8.3137	8.3137
0.60	8.6695	8.3879	8.3633	8.3386	8.3137	8.3137	8.3137	8.2886
0.65	8.6696	8.3879	8.3633	8.3386	8.3137	8.3137	8.2886	8.2886
0.70	8.6696	8.3879	8.3633	8.3386	8.3137	8.3137	8.2886	8.2886
0.75	8.6699	8.3879	8.3633	8.3386	8.3137	8.3137	8.2886	8.2886
0.80	8.5310	8.2711	8.2466	8.2218	8.1969	8.1969	8.1719	8.1719
0.90	8.5318	8.2711	8.2218	8.2218	8.1969	8.1719	8.1719	8.1719
1.00	8.5100	8.2466	8.2218	8.2218	8.1969	8.1719	8.1719	8.1719
1.25	8.3940	7.5276	7.5029	7.4780	7.4529	7.4529	7.4529	7.4277
1.50	8.3730	6.8793	6.8544	6.8544	6.8293	6.8293	6.8041	6.8041
1.75	7.8684	5.9687	5.9438	5.9187	5.8935	5.8935	5.8935	5.8681
2.00	7.2459	4.8502	4.8251	4.7999	4.7999	4.7745	4.7745	4.7745
2.50	7.2007	3.6016	3.5759	3.5500	3.5239	3.5239	3.4977	3.4977
3.00	7.6020	3.7208	3.6912	3.6782	3.6685	3.6535	3.6595	3.6398
3.20	7.4628	4.6289	4.6306	4.6317	4.6331	4.6340	4.6347	4.6350
3.39	7.4401	5.0678	5.0447	5.0448	5.0450	5.0451	5.0216	5.0217
3.50	7.6883	5.3251	5.3014	5.3015	5.3015	5.2777	5.2777	5.2777
3.75	7.6901	5.1142	5.1143	5.0900	5.0900	5.0657	5.0657	5.0657
4.00	7.7499	4.9510	4.9266	4.9266	4.9021	4.9021	4.8774	4.8774

4.50	7.8359	4.9287	4.9043	4.8796	4.8549	4.8549	4.8550	4.8299
5.00	7.6675	4.7653	4.7407	4.7159	4.7160	4.6910	4.6911	4.6911
5.50	7.4304	4.2702	4.2452	4.2199	4.2200	4.1946	4.1946	4.1946
6.00	7.0344	3.2572	3.2378	3.2161	3.2202	3.1980	3.1997	3.2005
6.20	7.7125	3.3959	3.3532	3.3320	3.3112	3.2894	3.2905	3.2910
6.50	7.7815	3.1190	3.0967	3.0737	3.0749	3.0516	3.0521	3.0523
7.20	7.0028	6.7837	6.7594	6.7598	6.7352	6.7355	6.7105	6.7106
7.90	4.2704	3.2814	3.2575	3.2580	3.2338	3.2341	3.2344	3.2346
8.20	2.1042	3.1629	3.1408	3.1180	3.1188	3.0959	3.0962	3.0964
8.50	6.6602	5.5719	5.5235	5.4991	5.4747	5.4749	5.4501	5.4502
8.70	16.4614	6.9331	6.8847	6.8355	6.8108	6.7859	6.7608	6.7608
9.00	17.5102	10.4074	10.3341	10.2844	10.2341	10.2088	10.1833	10.1833
9.20	15.7027	10.5807	10.5317	10.4818	10.4313	10.4059	10.3802	10.3803
9.50	13.1808	10.6608	10.6116	10.5868	10.5364	10.5111	10.4855	10.4856
9.80	12.3575	10.7319	10.6825	10.6321	10.5812	10.5557	10.5561	10.5300
10.00	11.8602	10.8020	10.7268	10.7018	10.6507	10.6250	10.5991	10.5992
10.60	11.1841	9.2959	9.2195	9.1943	9.1426	9.1167	9.1174	9.0906
11.00	10.7262	9.1901	9.1402	9.0885	9.0639	9.0383	9.0121	9.0125
11.50	10.2143	8.8227	8.7749	8.7248	8.6749	8.6501	8.6245	8.6252
12.50	9.5530	7.9190	7.8811	7.8637	7.8495	7.8305	7.8094	7.8115
13.00	9.5323	7.5807	7.5518	7.5395	7.5310	7.5158	7.4982	7.5007
14.00	8.8999	8.2793	8.2551	8.2723	8.2686	8.2582	8.2430	8.2468
14.80	7.6131	9.0011	9.0060	9.0006	8.9998	9.0152	9.0027	9.0067
15.00	7.8746	9.0316	9.0370	9.0320	9.0316	9.0471	9.0349	9.0389
16.40	11.4267	9.5953	9.5777	9.5718	9.5715	9.5854	9.5734	9.5773
17.20	14.7056	10.0710	10.0523	10.0244	10.0001	9.9906	9.9788	9.9813
18.00	13.9200	10.3007	10.2620	10.2559	10.2320	10.2232	10.2109	10.2134
18.50	10.1476	10.3330	10.3150	10.2878	10.2846	10.2748	10.2627	10.2652
20.00	14.9540	11.1490	11.1306	11.1233	11.1009	11.0916	11.0993	11.0825
21.30	14.5658	12.2388	12.2184	12.2100	12.1853	12.1748	12.1811	12.1644
22.50	14.1634	13.3055	13.2818	13.2711	13.2627	13.2500	13.2362	13.2373
25.00	13.3857	13.7350	13.7068	13.6932	13.6815	13.6668	13.6699	13.6522
27.90	13.1742	13.4507	13.4365	13.4213	13.4059	13.3894	13.3728	13.3728
30.00	13.0768	13.3004	13.2855	13.2693	13.2541	13.2377	13.2389	13.2211
35.00	14.5012	14.5128	14.4632	14.4367	14.4076	14.3833	14.3782	14.3588
40.00	15.4587	16.3784	16.2967	16.2426	16.1806	16.1343	16.0975	16.0909

APPENDIX C

Magnitude of effective polarizabilities of Continental Clean Aerosols at 61 wavelengths and 8 RH.

Wavelength $\lambda(\mu m)$	Effective Polarizabilities at 8 RH							
	RH00	RH50	RH70	RH80	RH90	RH95	RH98	RH99
0.25	0.4924	0.4924	0.4924	0.4924	0.4924	0.4924	0.4924	0.4924
0.30	0.4916	0.4916	0.4916	0.4916	0.4916	0.4916	0.4916	0.4916
0.35	0.4916	0.4916	0.4916	0.4916	0.4916	0.4916	0.4916	0.4916
0.40	0.4916	0.4916	0.4916	0.4916	0.4916	0.4916	0.4916	0.4916
0.45	0.4916	0.4916	0.4916	0.4916	0.4916	0.4916	0.4916	0.4916
0.50	0.4916	0.4916	0.4916	0.4916	0.4916	0.4916	0.4916	0.4916
0.55	0.4916	0.4916	0.4916	0.4916	0.4916	0.4916	0.4916	0.4916
0.60	0.4916	0.4916	0.4916	0.4916	0.4916	0.4916	0.4916	0.4916
0.65	0.4916	0.4916	0.4916	0.4916	0.4916	0.4916	0.4916	0.4916
0.70	0.4916	0.4916	0.4916	0.4916	0.4916	0.4916	0.4916	0.4916
0.75	0.4916	0.4916	0.4916	0.4916	0.4916	0.4916	0.4916	0.4916
0.80	0.4839	0.4839	0.4839	0.4839	0.4839	0.4839	0.4839	0.4839
0.90	0.4839	0.4839	0.4839	0.4839	0.4839	0.4839	0.4839	0.4839
1.00	0.4839	0.4839	0.4839	0.4839	0.4839	0.4839	0.4839	0.4839
1.25	0.4359	0.4359	0.4359	0.4359	0.4359	0.4359	0.4359	0.4359
1.50	0.3944	0.3944	0.3944	0.3944	0.3944	0.3944	0.3944	0.3944
1.75	0.3337	0.3337	0.3337	0.3337	0.3337	0.3337	0.3337	0.3337
2.00	0.2608	0.2608	0.2608	0.2608	0.2608	0.2608	0.2608	0.2608
2.50	0.1843	0.1843	0.1843	0.1843	0.1843	0.1843	0.1843	0.1843
3.00	0.1649	0.1649	0.1649	0.1649	0.1649	0.1649	0.1649	0.1649
3.20	0.2230	0.2230	0.2230	0.2230	0.2230	0.2230	0.2230	0.2230
3.39	0.2591	0.2591	0.2591	0.2591	0.2591	0.2591	0.2591	0.2591
3.50	0.2794	0.2794	0.2794	0.2794	0.2794	0.2794	0.2794	0.2794
3.75	0.2702	0.2702	0.2702	0.2702	0.2702	0.2702	0.2702	0.2702
4.00	0.2609	0.2609	0.2609	0.2609	0.2609	0.2609	0.2609	0.2609
4.50	0.2610	0.2610	0.2610	0.2610	0.2610	0.2610	0.2610	0.2610
5.00	0.2518	0.2518	0.2518	0.2518	0.2518	0.2518	0.2518	0.2518

5.50	0.2238	0.2238	0.2238	0.2238	0.2238	0.2238	0.2238	0.2238
6.00	0.1591	0.1591	0.1591	0.1591	0.1591	0.1591	0.1591	0.1591
6.20	0.1500	0.1500	0.1500	0.1500	0.1500	0.1500	0.1500	0.1500
6.50	0.1414	0.1414	0.1414	0.1414	0.1414	0.1414	0.1414	0.1414
7.20	0.3895	0.3895	0.3895	0.3895	0.3895	0.3895	0.3895	0.3895
7.90	0.1599	0.1599	0.1599	0.1599	0.1599	0.1599	0.1599	0.1599
8.20	0.1550	0.1550	0.1550	0.1550	0.1550	0.1550	0.1550	0.1550
8.50	0.3110	0.3110	0.3110	0.3110	0.3110	0.3110	0.3110	0.3110
8.70	0.3980	0.3980	0.3980	0.3980	0.3980	0.3980	0.3980	0.3980
9.00	0.6276	0.6276	0.6276	0.6276	0.6276	0.6276	0.6276	0.6276
9.20	0.6424	0.6424	0.6424	0.6424	0.6424	0.6424	0.6424	0.6424
9.50	0.6511	0.6511	0.6511	0.6511	0.6511	0.6511	0.6511	0.6511
9.80	0.6574	0.6574	0.6574	0.6574	0.6574	0.6574	0.6574	0.6574
10.00	0.6637	0.6637	0.6637	0.6637	0.6637	0.6637	0.6637	0.6637
10.60	0.5697	0.5697	0.5697	0.5697	0.5697	0.5697	0.5697	0.5697
11.00	0.5672	0.5672	0.5672	0.5672	0.5672	0.5672	0.5672	0.5672
11.50	0.5450	0.5450	0.5450	0.5450	0.5450	0.5450	0.5450	0.5450
12.50	0.4836	0.4836	0.4836	0.4836	0.4836	0.4836	0.4836	0.4836
13.00	0.4543	0.4543	0.4543	0.4543	0.4543	0.4543	0.4543	0.4543
14.00	0.4904	0.4904	0.4904	0.4904	0.4904	0.4904	0.4904	0.4904
14.80	0.5304	0.5304	0.5304	0.5304	0.5304	0.5304	0.5304	0.5304
15.00	0.5304	0.5304	0.5304	0.5304	0.5304	0.5304	0.5304	0.5304
16.40	0.5522	0.5522	0.5522	0.5522	0.5522	0.5522	0.5522	0.5522
17.20	0.5735	0.5735	0.5735	0.5735	0.5735	0.5735	0.5735	0.5735
18.00	0.5828	0.5828	0.5828	0.5828	0.5828	0.5828	0.5828	0.5828
18.50	0.5837	0.5837	0.5837	0.5837	0.5837	0.5837	0.5837	0.5837
20.00	0.6331	0.6331	0.6331	0.6331	0.6331	0.6331	0.6331	0.6331
21.30	0.7048	0.7048	0.7048	0.7048	0.7048	0.7048	0.7048	0.7048
22.50	0.7758	0.7758	0.7758	0.7758	0.7758	0.7758	0.7758	0.7758
25.00	0.8032	0.8032	0.8032	0.8032	0.8032	0.8032	0.8032	0.8032
27.90	0.7812	0.7812	0.7812	0.7812	0.7812	0.7812	0.7812	0.7812
30.00	0.7704	0.7704	0.7704	0.7704	0.7704	0.7704	0.7704	0.7704
35.00	0.8479	0.8479	0.8479	0.8479	0.8479	0.8479	0.8479	0.8479
40.00	0.9607	0.9607	0.9607	0.9607	0.9607	0.9607	0.9607	0.9607

APPENDIX D

Magnitude of effective polarizabilities of Urban Aerosols at 61 wavelengths and 8 RH.

wavelength $\lambda(\mu m)$	Effective Polarizabilities at 8 RH							
	RH00	RH50	RH70	RH80	RH90	RH95	RH98	RH99
0.25	0.0189	0.0135	0.0115	0.0099	0.0074	0.0053	0.0034	0.0024
0.30	0.0188	0.0135	0.0115	0.0099	0.0074	0.0053	0.0033	0.0024
0.35	0.0188	0.0135	0.0115	0.0099	0.0074	0.0053	0.0033	0.0024
0.40	0.0188	0.0135	0.0115	0.0099	0.0074	0.0053	0.0033	0.0024
0.45	0.0188	0.0135	0.0115	0.0099	0.0074	0.0053	0.0033	0.0024
0.50	0.0188	0.0135	0.0115	0.0099	0.0074	0.0053	0.0033	0.0024
0.55	0.0188	0.0135	0.0115	0.0099	0.0074	0.0053	0.0033	0.0024
0.60	0.0188	0.0135	0.0115	0.0099	0.0074	0.0053	0.0033	0.0024
0.65	0.0188	0.0135	0.0115	0.0099	0.0074	0.0053	0.0033	0.0024
0.70	0.0188	0.0135	0.0115	0.0099	0.0074	0.0053	0.0033	0.0024
0.75	0.0188	0.0135	0.0115	0.0099	0.0074	0.0053	0.0033	0.0024
0.80	0.0185	0.0133	0.0113	0.0098	0.0073	0.0052	0.0033	0.0024
0.90	0.0185	0.0133	0.0113	0.0098	0.0073	0.0052	0.0033	0.0024
1.00	0.0185	0.0133	0.0113	0.0098	0.0073	0.0052	0.0033	0.0024
1.25	0.0167	0.0119	0.0102	0.0088	0.0066	0.0047	0.0030	0.0022
1.50	0.0151	0.0108	0.0092	0.0079	0.0060	0.0043	0.0027	0.0020
1.75	0.0128	0.0091	0.0078	0.0067	0.0050	0.0036	0.0023	0.0017
2.00	0.0100	0.0071	0.0061	0.0053	0.0039	0.0028	0.0018	0.0013
2.50	0.0071	0.0051	0.0043	0.0037	0.0028	0.0020	0.0013	0.0009
3.00	0.0063	0.0045	0.0038	0.0033	0.0025	0.0018	0.0011	0.0008
3.20	0.0085	0.0061	0.0052	0.0045	0.0034	0.0024	0.0015	0.0011
3.39	0.0099	0.0071	0.0060	0.0052	0.0039	0.0028	0.0018	0.0013
3.50	0.0107	0.0077	0.0065	0.0056	0.0042	0.0030	0.0019	0.0014
3.75	0.0104	0.0074	0.0063	0.0054	0.0041	0.0029	0.0018	0.0013

4.00	0.0100	0.0072	0.0061	0.0053	0.0039	0.0028	0.0018	0.0013
4.50	0.0100	0.0072	0.0061	0.0053	0.0039	0.0028	0.0018	0.0013
5.00	0.0097	0.0069	0.0059	0.0051	0.0038	0.0027	0.0017	0.0013
5.50	0.0086	0.0061	0.0052	0.0045	0.0034	0.0024	0.0015	0.0011
6.00	0.0061	0.0044	0.0037	0.0032	0.0024	0.0017	0.0011	0.0008
6.20	0.0058	0.0041	0.0035	0.0030	0.0023	0.0016	0.0010	0.0007
6.50	0.0054	0.0039	0.0033	0.0029	0.0021	0.0015	0.0010	0.0007
7.20	0.0149	0.0107	0.0091	0.0079	0.0059	0.0042	0.0027	0.0019
7.90	0.0061	0.0044	0.0037	0.0032	0.0024	0.0017	0.0011	0.0008
8.20	0.0059	0.0042	0.0036	0.0031	0.0023	0.0017	0.0011	0.0008
8.50	0.0119	0.0085	0.0073	0.0063	0.0047	0.0034	0.0021	0.0015
8.70	0.0153	0.0109	0.0093	0.0080	0.0060	0.0043	0.0027	0.0020
9.00	0.0241	0.0172	0.0147	0.0127	0.0095	0.0068	0.0043	0.0031
9.20	0.0246	0.0176	0.0150	0.0129	0.0097	0.0069	0.0044	0.0032
9.50	0.0250	0.0178	0.0152	0.0131	0.0098	0.0070	0.0044	0.0032
9.80	0.0252	0.0180	0.0153	0.0133	0.0099	0.0071	0.0045	0.0033
10.00	0.0254	0.0182	0.0155	0.0134	0.0100	0.0072	0.0045	0.0033
10.60	0.0218	0.0156	0.0133	0.0115	0.0086	0.0062	0.0039	0.0028
11.00	0.0217	0.0155	0.0132	0.0114	0.0086	0.0061	0.0039	0.0028
11.50	0.0209	0.0149	0.0127	0.0110	0.0082	0.0059	0.0037	0.0027
12.50	0.0185	0.0133	0.0113	0.0097	0.0073	0.0052	0.0033	0.0024
13.00	0.0174	0.0124	0.0106	0.0092	0.0069	0.0049	0.0031	0.0023
14.00	0.0188	0.0134	0.0114	0.0099	0.0074	0.0053	0.0033	0.0024
14.80	0.0203	0.0145	0.0124	0.0107	0.0080	0.0057	0.0036	0.0026
15.00	0.0203	0.0145	0.0124	0.0107	0.0080	0.0057	0.0036	0.0026
16.40	0.0212	0.0151	0.0129	0.0111	0.0083	0.0060	0.0038	0.0027
17.20	0.0220	0.0157	0.0134	0.0116	0.0087	0.0062	0.0039	0.0028
18.00	0.0223	0.0160	0.0136	0.0117	0.0088	0.0063	0.0040	0.0029
18.50	0.0224	0.0160	0.0136	0.0118	0.0088	0.0063	0.0040	0.0029
20.00	0.0243	0.0174	0.0148	0.0128	0.0096	0.0068	0.0043	0.0031
21.30	0.0270	0.0193	0.0165	0.0142	0.0106	0.0076	0.0048	0.0035
22.50	0.0297	0.0213	0.0181	0.0156	0.0117	0.0084	0.0053	0.0038
25.00	0.0308	0.0220	0.0188	0.0162	0.0121	0.0087	0.0055	0.0040
27.90	0.0299	0.0214	0.0182	0.0157	0.0118	0.0084	0.0053	0.0039
30.00	0.0295	0.0211	0.0180	0.0155	0.0116	0.0083	0.0052	0.0038
35.00	0.0325	0.0232	0.0198	0.0171	0.0128	0.0092	0.0058	0.0042
40.00	0.0368	0.0263	0.0224	0.0194	0.0145	0.0104	0.0065	0.0048

APPENDIX E

Magnitude of effective polarizabilities of Desert/ Saharan Aerosols at 61 wavelengths and 8 RH.

wavelength	Effective Polarizabilities at 8 RH							
$\lambda(\mu m)$	RH00	RH50	RH70	RH80	RH90	RH95	RH98	RH99
0.25	0.1063	0.1063	0.1062	0.1062	0.1062	0.1062	0.1062	0.1062
0.30	0.1038	0.1038	0.1038	0.1038	0.1038	0.1038	0.1038	0.1038
0.35	0.1037	0.1037	0.1037	0.1037	0.1037	0.1037	0.1037	0.1037
0.40	0.1037	0.1037	0.1037	0.1037	0.1037	0.1037	0.1037	0.1037
0.45	0.1037	0.1037	0.1037	0.1037	0.1037	0.1037	0.1037	0.1037
0.50	0.1037	0.1037	0.1037	0.1037	0.1037	0.1037	0.1037	0.1037
0.55	0.1037	0.1037	0.1037	0.1037	0.1037	0.1037	0.1037	0.1037
0.60	0.1037	0.1037	0.1037	0.1037	0.1037	0.1037	0.1037	0.1037
0.65	0.1037	0.1037	0.1037	0.1037	0.1037	0.1037	0.1037	0.1037
0.70	0.1037	0.1037	0.1037	0.1037	0.1037	0.1037	0.1037	0.1037
0.75	0.1037	0.1037	0.1037	0.1037	0.1037	0.1037	0.1037	0.1037
0.80	0.1037	0.1037	0.1037	0.1037	0.1037	0.1037	0.1037	0.1037
0.90	0.1037	0.1037	0.1037	0.1037	0.1037	0.1037	0.1037	0.1037
1.00	0.1037	0.1037	0.1037	0.1037	0.1037	0.1037	0.1037	0.1037
1.25	0.1037	0.1037	0.1037	0.1037	0.1037	0.1037	0.1037	0.1037
1.50	0.1037	0.1037	0.1037	0.1037	0.1037	0.1037	0.1037	0.1037
1.75	0.1037	0.1037	0.1037	0.1037	0.1037	0.1037	0.1037	0.1037
2.00	0.1037	0.1037	0.1037	0.1037	0.1037	0.1037	0.1037	0.1037
2.50	0.1021	0.1020	0.1020	0.1020	0.1020	0.1020	0.1020	0.1020
3.00	0.1023	0.1023	0.1023	0.1023	0.1023	0.1023	0.1023	0.1023
3.20	0.1005	0.1005	0.1005	0.1005	0.1005	0.1005	0.1005	0.1005
3.39	0.1004	0.1004	0.1004	0.1004	0.1004	0.1004	0.1004	0.1004
3.50	0.1004	0.1004	0.1004	0.1004	0.1004	0.1004	0.1004	0.1004
3.75	0.0987	0.0987	0.0987	0.0987	0.0987	0.0987	0.0987	0.0987

4.00	0.0987	0.0987	0.0987	0.0987	0.0987	0.0987	0.0987	0.0987
4.50	0.0987	0.0987	0.0987	0.0987	0.0987	0.0987	0.0987	0.0987
5.00	0.0954	0.0954	0.0954	0.0954	0.0954	0.0954	0.0954	0.0954
5.50	0.0922	0.0922	0.0922	0.0922	0.0922	0.0922	0.0922	0.0922
6.00	0.0892	0.0891	0.0891	0.0891	0.0891	0.0891	0.0891	0.0891
6.20	0.0876	0.0876	0.0876	0.0876	0.0876	0.0876	0.0876	0.0876
6.50	0.0856	0.0856	0.0856	0.0856	0.0856	0.0856	0.0856	0.0856
7.20	0.0956	0.0956	0.0956	0.0956	0.0956	0.0956	0.0956	0.0956
7.90	0.0507	0.0507	0.0507	0.0507	0.0507	0.0507	0.0507	0.0507
8.20	0.0372	0.0372	0.0372	0.0372	0.0372	0.0372	0.0372	0.0372
8.50	0.0488	0.0488	0.0488	0.0488	0.0488	0.0488	0.0488	0.0488
8.70	0.0756	0.0755	0.0755	0.0755	0.0755	0.0755	0.0755	0.0755
9.00	0.1692	0.1691	0.1691	0.1691	0.1691	0.1691	0.1691	0.1691
9.20	0.2072	0.2071	0.2071	0.2071	0.2071	0.2071	0.2071	0.2071
9.50	0.2512	0.2512	0.2512	0.2512	0.2512	0.2512	0.2512	0.2512
9.80	0.2500	0.2500	0.2500	0.2500	0.2499	0.2499	0.2499	0.2499
10.00	0.2280	0.2280	0.2280	0.2280	0.2280	0.2280	0.2280	0.2280
10.60	0.1632	0.1632	0.1632	0.1632	0.1632	0.1632	0.1632	0.1632
11.00	0.1517	0.1517	0.1516	0.1516	0.1516	0.1516	0.1516	0.1516
11.50	0.1580	0.1580	0.1580	0.1580	0.1580	0.1580	0.1580	0.1580
12.50	0.1642	0.1641	0.1641	0.1641	0.1641	0.1641	0.1641	0.1641
13.00	0.1777	0.1777	0.1777	0.1777	0.1777	0.1777	0.1777	0.1777
14.00	0.1267	0.1267	0.1267	0.1267	0.1267	0.1267	0.1267	0.1267
14.80	0.1156	0.1156	0.1156	0.1156	0.1156	0.1156	0.1156	0.1156
15.00	0.1131	0.1131	0.1131	0.1131	0.1131	0.1131	0.1131	0.1131
16.40	0.1141	0.1141	0.1141	0.1141	0.1141	0.1141	0.1141	0.1141
17.20	0.1227	0.1226	0.1226	0.1226	0.1226	0.1226	0.1226	0.1226
18.00	0.1640	0.1640	0.1640	0.1640	0.1640	0.1640	0.1640	0.1640
18.50	0.1967	0.1967	0.1967	0.1967	0.1967	0.1967	0.1967	0.1967
20.00	0.2255	0.2255	0.2255	0.2255	0.2255	0.2255	0.2255	0.2255
21.30	0.2423	0.2423	0.2423	0.2423	0.2423	0.2423	0.2423	0.2423
22.50	0.2561	0.2561	0.2561	0.2561	0.2560	0.2561	0.2561	0.2560
25.00	0.2579	0.2579	0.2579	0.2579	0.2579	0.2579	0.2579	0.2579
27.90	0.2403	0.2403	0.2403	0.2403	0.2403	0.2403	0.2403	0.2403
30.00	0.2271	0.2271	0.2271	0.2271	0.2271	0.2271	0.2271	0.2271
35.00	0.2244	0.2244	0.2244	0.2244	0.2244	0.2244	0.2244	0.2244
40.00	0.2244	0.2244	0.2244	0.2244	0.2244	0.2244	0.2244	0.2244

APPENDIX F:

Magnitude of effective polarizabilities of Maritime tropical Aerosols at 61 wavelengths and 8 RH

Wavelength $\lambda(\mu m)$	Effective Polarizabilities at 8 RH							
	RH00	RH50	RH70	RH80	RH90	RH95	RH98	RH99
0.25	0.8409	0.3724	0.2952	0.2383	0.1605	0.1015	0.0487	0.0273
0.30	0.8409	0.3641	0.2884	0.2327	0.1566	0.0990	0.0473	0.0266
0.35	0.8409	0.3557	0.2816	0.2270	0.1566	0.0965	0.0473	0.0260
0.40	0.8269	0.3557	0.2816	0.2270	0.1526	0.0965	0.0460	0.0259
0.45	0.8269	0.3557	0.2749	0.2270	0.1526	0.0940	0.0460	0.0259
0.50	0.8269	0.3475	0.2747	0.2270	0.1526	0.0940	0.0460	0.0259
0.55	0.8269	0.3473	0.2747	0.2213	0.1526	0.0940	0.0460	0.0253
0.60	0.8128	0.3473	0.2747	0.2213	0.1487	0.0940	0.0460	0.0252
0.65	0.8128	0.3473	0.2747	0.2213	0.1487	0.0940	0.0448	0.0252
0.70	0.8128	0.3473	0.2747	0.2213	0.1487	0.0940	0.0448	0.0252
0.75	0.8128	0.3473	0.2747	0.2213	0.1487	0.0940	0.0448	0.0252
0.80	0.7986	0.3473	0.2680	0.2213	0.1487	0.0940	0.0448	0.0252
0.90	0.7986	0.3390	0.2678	0.2213	0.1487	0.0914	0.0448	0.0252
1.00	0.7843	0.3389	0.2678	0.2213	0.1487	0.0914	0.0448	0.0252
1.25	0.7843	0.3389	0.2678	0.2155	0.1446	0.0914	0.0448	0.0244
1.50	0.7698	0.3304	0.2609	0.2155	0.1446	0.0914	0.0435	0.0244
1.75	0.7553	0.3304	0.2609	0.2097	0.1406	0.0889	0.0435	0.0237
2.00	0.7553	0.3218	0.2539	0.2039	0.1406	0.0863	0.0422	0.0237
2.50	0.7260	0.2870	0.2254	0.1803	0.1201	0.0759	0.0358	0.0200
3.00	0.9755	0.4439	0.3558	0.2932	0.2030	0.1283	0.0641	0.0363
3.20	0.8128	0.4420	0.3593	0.2974	0.2058	0.1307	0.0647	0.0369
3.39	0.7986	0.4054	0.3223	0.2664	0.1839	0.1164	0.0561	0.0317
3.50	0.7986	0.3889	0.3087	0.2551	0.1761	0.1090	0.0535	0.0302
3.75	0.7843	0.3641	0.2952	0.2383	0.1644	0.1015	0.0498	0.0280

4.00	0.7986	0.3558	0.2816	0.2327	0.1566	0.0990	0.0473	0.0266
4.50	0.8128	0.3475	0.2749	0.2215	0.1488	0.0941	0.0461	0.0252
5.00	0.7843	0.3390	0.2680	0.2157	0.1488	0.0915	0.0448	0.0252
5.50	0.7112	0.3133	0.2470	0.1982	0.1367	0.0838	0.0410	0.0230
6.00	0.6965	0.2985	0.2367	0.1908	0.1324	0.0816	0.0401	0.0226
6.20	0.9631	0.3950	0.3079	0.2494	0.1687	0.1045	0.0515	0.0291
6.50	0.7699	0.3487	0.2760	0.2225	0.1536	0.0947	0.0464	0.0262
7.20	0.7113	0.3228	0.2549	0.2107	0.1414	0.0894	0.0425	0.0239
7.90	0.6816	0.3058	0.2410	0.1992	0.1334	0.0843	0.0413	0.0232
8.20	0.7121	0.3061	0.2412	0.1934	0.1335	0.0818	0.0400	0.0225
8.50	0.7999	0.3150	0.2414	0.1936	0.1295	0.0818	0.0388	0.0218
8.70	0.9638	0.3323	0.2556	0.1996	0.1336	0.0819	0.0388	0.0218
9.00	1.0275	0.3408	0.2557	0.1997	0.1297	0.0794	0.0376	0.0211
9.20	0.9764	0.3239	0.2488	0.1940	0.1257	0.0768	0.0363	0.0204
9.50	0.9366	0.3068	0.2348	0.1882	0.1217	0.0743	0.0351	0.0197
9.80	0.9098	0.2984	0.2280	0.1767	0.1137	0.0693	0.0339	0.0183
10.00	0.8827	0.2900	0.2140	0.1710	0.1098	0.0668	0.0314	0.0176
10.60	0.8273	0.2570	0.1874	0.1493	0.0951	0.0576	0.0270	0.0151
11.00	0.7990	0.2365	0.1793	0.1376	0.0918	0.0559	0.0263	0.0147
11.50	0.7990	0.2330	0.1800	0.1404	0.0921	0.0570	0.0272	0.0153
12.50	0.7118	0.2739	0.2233	0.1865	0.1315	0.0839	0.0413	0.0233
13.00	0.6970	0.3121	0.2577	0.2164	0.1533	0.0984	0.0485	0.0276
14.00	0.6974	0.3791	0.3148	0.2680	0.1904	0.1223	0.0607	0.0348
14.80	0.7279	0.4176	0.3496	0.2942	0.2083	0.1352	0.0674	0.0388
15.00	0.7578	0.4268	0.3576	0.3007	0.2128	0.1380	0.0688	0.0396
16.40	0.9220	0.5000	0.4096	0.3425	0.2406	0.1558	0.0778	0.0452
17.20	1.1518	0.5446	0.4440	0.3659	0.2537	0.1624	0.0812	0.0473
18.00	1.1995	0.5674	0.4569	0.3799	0.2628	0.1680	0.0842	0.0492
18.50	1.1898	0.5721	0.4645	0.3819	0.2665	0.1703	0.0853	0.0500
20.00	1.1838	0.5801	0.4692	0.3882	0.2670	0.1701	0.0860	0.0498
21.30	1.1881	0.5826	0.4696	0.3881	0.2664	0.1694	0.0856	0.0495
22.50	1.1935	0.5871	0.4723	0.3898	0.2700	0.1715	0.0857	0.0502
25.00	1.2034	0.5967	0.4791	0.3947	0.2727	0.1731	0.0874	0.0506
27.90	1.2478	0.6044	0.4876	0.4007	0.2757	0.1745	0.0870	0.0510
30.00	1.2619	0.6030	0.4857	0.3987	0.2739	0.1731	0.0871	0.0504
35.00	1.4019	0.6232	0.4925	0.4015	0.2735	0.1719	0.0861	0.0496
40.00	2.0094	0.7061	0.5474	0.4392	0.2929	0.1818	0.0894	0.0522

Table of Contents

Contents Page

List of Table

Table **Page**

List of Figures

Figure

Page

Missing References updated